Relative level of glucocorticoid and progesterone receptor: implications for immune and reproductive functions in women

Prettysha Appadoo

Thesis presented in fulfilment of the requirements for the degree of

Master of Science

Department of Molecular and Cell Biology

Faculty of Science

University of Cape Town

Abstract

Background: The glucocorticoid receptor (GR) and progesterone receptor (PR) are very closely related in terms of their amino acid sequence and three-dimensional structure. PR ligands have been previously reported to cross-react with the GR. The cross-talk effects of certain PR ligands via the GR may impact immune function and risk of acquiring sexually transmitted infections (STIs). This suggests that GR and PR expression levels are relevant to immunity against pathogens in the female genital tract (FGT) and systemic immunity. PR protein expression is well characterised *ex vivo* in FGT tissues while very little is known about GR protein expression *ex vivo* in the FGT. Immune cells patrol the FGT but the expression of GR as well as PR proteins in resident immune cells of the FGT has not been previously reported.

Aims and Hypotheses: This study aims to assess potential cross-reactivity of GR and PR primary antibodies as it is hypothesised that the antibodies exhibit cross-receptor binding, confounding data interpretation. Another aim is to evaluate GR and PR protein expression in FGT epithelial and stromal cells, with the hypothesis that both GR and PR proteins are expressed in FGT epithelial and stromal cells. The study also seeks to determine and compare GR and PR expression in FGT-resident $CD4^+$ and $CD8^+$ immune cells, hypothesising that these cells express more GR than PR proteins. Finally, the study aims to determine and compare GR and PR protein expression in systemic immune cells, hypothesising that systemic $CD3^+$, $CD4^+$, and $CD8^+$ T lymphocytes, as well as $CD14^+$ monocytes, express higher levels of GR than PR.

Models and methodologies: PR-negative COS1 cells overexpressing exogenous GR or PR proteins were used to assess cross-reactivity of primary antibodies by western blot analysis,

immunofluorescence staining and flow cytometry. FGT ectocervical tissue explants were used as a model for the FGT. These were stained by immunofluorescence for GR and PR as well as for $CD4^+$ and $CD8^+$ markers. Immunofluorescence staining in ectocervical tissue samples was visualised by confocal microscopy. Peripheral blood mononuclear cells (PBMCs) were used as a model to investigate protein expression levels of GR and PR in systemic $CD3^+$, $CD4^+$, $CD8^+$ and $CD14^+$ cells by flow cytometry.

Results: Western blotting, immunofluorescence staining and flow cytometry in COS1 cells overexpressing GR and/or PR confirmed that the anti-GR antibodies did not cross-react with PR proteins and the anti-PR antibodies did not cross-react with GR proteins. Confocal imaging of ectocervical tissue sections demonstrated relatively high levels of expression of GR in epithelial cells, whereas PR expression was predominantly observed in stromal cells. GR was also expressed in some, but not all, FGT $CD4^+$ and $CD8^+$ cells. In contrast, PR fluorescence was absent in $CD4^+$ and $CD8^+$ cells within the FGT. Additionally, no notable trend was observed in GR expression density, PR expression density and the relative expression density of GR versus PR between $CD4^+$ and $CD8^+$ cells. Flow cytometric analysis of PBMCs revealed a high frequency of GR^+ cells among the systemic immune cells including $CD3^+$, $CD4^+$ and $CD8^+$ T cells, with significantly lower frequency of $CD14^+GR^+$ cells. There was no significant difference in the expression density of GR among systemic $CD3^+$, $CD4^+$, $CD8^+$, and $CD14^+$ cells. Conversely, PR detection in systemic $CD3^+$, $CD4^+$, $CD8^+$, and $CD14^+$ cells was problematic due to non-specific signals and gating challenges. After adjusting for these issues with appropriate controls and gating strategies, flow cytometry data indicated a lack of PR protein expression in systemic $CD3^+$, $CD4^+$, $CD8^+$, and $CD14^+$ cells.

Conclusion: The lack of cross-reactivity of GR and PR primary antibodies ensures the reliability of antibody-based protein detection assays employed in the thesis. The widespread expression of GR across different FGT cells, including epithelial, stromal and specific T lymphocytes as well as systemic T lymphocytes and monocytes, signifies its diverse roles throughout the body. These findings suggest a pivotal role of GR in cells regulating FGT barrier function and systemic immunity. In contrast to the GR, PR expression is more restricted and is primarily found in FGT stromal cells. Its presence in FGT epithelial cells is minimal and absent in FGT and systemic T lymphocytes and/or monocytes. The limited expression of PR compared to GR suggests that certain progestogens, such as progesterone and medroxyprogesterone acetate (MPA), may exert off-target effects through the GR in cells crucial for women's immune and reproductive systems. Collectively these findings provide insights on the potential implications of progestins-based hormonal contraceptives (HCs) such as depot MPA (DMPA) for women's health.

Plagiarism declaration

I, Prettysha Appadoo, hereby declare that the work on which this thesis is based is my original work (except where acknowledgements indicate otherwise) and that neither the whole work nor any part of it has been, is being, or is to be submitted for another degree in this or any other university.

Signature: Signed by candidate

Acknowledgements

I extend my deepest gratitude to the following individuals whose invaluable contributions and unwavering support were instrumental in the completion of this master's project:

Professor Janet Hapgood, for her intellectual guidance, encouragement, and commitment to pushing the boundaries of my capabilities.

Dr. Chanel Avenant, for her invaluable assistance in facilitating my thought processes, technical planning, troubleshooting, and data analyses.

Gcina, Alexis, and Mosoko, whose expertise and invaluable assistance ensured the seamless progress of laboratory work. Their guidance, troubleshooting tips, and training in BSL II+ facilities were indispensable, along with their support in thesis writing.

Anne Hoffman, the research sister at Groote Schuur Hospital, for patient recruitment and the acquisition of cervical tissue specimens.

Dr. Ashwin Issacs from the Department of Human Biology, University of Cape Town, for his assistance with tissue sectioning and coordination of cryostat bookings.

Dr. Dirk Lang and Dr. Viantha Naidoo, from the Confocal and Light Microscope Imaging Facility at the Department of Human Biology, University of Cape Town, for their expertise, guidance, and training in the operation of the confocal microscope.

Mrs Lize Engelbrecht at the CAF Microscopy Unit of Stellenbosch University for assistance and training for the use of the confocal microscope.

Notemba and Shaldine, for their assistance in the ordering and collection of blood buffy coats at the Western Cape Blood Services (WCBS).

Dr. Michele Tomassichio, at the Division of Pulmonology, University of Cape Town for his expertise and support in running samples for flow cytometry analysis.

My family and friends, for their unconditional love and support during the course of this project.

I would also like to thank the National Institute of Health (NIH) and the Poliomyelitis Research Foundation (PRF) for funding this project.

List of abbreviations

AF: Alexa Fluor

AP-1: Activator protein-1

AR: Androgen receptor

ATCC: America Type Culture Collection

APC: Antigen-presenting cells

BSA: Bovine serum albumin

BSL: Biosafety Level (BSL)

CTZ: Cervical transformation zone

DBD: DNA binding domain

DMPA: Depot medroxyprogesterone acetate

E_2: Estrogen

ER: Estrogen receptor

FCS: Fetal calf serum

FGT: Female genital tract

FSH: Follicle stimulating hormone

GR: Glucocorticoid receptor

HC: Hormonal contraceptive

HPV: Human papillomavirus

Hr: Hour

HRP: Horseradish peroxidase

HSP: Heat shock protein

IFN: Interferon

IL: Interleukin

LB: Luria broth

LBD: Ligand binding domain

LH: Luteinising hormone

MAPK: Mitogen-activated protein kinase

Min: Minute

MIP: Maximum intensity projection

MHC: Major histocompatibility complex

MHT: Menopausal hormone therapy

MPA: medroxyprogesterone acetate

MR: Mineralocorticoid receptor

NFκB: Nuclear factor-kappa B

NK: Natural killer

OCT: Optimal cutting temperature

PBMCs: Peripheral blood mononuclear cells

PBS: Phosphate buffer saline

PCR: Polymerase chain reacion

PR: Progesterone receptor

qRT-PCR: Real-time quantitative reverse transcription PCR

RPMI: Roswell Park Memorial Institute

RT: Room temperature

SR: Steroid receptor

SRE: Steroid responsive element

STI: Sexually transmitted infection

TBS: TRIS-buffered saline

TNF: Tumor necrosis factor

U: Unit

WCBS: Western Cape Blood Services

Table of Contents

Chapter 1: Introduction

1. 1. Steroid receptors and their functions

Steroid receptors (SRs) are ligand-activated transcription factors that mediate the actions of steroid hormones. The steroid receptor family, a subfamily of the nuclear receptor superfamily, consists of the progesterone receptor (PR), glucocorticoid receptor (GR), androgen receptor (AR), mineralocorticoid receptor (MR), and estrogen receptor (ER) (Mangelsdorf et al., 1995). In the absence of ligands, SRs are localised in the cytoplasm, bound to heat-shock proteins (HSPs) such as HSP90. SRs undergo conformational changes upon binding to their respective hormones/ligands, releasing HSP90 (Gehring, 1998). The ligand-receptor complexes are then translocated to the nucleus where the activated SRs regulate gene transcription via transactivation or transrepression. Activated SRs upregulate gene transcription by binding directly to specific DNA sequences called steroid-responsive elements (SREs) (transactivation) and repress transcription of target genes by indirectly interacting with other transcription factors such as nuclear factor-kappa B (NFκB) and activator protein-1 (AP-1) (transrepression) (**Figure 1.1**) (Beato and Klug, 2000, Africander et al., 2011).

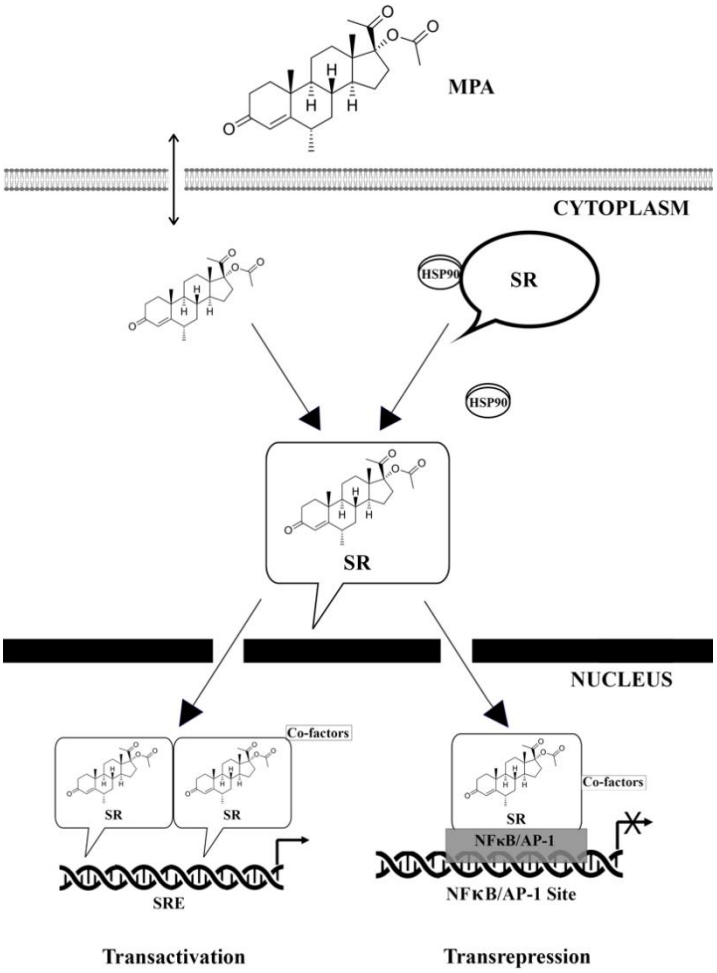

Figure 1.1: General mechanism of action of ligand-activated SRs in transcriptional gene regulation. SRs are activated by their cognate ligands and regulate gene transcription either by binding SRE and acting as a transcription factors or by interacting with other transcription factors to inhibit their actions. Image adapted from (Africander et al., 2011). HSP 90: heat-shock protein 90, MPA: medroxyprogesterone acetate, SR: steroid receptor, SRE: steroid response element, NFκB: as nuclear factor-kappa B, AP-1: activator protein-1.

1.1.1. Glucocorticoid receptor

The GR exists in two major isoforms, namely GRα and GRβ. GRα is the more transcriptionally active isoform, and GRβ is not activated by glucocorticoids (Oakley and Cidlowski, 2011, Timmermans et al., 2022). Inactivated GRα proteins reside in the cytoplasm in complex with chaperone proteins (Pratt and Toft, 1997, Grad and Picard, 2007) and are rapidly translocated to the nucleus when activated by glucocorticoids (Beato and Klug, 2000). The main glucocorticoid in humans is cortisol which is secreted in a circadian manner by the adrenal cortex and released in response to stress (Oakley and Cidlowski, 2013). Once in the nucleus, ligand-activated GRs transactivate and transrepress target genes (Oakley and Cidlowski, 2011), amounting to about 20% of the human genome (Galon et al., 2002). The GR is expressed in nearly all human tissues (Sapolsky et al., 2000, Oakley and Cidlowski, 2013). Hence, it is not surprising that glucocorticoids act on a diverse range of physiological processes involved in the proper functioning of the central nervous system, skeletal, hematopoietic, renal, and reproductive systems, as well as metabolism of carbohydrates, proteins and fats (Barnes, 1998, Sapolsky et al., 2000). Furthermore, GR signalling plays a major role in the control of inflammatory responses, mainly by inducing the transcription of anti-inflammatory genes and suppressing the transcription of proinflammatory genes (Oakley and Cidlowski, 2013, Vandevyver et al., 2013). For example, the GR promotes increased transcription of anti-inflammatory genes coding for lipocortin-1, serum leukoprotease inhibitor, Clara cell protein 10 (CC10), interleukin (IL)-1 receptor antagonist, IL-10, neural endopeptidase, and mitogen-activated protein kinase (MAPK) phosphatase-1, but represses the transcription of pro-inflammatory cytokine genes coding for TNF-α, GM-CSF, IL-1b, IL-2, IL-3, IL-6, IL-8, and IL-11 (Pace and Miller, 2009, Vandevyver et al., 2013, Cruz-Topete and Cidlowski, 2014, Nicolaides et al., 2018). Glucocorticoids are used to treat inflammatory diseases, autoimmune diseases, and organ transplant rejection due to their anti-inflammatory and immunosuppressive effects (Boumpas et al., 1993, Oakley and Cidlowski, 2011).

1.1.2. Progesterone receptor

The PR exists in two major isoforms, PR-A and PR-B, where PR-B is more transcriptionally active than PR-A (Mulac-Jericevic et al., 2000, Conneely et al., 2002). The PR mediates the actions of the endogenous hormone progesterone. Progesterone is involved in processes responsible for the development and normal functioning of the female reproductive system, including the maturation of oocytes, ovulation, embryo implantation, parturition, and maintenance of pregnancy (Graham and Clarke, 1997, Smith, 2007, Obr and Edwards, 2012, Salehnia and Zavareh, 2013). During the menstrual cycle, the PR is responsible for the functioning of ovarian cells to release eggs during ovulation (Salehnia and Zavareh, 2013). During pregnancy, the PR induces changes in uterine tissues to prepare for the fertilised egg to implant and grow (Navot et al., 1989, Dinh et al., 2019). The PR is also responsible for the normal proliferative activity and differentiation of epithelial and ductal cells in female mammary glands (Mulac-Jericevic et al., 2003). In males, the PR influences the functions of the male gametes and regulates fertility (Aquila and De Amicis, 2014). In addition to its well-documented reproductive functions, the PR is also activated by progesterone in the brain, thymus, bone, lungs and vasculature in both males and females (Lin et al., 2022). Furthermore, the PR is reported to play an anti-inflammatory role in female reproductive tissues by inhibiting the activation of the NFκB pathway (Hardy et al., 2006, Fedotcheva et al., 2022). Direct interaction of ligand-activated PR with the transcription factor NFκB suppresses the expression of pro-inflammatory cytokine genes such as TNF-α, IFN-γ and IL-12. The PR also upregulates gene transcription of anti-inflammatory cytokines such as IL-10, contributing to tissue repair and the reduction of inflammation (Patel et al., 2015).

1.1.3. Other SRs: estrogen receptor, androgen receptor and mineralocorticoid receptor

The ER mediates the actions of the endogenous hormone estrogen (E_2) that plays a role in the development of reproductive and mammary tissues. ER-mediated signalling regulates growth factor pathways that are involved in tissue repair, tumour growth and fibrogenesis, during morphogenesis in mammary glands, prostate, and lungs. In addition to the development and maintenance of reproductive tissues and mammary glands, the ER also exerts effects on the innate and adaptive immune system (Heldring et al., 2007).

In humans, the AR is activated by androgens, the male sex steroids. The main androgens include testosterone and the active metabolite of testosterone, dihydrotestosterone (DHT) (McEwan and Brinkmann, 2000). Androgens are responsible for male sexual differentiation, male reproductive functions and the development of prostate organs (McEwan and Brinkmann, 2000, Lu et al., 2006, Dehm and Tindall, 2007). Circulating concentrations of androgens are higher in men than in women. In both males and females, the AR regulates the transcription of genes involved in cell cycle progression, protein synthesis and cell death (Lu et al., 2006, Tan et al., 2015).

The mineralocorticoid receptor (MR) mediates the actions of the endogenous mineralocorticoid ligand, aldosterone. The MR is responsible for maintaining electrolyte homeostasis and blood pressure by regulating the transport of water, sodium and potassium, and it plays a role in metabolism and stress response, in both males and females (Gaeggeler et al., 2005).

Aldosterone, via the MR, regulates bone formation and bone resorption in osteocytes and osteoblasts (Altieri et al., 2018).

1.1.4. Cross-receptor binding of SRs ligands

The general structure of SRs is comprised of distinct domains: a transcriptional activation function-1 (AF-1) domain, a DNA-binding domain (DBD) and a C-terminal ligand binding domain (LBD). SRs display homology in their amino acid sequences and three-dimensional structures (**Figure 1.2**) (Griekspoor et al., 2007). The DBD is highly conserved among the SRs with about 90% homology, while the LBD of PR, GR, AR and MR share about 50-57% homology (Szapary et al., 2008, Africander et al., 2011). The GR and PR are very closely related. Their DBDs and LBDs are 90% and 55% identical, respectively (Szapary et al., 2008).

Figure 1.2: The structure of SRs consists of an activation domain (A/B), a DNA binding domain (DBD) and a ligand binding domain (LBD). The amino acid sequences of the SRs

suggest that they share structural similarities, particularly in their LBD. Figure taken from (Griekspoor et al., 2007).

Given the structural similarities between the SRs (**Figure 1.2**), it is not surprising that many SR ligands have been shown to cross-react with other SRs. For example, progesterone antagonises the activation of the AR and the MR (Rupprecht et al., 1993, Africander et al., 2014). The MR is not selective for aldosterone and binds to the glucocorticoid cortisol with a similar affinity (Arriza et al., 1987, Gorini et al., 2019). While these various cross-reactivities of endogenous steroids are physiologically important, and important for women's health, it is beyond the scope of this study to discuss and investigate all of them. Therefore, for the rest of the introduction, crosstalk between only GR and PR ligands will be discussed.

Progestogens are compounds that exert progestogenic effects by binding to PR. These include both endogenous progesterone and synthetic progestogens known as progestins (Hapgood et al., 2014a). Progesterone, at high concentrations, i.e. greater than 200 nM, can also bind to the GR as a weak agonist (Stanczyk et al., 2013). Progestins such as medroxyprogesterone acetate (MPA), norethisterone (NET), levonorgestrel (LNG) and etonogestrel (ETG) (**Figure 1.3**) are commonly used in menopausal hormone therapy (MHT) and as hormonal contraceptives (HCs) (Bick et al., 2021, Africander et al., 2011). They were designed to mimic progestational actions of progesterone and possess higher affinity, relative to progesterone, for the human PR (Africander et al., 2011). However, MPA binds to the GR with an equilibrium dissociation constant (K_d) of 4 – 11 nM and has a higher affinity for the GR than the endogenous glucocorticoid cortisol (Koubovec et al., 2004). MPA is a partial to full agonist for the GR, while NET, LNG and ETG have lower affinity for the GR and are less efficacious via the GR

than MPA (Africander et al., 2011, Huijbregts et al., 2014, Komane et al., 2022). Both MPA and NET are also partial to full agonists for the AR (Stanczyk et al., 2013).

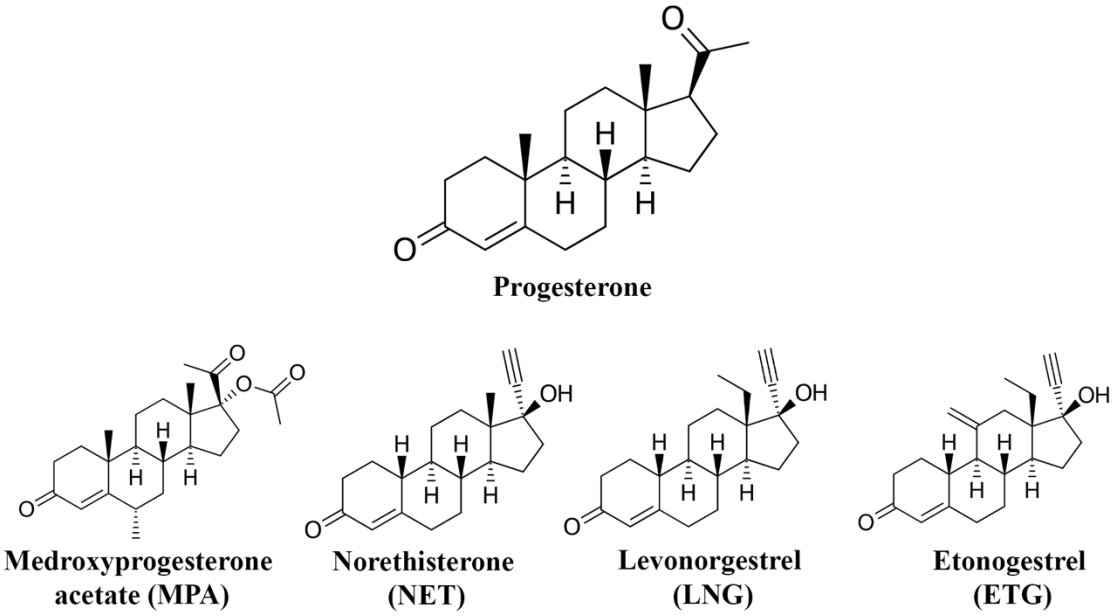

Figure 1.3: Commonly used progestins in MHT and HC, such as MPA, NET, LNG and ETG in HCs, share chemical structural similarities with the endogenous hormone, progesterone. Taken from (Bick et al., 2021).

Cross-reaction of PR ligands to the GR is physiologically relevant at different reproductive stages in women, particularly when progesterone levels increase. For example, when ovulation occurs, progesterone levels start to increase and continue to do so for approximately 7 days, at which time the levels peak, before decreasing prior to menstruation. The period of high progesterone levels is also known as the luteal phase of the menstrual cycle, where concentrations of progesterone increase to approximately 80 nM (Thurman et al., 2016, Bick et al., 2022). At the onset of pregnancy, progesterone levels also increase and can reach a concentration of up to 1 μM (Lissauer et al., 2015, Polikarpova et al., 2019). Additionally,

women taking HCs or MHT, particularly DMPA, possess serum concentrations of MPA of up to 420 nM (Hedley et al., 1985, Hapgood et al., 2018).

Altogether, receptor binding theory and the biological concentrations of progestogens during specific reproductive phases or following progestin administration suggest that cross-talk between PR ligands and GR is likely to occur, potentially impacting women's health.

1.1.5. Involvement of the GR and PR in physiological disorders, immunity and sexually transmitted infections

SRs are involved in several physiological disorders, including atherosclerosis, vascular inflammation, osteoporosis, and the incidence and progression of cancers (Caratti et al., 2015, Moss and Jaffe, 2015, Altieri et al., 2018, Dehm and Tindall, 2007). These are generally associated with increased SR levels, abnormal concentrations of steroid hormones and/or increased activation of SRs. For example, effects mediated via the GR impair bone remodelling in osteoblasts, osteocytes, and osteoblasts, causing plaques (Altieri et al., 2018). Differential GR expression levels have also been demonstrated to alter pathological states in patients with systemic lupus erythematosus and leukaemia (Lauten et al., 2003, Du et al., 2009). Steroid hormones used in HCs are reported to increase the risk of invasive cervical cancers and are associated with increased PR levels in higher-grade carcinomas (Monsonego et al., 1991, Moodley et al., 2003). Therefore, during cancer screening, PR expression is analysed to diagnose the type of cancer and to determine appropriate treatments. Furthermore, activation of the PR affects the incidence and progression of cancer cells in mammary glands (Ogara et al., 2019). PR is also associated with pancreatic and periampullary cancers (Andersson et al., 2019).

SRs are key immune regulators, modulating the production of cytokines, chemokines and inflammatory markers by targeting transcription factors such as NFκB and AP-1 (Lawrence, 2009, Cruz-Topete and Cidlowski, 2014, Moss and Jaffe, 2015, Fedotcheva et al., 2022). GCs, via the GR, display potent anti-inflammatory and immunosuppressive effects. They suppress inflammation by suppressing pro-inflammatory genes encoding cytokines, chemokines, cell adhesion molecules, inflammatory enzymes and receptors (McMaster and Ray, 2008, Cruz-Topete and Cidlowski, 2014). Moreover, fluctuating levels of sex hormones, particularly progesterone, is one of the key regulators of the function of epithelial, stromal, and immune cells in the FGT. The luteal phase, characterised by an increased concentration of progesterone, is regarded by some researchers as a 'window of vulnerability' to increased HIV/STI infection period (Wira and Fahey, 2008). During this phase, the innate and adaptive systems in female reproductive tissues undergo changes to optimise conditions for fertilisation and implantation. In the FGT, components of adaptive, innate, humoral and cell-mediated immunity, such as migration of immune cells, expression of coreceptors, secretion of antibodies, antimicrobial peptides, cytokines, and chemokines are suppressed during the luteal phase (White et al., 1997, Yeaman et al., 2003, Wira and Fahey, 2008). Similar to the luteal phase, high progesterone levels during pregnancy are associated with dampened immunity, where protective functions of the adaptive immune system are impaired to promote maternal-foetal tolerance (Hardy et al., 2006, Yao et al., 2017, Hellberg et al., 2021).

Furthermore, increased progesterone concentrations and the administration of progestin-based HCs also predispose women to viral infection, such as by human papillomavirus (HPV) and HIV, in the FGT (Wira and Fahey, 2008, Moodley et al., 2003, Bick, 2018, Bick et al., 2022, Hapgood et al., 2014b). The mechanisms associated with this reportedly include changes in the

recruitment or differentiation of viral target cells, suppression of innate and adaptive immune functions, enhanced expression of coreceptors that aid binding to viruses, a thinner epithelial layer, and modulation of pro- and anti-inflammatory cytokines and chemokines (Wira and Fahey, 2008, Wira et al., 2014, Hapgood et al., 2018). However, some but not all of these mechanisms are consistent with the reported effects of high progesterone in the luteal phase. Investigators carried out *ex vivo* and *in vitro* studies, which suggested that the actions of certain progestogens, such as progesterone and MPA, on suppression of immune function could be mediated via the GR and not the PR (Lei et al., 2012, Bick et al., 2022, Bick, 2018, Ray et al., 2019, Hapgood et al., 2014b). The presence of GR antagonist, and not PR antagonist, was able to prevent progesterone- or MPA-induced responses in human myometrial cells (Lei et al., 2012), cultured $CD4^+$ T cells (Tomasicchio et al., 2013) and PBMCs (Bick, 2018). Moreover, GR knockdown using siRNA reversed the effects of progesterone and MPA in both FGT cell lines and PBMCs (Lei et al., 2012, Govender et al., 2014, Louw-du Toit et al., 2014, Bick, 2018). Lastly, it was demonstrated that the relative levels of GR and PR affect inflammatory and immune responses of HIV-1 target cells to progestins *in vitro* (Bick, 2018).

Altogether, the above-mentioned studies suggest that GR and PR receptor levels, along with endogenous hormone and progestin concentrations, can modulate the responses of certain tissues to hormonal ligands, thus affecting susceptibility to pathogens and the progression of cancers. Additionally, high physiological concentrations of progesterone or administration of progestin-only HCs suppress immunity in the FGT, thus predisposing to sexually transmitted infections (STIs). Further research indicates that the relative expression of GR to PR is associated with differential responses to progestogens. Hence, the interplay between the endocrine and immune systems influences women's health and is a major area of research.

1.2. The role of the FGT and systemic immune cells in controlling infections

1.2.1 Structural and immunoregulatory functions of FGT compartments

The cervix is subdivided into the ectocervix, transformation zone (CTZ) and endocervix (**Figure 1.4A**). The ectocervix, endocervix and CTZ constitute of mainly epithelial and stromal cells (**Figure 1.4B**). The endocervix is lined by a single layer of tall columnar mucinous epithelial cells and forms part of the upper FGT (**Figure 1.4A**). The endocervix is not directly exposed to the external environment and is thus considered to be more sterile than the ectocervix. The CTZ is the region where the endocervix and ectocervix meet and is characterised by the transition of simple columnar epithelial cells to stratified squamous epithelial cells. The ectocervix, unlike the endocervix, is lined by layers of nonkeratinized stratified squamous epithelial cells and constitute the lower FGT (**Figure 1.4A**) which is associated with heavy microbial presence. Furthermore, the lower FGT is considered as the first site of contact with pathogens during heterosexual transmission. In the ectocervix, the epithelial and stromal tissues are separated by a layer of cells known as the basal layer (**Figure 1.4B**). The stromal tissue layer which is composed of fibroblasts, smooth muscles, lymphatic, nerve and vascular connections that collectively provide structural tissue support (Shukla et al., 2018). Both the epithelial and stromal tissues play important roles in mounting immunity against pathogens through several mechanisms (De Tomasi et al., 2019).

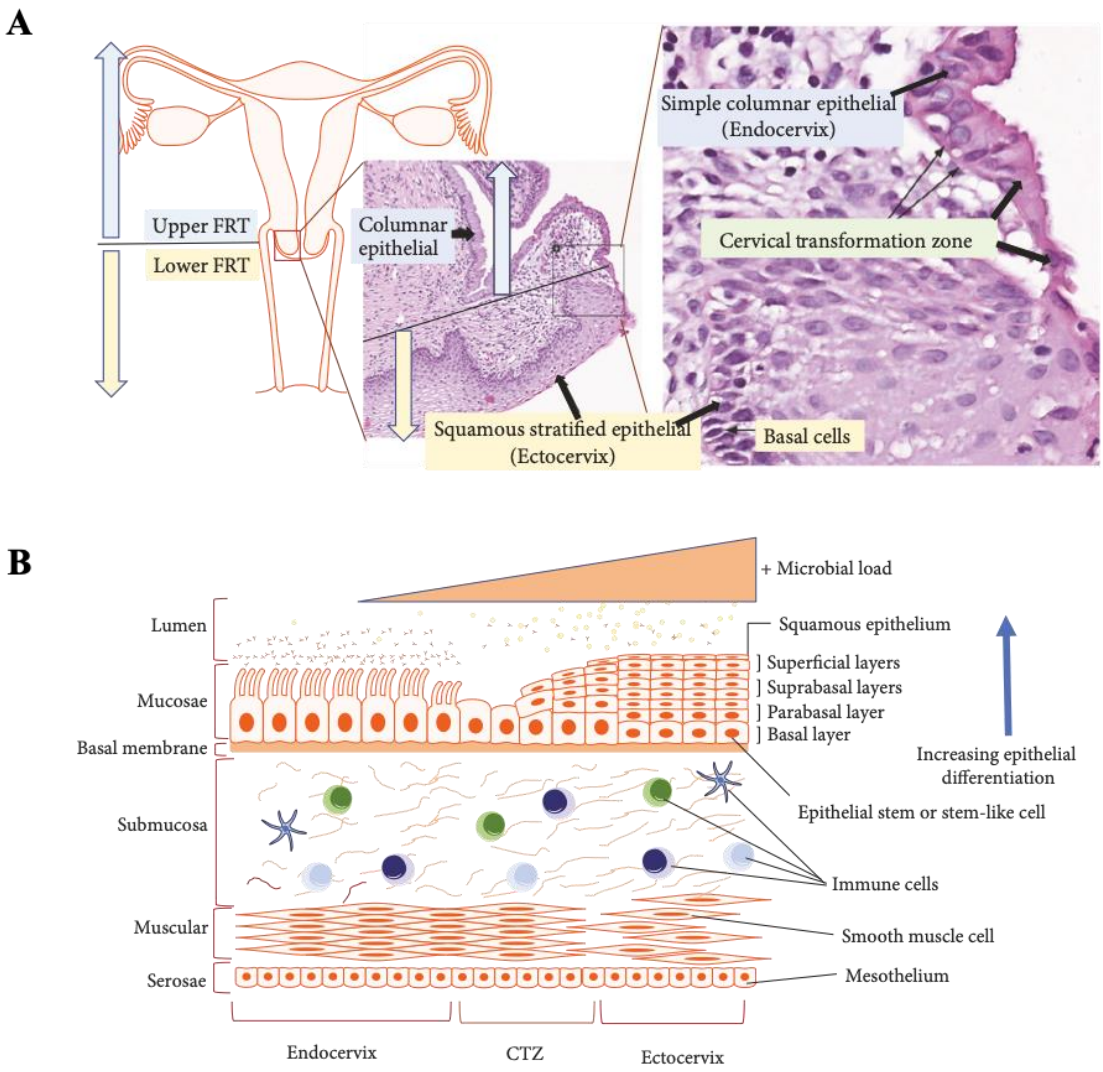

Figure 1.4: Anatomical and histological overview of the cervix within the female reproductive tract (FRT). (**A**) Figure showing the anatomy of the FRT as well as the location of the endocervix, the CTZ and ectocervix within the FRT. (**B**) Figure illustrating the histological structure of the cervix. CTZ: cervical transformation zone; FRT: female reproductive tract. Figures taken from (De Tomasi et al., 2019).

In the FGT, epithelial cells separate the lumen from the underlying tissue. They act as a physical barrier by either forming layers (ectocervix) or secreting mucus to fight pathogens (endocervix), conferring immune protection (Wira et al., 2005b). The consistency of mucus produced by epithelial cells is dynamic, serving as a semi-permeable barrier that prevent and

allow entry of pathogens and sperm respectively. Epithelial cells also secrete antimicrobial peptides, cytokines and chemokines. Cytokine and chemokine signalling act on immune cells such as dendritic, B, T and NK cells, leading to their differentiation or migration to provide appropriate immune responses (Wira et al., 2015, De Tomasi et al., 2019).

The stroma is a collagen-rich matrix and plays an important role in cervical remodelling during pregnancy and parturition (Socha et al., 2022). Furthermore, immune cells are also found to be scattered in the stroma and are responsible for fighting pathogens that infiltrate the cervix pass the epithelial barrier (Wira et al., 2015, De Tomasi et al., 2019). Other studies also suggest that stromal cells can indirectly influence functions of epithelial cells through paracrine signalling of cytokines and chemokines secreted by stromal fibroblasts (Wira et al., 2005b).

1.2.2 Functional roles of FGT immune cells

Besides epithelial cells and stromal fibroblasts, the ectocervix comprises of immune cells that patrol the epithelium and the stroma. Dynamic immune cell populations migrate throughout various sites of the FGT including the fallopian tubes, uterus, cervix and vagina, providing protection against foreign pathogens (Wira et al., 2005a, De Tomasi et al., 2019). Leukocytes account for 6-20% of the total number of cells in the FGT, with T lymphocytes ($CD3^+$ cells) representing the predominant immune cell subset. Other immune cells, such as B lymphocytes, macrophages, granulocytes, and monocytes, are present in lower proportions (Givan et al., 1997). Additionally, lymphoid aggregates, which comprise of macrophages, B lymphocytes, and T lymphocytes, are also present but are uniquely localized to the uterus (De Tomasi et al., 2019). The leukocyte population in the ectocervix consists predominantly of T lymphocytes

accounting 30-60% of all leukocytes (Givan et al., 1997, Poppe et al., 1998). $CD3^+$ cells are further subdivided to $CD4^+$ and $CD8^+$ cells and $CD3^+$, $CD4^+$, $CD8^+$ T cells are distributed across the epithelium and the stroma of the ectocervix (Trifonova et al., 2014, Zhou et al., 2018). $CD8^+$ T cells are more abundant than $CD4^+$ T cells, constituting of 60% and 40% of T cells, respectively (Trifonova et al., 2014). During pregnancy, $CD4^+$ T cells play important role by maintaining inflammation for foetal-maternal acceptance (Polikarpova et al., 2019). $CD4^+$ T cells are also the most preferred target cell of HIV since during the early steps required for HIV cell entry, gp120 attaches to the extracellular receptor, CD4, on host cells (Trifonova et al., 2014, Hapgood et al., 2018). $CD8^+$ T cells are cytotoxic cells and are able to sustain pathogens by inducing effective local cellular responses against microbes. Their antiviral effects allow them to control further transmission of viruses in the FGT (Koh et al., 2023). Macrophages ($CD14^+$ cells), natural killer (NK) cells ($CD56^+$ cells) and B lymphocytes are also present in the FGT and represent very small percentage of total immune cells (Mselle et al., 2007, Trifonova et al., 2014, Zhou et al., 2018, De Tomasi et al., 2019). $CD14^+$ cells in the FGT act as antigen-presenting cells (APCs) to $CD4^+$ and $CD8^+$ cells. Cervical $CD14^+$ cells may also transmit pathogens such as HIV-1 viruses to $CD4^+$ and $CD8^+$ cells (Donaghy et al., 2004, Trifonova et al., 2014, Trifonova et al., 2018). Some dendritic cells, which are also $CD14^+$ cells, express cell surface receptors known as DC-SIGN that bind and internalise viruses (Su et al., 2003).

1.2.3 Functional roles of peripheral blood mononuclear cells (PBMCs)

PBMCs consist of heterogenous cell populations that include lymphocytes, monocytes and dendritic cells. In humans, lymphocytes account for 70-90%, monocytes range from 10-20%

and dendritic cells represent 1-2% of total PBMCs (Kleiveland, 2015, Polikarpova et al., 2019). The lymphocytes population comprise of mainly of $CD3^+$ T cells (70-85%) while the minority are B cells (5-10%) and NK cells (5-20%) (Kleiveland, 2015). $CD4^+$ and $CD8^+$ T cells form part of the adaptive immune system and mount appropriate immune responses by secreting cytokines and chemokines. $CD4^+$ T cells differentiate to helper T cells which then induce activation of B cells' antibody production and cytotoxic $CD8^+$ T cells (Swain et al., 2012). $CD8^+$ T cells are cytotoxic cells that recognise and kill infected cells by releasing cytotoxic chemokines, cytokines or granules (Koh et al., 2023). $CD14^+$ cells in the blood are primarily monocytes but macrophages and dendritic cells also express CD14. $CD14^+$ cells express major histocompatibility complex (MHC) molecules such as HLA-DR enabling them to function as APCs to $CD4^+$ T and $CD8^+$ T cells (MacDonald et al., 2002).

Taken together, the above data suggests that the structure of the cervix, features of the epithelial and stromal tissues and distribution of immune cells make the cervix well equipped to support immunological and reproductive functions. Collectively, the epithelial cells, stromal fibroblasts and immune cells of the FGT contribute to a pool of cytokines, chemokines and antimicrobial peptides, conferring protection to the FGT. FGT $CD4^+$ and $CD8^+$ T cells are the predominant leukocytes, exhibiting specific function and differential susceptibility to STIs compared to each other. Hence, FGT cells, FGT $CD4^+$ and $CD8^+$ immune cells are appropriate models to investigate GR and PR expression. PBMCs are also suitable models as they consist of several immune cells including T lymphocytes ($CD3^+$ cells), $CD4^+$ T cells, $CD8^+$ T cells and $CD14^+$ monocytes that are relevant for establishment, control or progression of STIs.

1.3. Expression of GR and PR in FGT tissues and systemic immune cells

1.3.1. Expression of GR and PR in FGT tissues

Data on GR expression in the FGT is limited while the expression of PR is well-characterised across various FGT tissues (**Table 1.1**). In the endometrial tissue, GR protein has been reported to be expressed in stromal fibroblasts, endothelial cells and lymphocytes but not in endometrial glands (Bamberger et al., 2001). One study demonstrated the presence of GR proteins in the ectocervical epithelium but GR expression in the stroma was not investigated (Buxant et al., 2009). In the cells of the endometrium and the ectocervical epithelium, GR proteins appeared to localise to the nuclei (Bamberger et al., 2001, Buxant et al., 2009). GR mRNA was also detected in normal ectocervical tissue explants (Ray et al., 2019).

In contrast to GR, expression of PR protein in fresh FGT tissues such as the endometrium, the endocervix and the ectocervix is well documented. Both PR isoforms, i.e PR-A and PR-B were expressed in normal endometrium tissues (Wang et al., 1998) and previous work conducted in the Hapgood research group also confirmed the expression of both isoforms at the protein level in ectocervical tissue explants (Ray, 2015). Other studies have shown that PR proteins were expressed in glandular and stromal cells, but not in endothelial cells of the endometrium (Wang et al., 1998, Bamberger et al., 2001, Patel et al., 2015). In the endometrial tissues of pregnant women, PR proteins were observed in stromal cells but were absent in glandular epithelial cells (Perrot-Applanat et al., 1994). PR proteins were detected in columnar endocervical epithelial cells but were absent in the ectocervical epithelium of fresh human cervical tissues (Cano et al., 1990). However, a more recent study demonstrated PR protein expression in basal epithelial and stromal ectocervical cells (Ackerman et al., 2016). Similar to the GR, PR proteins were

localised to nuclei of FGT cells specified above (Cano et al., 1990, Bamberger et al., 2001, Ackerman et al., 2016). PR expression, at the mRNA level, was also detected in normal ectocervical tissue explants (Ray et al., 2019).

1.3.2. Expression of GR and PR in primary FGT cells and cell lines

Primary cell cultures of cervical stromal fibroblasts were shown to express GR protein whereas PR protein expression was lost in those cells when cultured *in vitro* (Ackerman et al., 2016). In FGT cell lines such as HeLa, End1/E6E7 endocervical epithelial, Ect1/E6E7 ectocervical epithelial, TZM-bl cervical cancer and Vk2/E6E7 vaginal epithelial cell lines, GR was shown to be expressed at both mRNA and protein levels (**Table 1.1**) (Africander et al., 2011, Govender et al., 2014, Louw-du Toit et al., 2014, Maritz et al., 2018). PR, on the other hand, was not detected in those FGT cell lines at protein level nor at mRNA level (Govender et al., 2014, Maritz et al., 2018, Mahajan et al., 2022).

Table 1.1: Summary of GR and PR expression in frozen FGT tissues, primary FGT cells and FGT cell lines. The methodologies employed to detect expression at protein or mRNA level are also recorded.

Receptors	GR and PR protein or mRNA expression	Stimulated or non-stimulated	References
FGT tissue			
PR	Immunocytochemistry (**protein**): PR was detected in the stromal and basal epithelial cells of ectocervix Immunohistochemistry (**protein**): PR was expressed in stromal cells and arterial cell wall cells of endometrium Immunohistochemistry (**protein**): PR was expressed in endometrial glands Western blot (**protein**): PR-A and PR-B was expressed in ectocervical tissue explants. Higher expression in follicular than luteal phase qRT PCR (**mRNA**): PR mRNA was expressed in ectocervical tissue	Non-stimulated	(Ackerman et al., 2016) (Perrot-Applanat et al., 1994) (Bamberger et al., 2001) (Ray, 2015) (Ray et al., 2019)
GR	Immunohistochemistry (**protein**): GR was expressed in stromal compartment of endometrium but not in endometrial glands Immunohistochemistry (**protein**): GR was expressed in the ectocervix qRT PCR (**mRNA**): GR mRNA was expressed in ectocervical tissue	Non-stimulated	(Bamberger et al., 2001) (Buxant et al., 2009) (Ray et al., 2019)

Primary cervical stromal fibroblasts			
PR	Immunofluorescence staining (**protein**): PR was expressed in the nuclei Western blot (**protein**): PR-A and PR-B were expressed qRT-PCR (**mRNA**): PR-A and PR-B were expressed	Estrogen (17β-E2) priming	(Ackerman et al., 2016)
GR	Immunofluorescence staining (**protein**): GR was constitutively expressed in the nuclei	Non-stimulated	(Ackerman et al., 2016)
FGT cell lines			
PR	Western blot (**protein**): PR was not detected in AN3 endometrial cancer cell line, RL95-2 endometrial cancer cell line, HeLa, End1/E6E7 endocervical epithelial cell line, Ect1/E6E7 ectocervical epithelial cell line, TZM-bl cervical cancer cell line and Vk2/E6E7 vaginal epithelial cell line qRT-PCR (**mRNA**): PR was not detected in AN3, RL95-2, HeLa, End1/E6E7, Ect1/E6E7 and TZM-bl cells	Non-stimulated or progesterone-estrogen treatment	(Mahajan et al., 2022) (Govender et al., 2014) (Maritz et al., 2018) (Louw-du Toit et al., 2014) (Africander et al., 2011)
GR	Western blot (**protein**): GR was detected in HeLa, End1/E6E7, TZM-bl and Ect1/E6E7 cells qRT-PCR (**mRNA**): GR was detected in HeLa, End1/E6E7 and TZM-bl cells	Non-stimulated	(Govender et al., 2014) (Maritz et al., 2018) (Louw-du Toit et al., 2014) (Africander et al., 2011)

1.3.3. Expression of GR and PR in systemic immune cells

Other studies also analysed the expression of GR and PR in systemic immune cells. It was shown that GR protein was expressed in peripheral blood mononuclear cells (PBMCs) (Tomasicchio et al., 2013, Bick et al., 2022) but PR protein expression was not detected (Tomasicchio et al., 2013). Similarly, RNA analyses of GR and PR in total PBMCs revealed that GR mRNA was expressed but PR mRNA was undetectable (Tomasicchio et al., 2013, Polikarpova et al., 2019, Brundin et al., 2021). In specific immune cell types, GR protein was identified in $CD3^+$ and $CD14^+$ cells, where $CD3^+$ cells were positive for GR at higher frequency than $CD14^+$ cells (Du et al., 2009). PR protein was found to be expressed in innate immune cells such as $CD56^+$ NK cells (Arruvito et al., 2008) whereas in the same study and others, low to no immunoreactivity to PR proteins was observed in $CD3^+$ T cells, $CD4^+$ T cells and $CD20^+$ B cells (Arruvito et al., 2008, Dosiou et al., 2008). High expression of GR mRNA was detected in $CD4^+$ T cells, $CD8^+$ T cells, $CD14^+$ monocytes, $CD56^+$ natural killer (NK) cells and $CD19^+$ B cells sorted from PBMCs (Brundin et al., 2021), while PR mRNA expression was not observed in peripheral blood leukocytes or $CD4^+$ T cells, $CD8^+$ T cells and dendritic cells (Dosiou et al., 2008, Hughes, 2011, Polikarpova et al., 2019).

Table 1.2: GR and PR expression in PBMCs and immune cell subsets sorted from PBMCs. The methods used to detect their expression at mRNA or protein level are also noted.

Receptors	GR and PR protein or mRNA expression	Stimulated or non-stimulated	References
PBMCs (whole population)			
PR	Western blot (**proteins**): PR was not detected qRT-PCR (**mRNA**): Nuclear *[1] PR mRNA was not detected	Non-stimulated	(Dosiou et al., 2008) (Hughes, 2011) (Tomasicchio et al., 2013) (Polikarpova et al., 2019) (Brundin et al., 2021)
GR	Western blot (**protein**): GR was detected qRT PCR (**mRNA**): GR mRNA was detected	Non-stimulated	(Tomasicchio et al., 2013) (Brundin et al., 2021) (Bick et al., 2022)
PBMCs (sorted)			
PR	Western blot (**protein**): PR-A and PR-B in peripheral blood natural killer (NK) cells was detected RT-PCR (**mRNA**): PR was not detected in peripheral blood leukocytes IF staining/confocal microscopy (**protein**): PR in ***CD56***$^+$ NK cells was detected Flow cytometry (**protein**): Expression of PR was observed in **NK** cells (63.63 %). Very low immunoreactivity was observed in peripheral blood purified ***CD3***$^+$ T cells, ***CD4***$^+$ T cells and ***CD20***$^+$ B cells	Non-stimulated Non-stimulated P_4 stimulation (2h) Non-stimulated	(Dosiou et al., 2008) (Arruvito et al., 2008) (Polikarpova et al., 2019)
GR	Flow cytometry (**protein**): GR was expressed in $CD3^+$ T cells and $CD14^+$ monocytes $\%CD3^+GR^+$ cells > $\%CD14^+GR^+$ cells Manual qPCR (**mRNA**): GR was highly expressed in $CD4^+$ T cells, $CD8^+$ T cells, $CD14^+$ monocytes, $CD56^+$ NK cells and $CD19^+$ B cells	Non-activated	(Du et al., 2009) (Brundin et al., 2021)

*[1] It is important to note that in this study, the authors also explored the expression of membrane progesterone receptors (PRs) (Polikarpova et al., 2019). However, for the purposes of the present investigation, the primary focus is on the classical nuclear PR.

In summary (data summarised in **Table 1.1** and **Table 1.2**), GR expression was detected in almost all types of FGT tissues, cultured primary stromal fibroblasts, FGT cell lines and primary systemic immune cells. Nevertheless, there is limited data on GR protein expression in the lower FGT, more specifically in the epithelial and stromal compartments of the ectocervix. Additionally, differences in GR expression and protein expression density among $CD3^+$, $CD4^+$, $CD8^+$ and $CD14^+$ cellular subsets are yet to be elucidated. PR expression is well established in the ectocervix at the protein level while its expression in specific systemic immune cells such as $CD3^+$, $CD4^+$, $CD8^+$ and $CD14^+$ cells is questionable. Besides, no studies by thus have investigated the expression of GR and PR in immune cells residing in the FGT.

1.4. Strategies, methodologies and challenges in detecting GR and PR in FGT tissues and systemic immune cells

Both GR and PR protein were observed in fresh FGT tissues by immunohistochemistry (Perrot-Applanat et al., 1994, Bamberger et al., 2001, Buxant et al., 2009, Ackerman et al., 2016). Immunohistochemistry is recognised as a powerful technique to visualise protein expression in tissues *ex vivo* (Gremel et al., 2014). It enables detection of the proteins in their native form and can provide information on their spatial localisation in tissues or subcellular compartments. Previously in the Hapgood research group, western blot analyses were conducted on homogenised cervical tissue explants to probe for GR and PR proteins (Ray, 2015). The

expression GR and PR proteins were detected but the spatial localisation of the proteins could not be determined using this technique. Nevertheless, the molecular weights of the signal obtained confirmed the identity of the proteins of interest and revealed the presence of different isoforms of the proteins (Ray, 2015). Further studies cultured cervical fibroblasts *in vitro* and explored GR and PR protein expression by immunofluorescence microscopy. This method generated high resolution images demonstrating that GR and PR proteins were expressed in the nuclei of primary cervical fibroblasts (Ackerman et al., 2016). Moreover, protein expression of GR and PR was investigated in FGT cell lines by western blot analyses which is less complex to perform and less expensive compared to immunocytochemistry techniques using tissue samples (Bamberger et al., 2001, Govender et al., 2014, Louw-du Toit et al., 2014, Maritz et al., 2018). However, *in vitro* analyses may not fully replicate the *in vivo* environment and potentially lead to inaccurate conclusions. Indeed, PR proteins were reportedly expressed in fresh FGT tissues but were not detected in any of the FGT cell lines summarised in **Table 1.1** (Perrot-Applanat et al., 1994, Bamberger et al., 2001, Govender et al., 2014, Louw-du Toit et al., 2014, Ackerman et al., 2016, Maritz et al., 2018). Several studies also performed mRNA analyses by using real-time quantitative reverse transcription PCR (qRT-PCR) to examine and quantify mRNA transcripts of GR and PR in FGT tissues, primary FGT cells and FGT cell lines (Govender et al., 2014, Ackerman et al., 2016, Maritz et al., 2018, Ray et al., 2019, Mahajan et al., 2022). However, the presence of mRNA does not necessarily mean that the protein is expressed.

For determination of GR and PR in systemic tissues, PBMCs isolated from human blood samples are repeatedly used as a model as they constitute of several types of immune cells. Western blotting has been conducted previously on whole population PBMCs to check for protein expression of GR and PR (Tomasicchio et al., 2013). Conventional PCR was also

performed on whole population PBMCs to examine mRNA expression of GR and PR (Tomasicchio et al., 2013). GR protein and mRNA was easily detected in the whole PBMC population, while PR protein and mRNA could not be detected using Western blot analysis and PCR (Tomasicchio et al., 2013). However, PR proteins were detected by flow cytometry or by immunofluorescence in certain immune cells such as natural killer cells ($CD56^+$ cells) following sorting of PBMCs. PBMCs constitute of 70% of T cells which do not express PR (Brundin et al., 2021) and hence the lack of expression of PR in T cells could mask the expression of PR in other immune cells such as macrophages and NK cells (Dosiou et al., 2008). Fluorescence-activated cell sorting (FACS) is a more advanced method that enables sorting of immune cell subtypes and therefore, protein or mRNA analyses can be conducted in specific immune cell population (Arruvito et al., 2008, Brundin et al., 2021). Flow cytometry is a direct method for detection of specific markers in sorted immune cells whereas other researchers harvested the sorted immune cells and performed immunofluorescence staining, western blotting (Arruvito et al., 2008) or PCR (Brundin et al., 2021).

Taken together, the information gathered from literature suggest that immunofluorescence technique coupled with confocal microscopy is the most powerful method to use for protein detection of GR and PR in the FGT, as it provides information on spatial expression of proteins in tissues and expression density can also be quantified in specific cells. However, no such study has investigated or quantified GR or PR expression in specific FGT immune cells such as $CD4^+$ and $CD8^+$ cells. In PBMCs, the flow cytometry method is the most suitable method where the immune cells can be sorted as well as determination of the frequency of specific immune cell subset and the expression density of the protein of interest. However, none of the studies in **Table 1.1** and **Table 1.2** that investigated GR and PR proteins expression, demonstrated that the primary antibodies used to detect GR and/or PR do not cross-reacted

with the non-target receptor. Given the sequence and structural homology among SRs, as discussed earlier, this is of extreme importance.

1.5. Thesis rationale, research gap, hypotheses and aims

1.5.1. Thesis rationale and research gap

As mentioned previously, progesterone concentration fluctuates during the menstrual cycle, menopausal stages and at the onset of pregnancy. During these fluctuations, steroid receptor theory and binding affinities suggest that the PR is the main SR through which progesterone acts at low progesterone concentrations (Graham and Clarke, 1997, Africander et al., 2011, Hapgood et al., 2018). However, when progesterone concentrations are very high, particularly during the luteal phase and pregnancy, progesterone could also be acting via the GR (Africander et al., 2011, Stanczyk et al., 2013, Hapgood et al., 2018). Similarly, certain progestins such as MPA also react with the GR at physiological concentrations in women taking HCs or MHT (Hapgood et al., 2018). Several lines of evidence suggest that high progesterone levels during the luteal phase and the use of progestin-based HCs impact immune function in women and increase their risk of acquiring STIs (Asin et al., 2008, Saba et al., 2013, Morrison and Nanda, 2012, Morrison et al., 2015, Byrne et al., 2016, Polis et al., 2016, Bick et al., 2022). Some of these biological responses are likely due to the crosstalk effects of certain progestogens with the GR (Lei et al., 2012, Hapgood et al., 2014a, Hapgood et al., 2018, Bick et al., 2022, Komane et al., 2022). This is particularly relevant in the FGT, which is the primary site of STIs. Epithelial cells and resident immune cells in the FGT are target cells for viruses such as HIV-1, HPV and herpes (Horvath et al., 2010, Wira et al., 2014, Wira et al., 2015).

Additionally, systemic immune cells are exposed to progestogens in circulation, where their responses are regulated by hormonal changes (Omollo et al., 2021, Bick et al., 2022).

It is unclear via which SRs progestogens exert their biological effects in these tissues. Most FGT cell lines (summarised in **Table 1.1**), including Ect/E6E7 cells (Louw-du Toit et al., 2014), have been demonstrated to respond to progesterone and progestins but lack expression of PR protein (Africander et al., 2011, Govender et al., 2014, Maritz et al., 2018, Mahajan et al., 2022). On the other hand, very little is known about GR protein expression *in vivo* in lower FGT tissues and its cellular compartments. Moreover, protein expression of GR and PR is not characterised in FGT $CD4^+$ and $CD8^+$ immune cells. Similarly, a comparison of GR and PR expression at the protein level among systemic T lymphocytes ($CD3^+$, $CD4^+$, $CD8^+$ cells) and monocytes ($CD14^+$ cells) has not been previously investigated.

1.5.2. Hypotheses and aims

The primary aim of this study is to investigate GR and PR protein expression in tissues that regulate women's reproductive and immune systems.

Due to structural and amino acid sequence homology between GR and PR (Szapary et al., 2008, Africander et al., 2011), it is possible that the anti-GR and anti-PR antibodies used for protein detection methods can non-specifically bind to the PR and GR, respectively. This may have confounded the results of published data (**Table 1.1** and **Table 1.2** and references therein) since cross-reactivity testing of the antibodies was not reported.

It is therefore hypothesised that the primary antibodies used for detection GR and PR bind non-specifically to each other's receptors, leading to potential cross-reactivity.

Hence, for this project, the first aim is to assess whether the primary antibodies used for GR and PR detection display reciprocal receptor cross-reaction and whether the antibodies are optimal for sensitive protein detection methods.

Ex vivo, PR protein has previously been detected in basal epithelial and stromal cells of the ectocervix (Ackerman et al., 2016). GR protein was previously detected in primary ectocervical stromal fibroblasts and the ectocervical epithelial cell line, Ect/E6E7 (Louw-du Toit et al., 2014, Ackerman et al., 2016).

It is therefore hypothesised that the ectocervical epithelial and stromal cells express both GR and PR.

This study aims to characterise GR and PR protein expression in the epithelial and stromal compartments of the ectocervix using immunofluorescent microscopy.

Additionally, $CD4^+$ and $CD8^+$ immune cells located in the ectocervix protect the FGT and act as potential target cells for certain viruses (Trifonova et al., 2014, Hapgood et al., 2018) (Koh et al., 2023). Their immune responses are also regulated by fluctuating levels of progestogens (Chandra et al., 2012, Edfeldt et al., 2022). Currently, no information is available on GR or PR protein levels in immune cells within the FGT. Nevertheless, previous research demonstrated that GR but not PR was expressed in systemic T lymphocytes (Arruvito et al., 2008, Dosiou et al., 2008).

Based on this, the second hypothesis is that as in the case of systemic T lymphocytes, all FGT $CD4^+$ and $CD8^+$ cells express GR and a relatively low amount of PR protein. There may also be differences in the expression density of GR and PR between FGT $CD4^+$ and $CD8^+$ cells.

Another aim is to investigate GR and PR protein expression in ectocervical $CD4^+$ and $CD8^+$ cells using immunofluorescent microscopy.

It has been previously demonstrated that tissue-resident immune cells in the FGT display different functions compared to systemic immune cells (De Tomasi et al., 2019, Wira et al., 2015). According to previous studies (summarised in **Table 1.2**), GR but not PR was detected in total PBMCs. Within the PBMC population, T lymphocytes constitute the majority while macrophages and monocytes represent minor components (Kleiveland, 2015). Interestingly, when looking at specific cells within the total PBMC population, one study reported that $CD3^+$ T lymphocytes express GR at a higher frequency than $CD14^+$ monocytes (Du et al., 2009) (**Table 1.2**). The expression of GR in other immune cell types, such as $CD4^+$ T cells, $CD8^+$ T cells and $CD14^+$ monocytes, is unknown. Similarly, while PR protein expression has been observed in $CD56^+$ natural killer (NK) cells and detected at low levels in $CD3^+$ T cells, $CD4^+$ T cells, and $CD20^+$ B cells (Polikarpova et al., 2019), there is no information on PR protein expression in $CD8^+$ T cells or $CD14^+$ monocytes. (summarised in **Table 1.2**). While a thorough investigation of GR and PR expression in all the cell types comprising total PBMCs is required, such a comprehensive study is beyond the scope of this thesis. As a starting point, this study set out to determine GR and PR expression in T cells, which are the most prevalent immune cell type in total PBMCs, and monocytes, which are the second most prevalent.

Taking all known literature into account, the third hypothesis is that systemic T lymphocytes and monocytes express relatively more GR than PR protein. It is also hypothesised that a higher

proportion of T lymphocytes ($CD3^+$ cells; including $CD4^+$ and $CD8^+$ cells) compared to monocytes ($CD14^+$ cells) express GR.

Lastly, the present study seeks to determine and compare GR and PR protein expression levels among $CD3^+$, $CD4^+$, $CD8^+$ T cells and $CD14^+$ monocytes using flow cytometry.

Chapter 2: Material and Methods

2.1. Ethics and biosafety

This research is a sub-study linked to HREC 210/2011. This study was approved for the use of human cervical explant tissue from Groote Schuur Hospital and blood bank buffy coats from Western Cape Blood Services by the Human Research Ethics Committee at the University of Cape Town with reference number HREC REF: 590/2022. The ethics approval letters are uploaded in **Section 6.4.**

All biosafety procedures, with approval number BSC 004-2018, established by the Health and Safety Committee of the Department of Molecular Cell Biology at the University of Cape Town were followed for all experiments carried out in Biosafety Level (BSL) II and II+ facilities.

2.2. Antibodies and reagents

Unconjugated primary antibodies for GR (mouse anti-GR, G-5; Santa Cruz Biotechnology, USA), PR (mouse anti-PR, NCL- LPGR-312; Leica Biosystems, UK) and GAPDH (mouse anti-GAPDH; Santa Cruz Biotechnology, USA) were used for immunofluorescence staining and/or western blot analysis. Fluorescently labelled secondary antibodies, anti-mouse Alexa Fluor (AF) 488 (Jackson ImmunoResearch, USA) and anti-rabbit Cy3 (Jackson ImmunoResearch, USA) were used for immunofluorescence and HRP-linked anti-mouse secondary antibodies (Santa Cruz Biotechnology, USA) were used for western blot analysis.

The unconjugated primary antibodies mouse anti-GR, G-5, mouse anti-PR, NCL- LPGR-312 and the secondary antibodies anti-mouse AF488 and anti-mouse AF647 (Jackson ImmunoResearch, USA) were also used for flow cytometry.

Primary antibodies conjugated to fluorochromes were used for staining by flow cytometry. A panel was designed for the antibodies such that their excitation and emission spectral profiles do not overlap. The antibodies mouse anti-human CD3 AF700, mouse anti-human CD4 APC Fire 750, mouse anti-human CD8 PerCP and mouse anti-human CD14 PE Dazzle were purchased from Biolegend, USA, while the monoclonal anti-GR FITC and anti-PR eFluor™ 660 antibodies were obtained from Thermo Scientific, South Africa, and mouse anti-CXCR4 BV605 from BD, USA.

The dilution or volume titre of all antibodies is tabulated below in **Tables 2.1-2.3**.

Table 2.1: Dilutions of primary and secondary antibodies used for western blot analysis.

Markers	**Primary antibody dilution**	**Secondary antibody dilution**	**Conjugate**
GR	mouse anti-GR 1:3000	anti-mouse HRP 1:3000	Horseradish peroxidase (HRP)
PR	mouse anti-PR 1:1000	anti-mouse HRP 1:3000	HRP
GAPDH	mouse anti-GAPDH 1:2000	anti-mouse HRP 1:3000	HRP

Table 2.2: Dilutions of primary and secondary antibodies used for immunofluorescence staining of COS1 cells or cervical tissue explants.

Markers	**Primary antibody dilution**	**Secondary antibody dilution**	**Fluorophore (colour)**
Single marker staining			
GR	mouse anti-GR 1:250	anti-mouse AF488 1:500 dilution	AF488 (green)
PR	mouse anti-PR 1:1000 dilution	anti-mouse AF488 1:500 dilution	AF488 (green)
Double markers staining			
GR	mouse anti-GR 1:250 dilution	anti-mouse AF488 1:500 dilution	AF488 (green)
PR	mouse anti-PR 1:1000 dilution	anti-mouse AF488 1:500 dilution	AF488 (green)
CD3	rabbit anti-CD3 1:1000 dilution	anti-rabbit Cy3 1:1000 dilution	Cy3 (red)
CD4	rabbit anti-CD4 1:200 dilution	anti-rabbit Cy3 1:1000 dilution	Cy3 (red)
CD8	rabbit anti-CD8 1:1000 dilution	anti-rabbit Cy3 1:1000 dilution	Cy3 (red)

Table 2.3: Volume titres and fluorochromes of conjugated primary antibodies used for flow cytometry.

Marker	**Antibody**	**Volume (µL)*[1]**	**Fluorochrome**
CD3	mouse anti-CD3 AF700	0.5	AF700
CD4	mouse anti-CD4 APC Fire 750	0.5	APC Fire 750
CD8	mouse anti-CD8 PerCP	1	PerCP
CD14	mouse anti-CD14 PE Dazzle 594	2	PE Dazzle 594
GR	mouse anti-GR FITC	5	FITC
PR	mouse anti-PR efluor660	5	Efluor660
CXCR4*[2]	mouse anti-CXCR4 BV605	-	BV605

*[1] titre of antibodies in µL used per test for staining 1 million cells

*[2] CXCR4 was used as a marker for Zombie to distinguish between live and dead cells

The media used for cell culture was Dulbecco's modified Eagle's medium (DMEM; D6429, Sigma Aldrich, South Africa). For tissue culture or storage, tissue freezing medium (Leica Biosystems, United Kingdom), also known as optimal cutting temperature (OCT) medium, and Roswell Park Memorial Institute (RPMI)-1640 medium (Sigma Aldrich, South Africa) were used. Supplements for the media were foetal calf serum (FCS; Thermo Scientific, South Africa), L-glutamine (Sigma Aldrich, South Africa), Penicillin, Streptomycin (Gibco, Invitrogen, UK) and IL-2 (Gentaur, United Kingdom).

The reagents for preparing Luria Broth (LB) medium for bacterial culture were tryptone, yeast extract, NaCl and ampicillin (Sigma Aldrich, South Africa). Either Dulbecco's PBS (Sigma Aldrich, South Africa) or 1X PBS solution (Thermo Scientific, South Africa) were used for washes and dilutions.

Other reagents used for western blot analysis, including Dodecyl sodium sulfate (SDS), bromophenol blue, ammonium persulfate (APS), glycerol, methanol and β-mercaptoethanol were purchased from Sigma Aldrich, South Africa. N,N,N′,N′-tetramethylethylene-diamine (TEMED) and acrylamide were obtained from Bio-Rad.

For plasmid preparations, the pcDNA-hGR plasmid, which is a pcDNA3 vector containing full-length human GR, was a gift from D. W. Ray, University of Manchester, UK (Ray et al., 1999) , and the pMT-hPRB plasmid, which is a pMT vector consisting of the full-length human PR-B was a gift from S. Okret, Karolinska Institute, Sweden (Cairns et al., 1993).

2.3. Mammalian cell culture

COS1 cells (America Type Culture Collection (ATCC), USA) isolated from the kidney of an African green monkey were cultured in Full DMEM, which is DMEM solution containing 10% (v/v) FCS, 2 mM L-glutamine, 100 IU/mL Penicillin and 100 mg/mL Streptomycin. The cells were maintained in 75 cm^2 flasks (Greiner Bio-one International, Austria) in humidified chambers at 37°C and 5% CO2. The cultured cells were routinely checked for mycoplasma by staining the cells with Hoescht (ThermoFisher, South Africa) as described in **Section 2.10.1**. The stained cells were then visualised under a Nikon Ti-E Inverted Microscope with a Double Port FRET System at the Department of Molecular and Cell Biology, University of Cape Town. Cells that were negatively tested for mycoplasma were used for subsequent experiments.

2.4. Sample collection and storage

Ectocervical tissue samples were obtained from pre-menopausal and HIV-1 negative female donors undergoing hysterectomy for benign reasons with approved consent at the Groote Schuur hospital in Cape Town, South Africa. The tissue sample from one of the patients who was using contraception was harvested 3 days after the last dose (Tissue sample ID: Prog 179). Blood samples of the tissue donors were tested for endogenous luteinising hormone (LH), follicle-stimulating hormone (FSH), estrogen (E_2) and progesterone by the National Health Laboratory Services (NHLS, Groote Schuur Hospital, South Africa). Tissue samples were washed with Dulbecco's PBS followed by RMPI-1640 medium supplemented with 10% (v/v) charcoal stripped-FCS (cs-FCS), 2 mM L-glutamine, 100 IU/mL Penicillin and 100 μg/mL

Streptomycin. Harvested tissues were flash frozen in OCT and were stored at -80°C in the BSL II+ facility at the Department of Molecular and Cell Biology, University of Cape Town.

Blood bank buffy coats from female donors aged 16-40 years old were collected at the WCBS, and PBMCs were isolated on the same day of collection as described in **Section 2.5**.

2.5. PBMC isolation

PBMCs were isolated according to procedures previously described (Tomasicchio et al., 2013). Briefly, pre-warmed 15 ml Histopaque (Sigma Aldrich, South Africa) was added in Leucosep tubes (Greiner, Cape Town) and the tubes were centrifuged in a swing-bucket centrifuge (Heraeus Megafuge 40 centrifuge; Thermo Scientific, South Africa) at 2500 revolutions per minute (rpm) for 1 minute (min). Blood was diluted by adding 20 mL blood to 10 mL of RMPI-1640 medium and 10 mL of Dulbecco's PBS. The diluted blood was added to the Histopaque-containing Leucosep tubes and centrifuged at 2500 rpm for 15 mins with brakes off. Following centrifugation, the white buffy PBMC layer was harvested, transferred to a clean 50 mL tube and washed by adding 40 mL PBS Wash solution (Dulbecco's PBS supplemented with 1% (v/v) cs-FCS) and centrifuged at 1200 rpm for 5 mins. The supernatant was discarded, the cell pellet resuspended in dead volume, and 40 mL Full RMPI medium (RPMI medium containing 10% (v/v) cs-FCS, 2 mM L-glutamine, 100 IU/mL Penicillin, 100 μg/mL Streptomycin, 30 U/mL IL-2) was added. The PBMCs were incubated overnight at 37°C and used the following day for staining by flow cytometry.

2.6. Plasmid purification

Glycerol stocks of pcDNA-hGR and pMT-hPRB were inoculated in 5 mL LB. LB was prepared using 1% (w/v) tryptone, 0.5% (w/v) yeast extract, 0.5% (w/v) NaCl and was supplemented with 100 µg/mL ampicillin. The cells were incubated for 8 hours (hrs) at 37°C with shaking, and 500 µL of this culture was inoculated in 200 mL LB containing 100 µg/mL ampicillin. The cultures were incubated overnight for 16 hrs at 37°C with shaking. Following incubation, plasmid DNA was purified using the Nucleobond Xtra Midi kit for transfection-grade plasmid DNA (Thermo Scientific, USA) as per the manufacturer's instructions.

2.7. Restriction enzyme digestion and agarose gel electrophoresis

The integrity and identity of the plasmids was confirmed by restriction enzyme digestion. The digestion reaction was carried out according to the manufacturer's instructions by incubating 300 ng DNA with 1 unit (U)/µl restriction enzyme (Fermentas, Thermo Scientific, USA) or an equivalent volume of water for undigested control in 1X FastDigest universal buffer for 10 mins at 37°C.

Digested and undigested DNA samples were separated by electrophoresis on a 0.8% (w/v) agarose gel made in 1 X Tris-Acetate-EDTA buffer containing 10 µg/mL ethidium bromide (Sigma Aldrich, South Africa). The gel was viewed under ultraviolet light using a Syngene, G:Box (Vacutec, England) to confirm the identity of plasmids by their digestion patterns.

2.8. Overexpression of GR and PR by transfection

Constructs of human SR were transfected in COS1 cells using XtremeGENE-9 transfection reagent (Roche Applied Science, South Africa) according to the manufacturer's instructions. For immunofluorescence staining, 1.0 x 10^4 COS1 cells were seeded on coverslips in a 6-well plate, allowed to grow for 48 hrs, and transfected with 300 ng of DNA. For western blot analysis, 1.5 x 10^5 COS1 cells were seeded in a 12-well plate and transfected with 500 ng of DNA, while for flow cytometry, 1.5 x 10^6 cells COS1 cells were seeded in a 10 cm dish and transfected with 5µg of DNA. The transfection mix containing DNA was added dropwise to COS1 cells. For mock transfection, no DNA was added to the transfection mix. The cells were incubated for 24 hrs at 37 °C and 5% CO2.

2.9. Western blot analysis

Western blot analysis was performed according to the procedures previously described (Sambrook et al., 1989). Following transfection, the cells were washed with 1X PBS and lysed by adding 50µl of 5X SDS sample buffer (62.5 mM Tris-HCl, pH 6.8, 25% glycerol, 2% SDS, 0.01% bromophenol blue and 5% β-mercaptoethanol). The cell lysates were harvested, and equal volumes of 10 µL of cell lysates were loaded on SDS-polyacrylamide gels. The protein samples were stacked on a 4% SDS-polyacrylamide gel (30% acrylamide, 0.5 mM Tris-HCl pH 6.8, 10% SDS, TEMED, 10% APS) and were separated on an 8 % SDS-polyacrylamide gel (30% acrylamide, 1.5 mM Tris-HCl pH 8.8, 10% SDS, TEMED, 10% APS). The gels were run at 70 V for 30 mins (for stacking) and at 120 V for 1 hr (for separation) in 1X SDS running buffer (25 mM TRIS-HCl, 250 mM glycine, and 0.1% (v/v) SDS pH 8.4) to separate the

proteins. The samples were then transferred onto a Hybond-ECL nitrocellulose membrane (Amersham, South Africa) at 180 mA in ice-cold 1X transfer buffer (25 mM TRIS, 200 mM glycine, 20% (v/v) methanol) for 1 hr using the Mini Protean III blotting system (Bio-Rad, USA). After protein transfer, the membranes were blocked with 4% ECL blocking reagent, that is, 4% (w/v) ECL Advance blocking powder (Amersham, South Africa) made in 1X TRIS-buffered saline (50 mM TRIS, 150 mM NaCl, pH 7.6; TBS) containing 0.1% (v/v) Tween (TBS-Tween; TBST). The membranes were subsequently incubated, shaking overnight at 4°C with primary antibodies. Primary antibodies were made in 4% ECL-TBST using appropriate dilutions (**Table 2.1**). The following day, the membranes were washed once for 10 mins and twice for 5 mins with 1X TBST. The membranes were then incubated with anti-mouse HRP-linked secondary antibodies (sc-516102; Santa Cruz Biotechnology, USA) at appropriate dilutions (**Table 2.1**) prepared in 5% (w/v) skim milk powder in 1X TBST with shaking for 1 hr at RT. The washes were repeated as described previously with 1X TBST, and the membranes were incubated for 1 min in ECL-chemiluminescent western blotting substrate (Amersham, South Africa). The membranes were then exposed to Amersham HyperfilmTM MP higher-performance autoradiography film (Amersham, South Africa), and films were incubated in a development buffer (Bio-Rad, USA) to visualise the protein bands. The films were rinsed with water, fixed with fixing buffer (Bio-Rad, USA) and were allowed to dry.

2.10. Immunofluorescent microscopy

2.10.1. Staining of COS1 cells

Following transfection, the cells seeded on coverslips were washed twice with 2 mL ice-cold 1X PBS solution, and 2 mL ice-cold methanol was added to fix the cells. The cells were incubated for 10 mins at -20°C, methanol was aspirated, and the cells were washed with 1X PBS solution. The cells were then blocked with 5% Bovine Serum Albumin (BSA) (Sigma Aldrich, South Africa) for 30 mins at RT before the coverslips were transferred to a clean 6-well plate. The cells were incubated with primary antibodies made up in 5% BSA at their appropriate dilutions (**Table 2.2**) in a humidified chamber for 1 hr at RT. Following incubation, the primary antibodies were discarded, and the cells were washed thrice with 2 mL 1% BSA for 5 mins each. Fluorescently labelled secondary antibodies were prepared in 5% BSA at their appropriate dilutions (**Table 2.2**) and added to the cells. The cells were incubated in the dark at RT for 1 hr and washed afterwards thrice with 1% BSA. Thereafter, the cells were incubated with 1 µg/mL Hoescht for 5 mins at RT in the dark to stain cell nuclei and washed once with 1X PBS. The coverslips containing the cells were then removed and mounted on microscope slides with 30 µL Mowiol (Merck, South Africa) containing antifade. The slides were allowed to dry in the dark overnight at RT before being stored at 4°C in the dark until used for microscopy.

2.10.2. Staining of ectocervical tissue explants

Frozen ectocervical tissue samples in OCT medium were sectioned at 8 µm using a Leica Cryotome cryostat (Leica Biosystems, Germany. The tissue sections were mounted onto SuperFrost Plus slides (ThermoFisher Scientific, USA) by inverting and placing the slides onto the tissue slices. The tissue sections were fixed with 2% Formaldehyde diluted in 1X PBS solution for 15 mins at RT, washed twice with ice-cold 1X PBS solution for 5 mins and

permeabilised for 10 mins with 1X PBS solution containing 0.25% Triton-X-100 (Sigma Aldrich, South Africa). All subsequent washes were done by shaking the slides gently with 1X PBS solution three times for 5 mins. Following permeabilization, tissue sections were washed and blocked with 1% BSA made in PBS containing 1% Tween-20 (Sigma Aldrich, United Kingdom) (PBS-T) for 30 mins at RT. Primary and secondary antibodies were made in 1% BSA in PBS-T at their respective dilutions (**Table 2.2**). After blocking, the tissue sections were incubated overnight in the dark with appropriate primary antibodies or with 1% BSA in PBS-T for the controls at 4°C in a humidified incubation chamber to avoid evaporation of antibodies. Thereafter, the sections were washed, incubated with fluorescently labelled secondary antibodies for 1 hr in the dark and washed following incubation. For double staining, the tissue sections were blocked again and stained with primary and secondary antibodies, as described above. After the washes, the tissue sections were incubated with 1 μg/mL Hoescht for 5 mins at RT in the dark to stain cell nuclei. The slides containing the tissue sections were rinsed with 1X PBS and coverslips were mounted on the slides with 30 μL Mowiol. The prepared slides were allowed to dry overnight at RT in the dark before being stored at 4°C in the dark until further use.

2.10.3. Confocal microscope imaging and image analysis

The stained tissue sections were viewed either under the Carl Zeiss 880 LSM confocal microscope with Fast Airyscan technology at the Confocal and Light Microscope Imaging Facility, Department of Human Biology, University of Cape Town (tissue sample IDs PROG 173 and PROG 175) or under ZEISS LSM780 confocal microscope at the Department of Physiological Sciences, Stellenbosch University (tissue sample ID PROG 179).

The slides were first viewed with 20X magnification to obtain a greater field of view and locate the epithelial and stromal tissues. Three regions in the epithelium and three regions in the stroma were chosen at random for the visualisation of stained cells at higher magnification (63X). Z-stack images were captured at 63X magnification and were converted to maximum intensity projection (MIP) 2D images. The images were analysed on the Carl ZEISS ZEN lite software (blue and black editions) version 2009, where the mean fluorescence intensity (MFI) in ectocervical cells was determined. Cells were selected manually on the images and the MFI was generated by the software. The steps for determining MFI in the cells are described in detail in **Section 3.1.4**.

2.11. Flow cytometry

2.11.1. Staining of COS1 cells

For the cross-reactivity experiment, transfected COS1 cells, as described earlier, were lifted from the transfection dish using Accutase buffer (Sigma-Aldrich, South Africa) according to the manufacturer's instructions and centrifuged at 400 x relative centrifugal force (rcf). The buffer was discarded, and cells were resuspended in PBS Wash. The cells were counted on the TC20 automatic cell counter (Bio-Rad) by staining 10 µl of resuspended cells in PBS Wash with Trypan blue (Sigma Aldrich, South Africa) in a 1:1 ratio. The remaining resuspended cells were centrifuged at 400 rcf to pellet the washed cells. The supernatant was discarded, and depending on the number of cells obtained, the cell pellet was resuspended in the appropriate amount of Full DMEM solution for a concentration of 5 x 10^5 cells per mL. The cells were

seeded in Corning Falcon round bottom tubes at 6 x 10^5 cells per tube, and the tubes were centrifuged at 400 rcf. Each transfection group had their own set of controls, which included an unstained control (no Zombie dye, no antibody) and a Zombie-only control (Zombie dye only, no antibody). The Zombie dye stain is used to distinguish between live and dead cells. The Zombie dye staining was performed using Zombie Aqua™ Fixable Viability Kit (Biolegend, USA) by adding 0.5 µL of Zombie Aqua™ made up to 50 µL with 1X PBS to each sample, except for the unstained control, and incubating at 4°C for 15 mins in the dark. The cells were washed by adding 1 mL of PBS Wash and centrifuging at 400 rcf for 5 mins at RT. The supernatant was discarded, and the cells were permeabilised using the Transcription Factor Buffer Set (BD Pharmigen, USA) by incubating the cells in 1 mL 1X Fix/Perm Transcription Factor Buffer (4X Fix/Perm diluted with TF diluent buffer) for 40 mins at 4°C in the dark. The cells were subsequently washed with 1 mL 1X Perm/Wash solution and centrifuged at 400 rcf for 5 mins to pellet the cells. The supernatant was discarded, and the cells were incubated for 45 mins at 4°C in the dark with the monoclonal GR FITC and/or PR eFluor™ 660 antibodies made up to 50 µL in 1X Perm/Wash solution. Following incubation, the cells were washed by adding 1 mL 1X Perm/Wash and centrifuging at 400 rcf for 5 mins. The supernatant was discarded, and another wash was performed by adding 2 mL 1X Perm/Wash and centrifuging at 400 rcf for 5 mins. The supernatant was discarded, and the cells were resuspended in 1X Cell Fix (BD, USA). The samples were then stored overnight at 4°C. On the following day, the cells were acquired on an LSRII flow cytometer (BD, USA) by Dr Michele Tomasicchio, Division of Pulmonology, University of Cape Town.

2.11.2. Staining of PBMCs

2.11.2.1 PBMC counting and Zombie staining

For staining of PBMCs, isolated PBMCs in full RPMI medium were centrifuged at 1200 rpm for 5 mins in a swing bucket-centrifuge. The supernatant was discarded, the PBMC pellet was resuspended in dead volume, and 40 ml PBS Wash was added. The cells were counted following the same procedure as described previously using Trypan blue, and the remaining cells in PBS Wash were centrifuged at 1200 rpm for 5 mins. The supernatant was discarded, the cells were resuspended in dead volume, and an appropriate volume of full RPMI medium was added to obtain a concentration of 5 x 10^5 cells per mL. Thereafter, 1 x 10^6 cells were aliquoted in Corning Falcon round bottom tubes and centrifuged at 1200 rpm to pellet the cells. The cells were washed by adding 1 mL of PBS Wash to each tube and centrifuging at 1200 rpm, followed by staining for Zombie with the Zombie Aqua™ Fixable Viability Kit for 15 mins at 4°C in the dark as described in **Section 2.10.1**.

2.11.2.2 Staining of extracellular markers

Cells were washed with PBS Wash solution and stained for extracellular markers with the following conjugated antibodies: mouse anti-CD3, mouse anti-CD4, mouse anti-CD8 and mouse anti-CD14 with their respective titres (**Table 2.3**) made up to 50 µL with Brilliant Stain buffer (BD, USA) for 30 mins at 4°C in the dark. The cells were washed by adding 1 mL PBS Wash and centrifuging at 1200 rpm for 5 mins at RT.

2.11.2.3 PBMC permeabilization and staining of intracellular receptors (GR and PR)

The supernatant was discarded, and the cells were permeabilised by incubation in 1 mL 1X Fix/Perm Transcription Factor Buffer for 40 mins at 4°C in the dark. The cells were subsequently washed with 1 mL 1X Perm/Wash solution and centrifuged at 1200 rpm for 5 mins. The supernatant was discarded and the cells were incubated for 45 mins at 4°C in the dark with the monoclonal GR FITC and PR eFluor™ 660 antibodies made up to 50 μL in 1X Perm/Wash solution (**Table 2.3**).

A different antibody mixture for the detection of GR and PR by flow cytometry was previously used, which consisted of primary antibodies for GR and PR raised in mice that were not conjugated to fluorophores. Anti-mouse secondary antibodies conjugated to fluorophores were therefore pre-incubated with the unconjugated mouse primary antibodies. The antibody mixtures for intracellular staining of GR and PR were prepared by incubating mouse anti-GR with anti-mouse AF488 and mouse anti-PR with anti-mouse AF647 for 1 hr at 4°C in the dark. The ratio of primary antibody to secondary antibody used was 5:1. Aliquots of 5 μL and 2 μL of GR and PR antibody mixes, respectively, were added to PMBCs for staining following permeabilization as described above.

For this experiment, a set of fluorescence minus one (FMO) controls were included and are described in **Section 2.11.3**. Following incubation, the cells were washed by adding 1 mL 1X Perm/Wash and centrifuging at 1200 rpm for 5 mins.

2.11.2.4 PBMC washing and fixing

The supernatant was discarded, and another wash was performed by adding 2 mL 1X Perm/Wash and centrifuging at 1200 rpm for 5 mins. The supernatant was discarded, and the cells were resuspended in 1X Cell Fix. The samples were then stored overnight at 4°C and then acquired on an LSRII flow cytometer the following day by Dr Michele Tomasicchio at the Division of Pulmonology, University of Cape Town.

2.11.3. Compensation and FMO controls

Compensation controls were included for each antibody for all flow cytometry experiments. The ABC Total Antibody Compensation Bead Kit (ThermoFisher Scientific, USA) was used. Two drops of negative compensation beads, 2 drops of positive compensation beads and 2 µL of antibody were added. The samples were incubated for 20 mins in the dark at RT and 1 mL PBS Wash was added. The samples were centrifuged at 250 x g for 5 mins, supernatants were discarded, and the beads were resuspended in 500 µL Dulbecco's PBS. All the samples were then stored overnight at 4°C. On the following day, the beads were acquired on the LSRII flow cytometer.

To identify negative and positive populations used to set the gates of specific cells or markers during FACS analysis, FMO controls were included. For FMO controls the cells were seeded and stained as described in **Section 2.10.2**, but one specific antibody was excluded during antibody staining. For example, in the CD3 FMO, the cells were stained with Zombie dye and all the antibodies except the anti-CD3 antibody. Similar FMO controls were made for all the

antibodies. Other controls included an unstained control where Zombie dye and antibodies were not added, as well as a Zombie-only control where Zombie dye was added, but antibodies were not added. For the unconjugated antibody mixture, a control was included where the primary antibodies for GR and PR were excluded, but the secondary antibodies were added to the antibody mixture. For the conjugated antibodies, 'no GR and PR control' was also included, where antibodies for GR and PR were not added, but Zombie dye and antibodies for extracellular markers were added. These staining controls were intended to act as negative controls for GR and PR, where it was expected to obtain negative signals for GR and PR in the immune cell subsets.

2.11.4. Flow cytometry data analysis and statistics

Flow cytometry data was analysed on FlowJo software version 10.9.0 (Treestar Inc., Ashland, Ore). The cells were gated using the unstained, Zombie-only and FMO controls. The frequency of $CD3^+$, $CD4^+$, $CD8^+$ and $CD14^+$ cells positive for GR and PR were determined. The expression density of GR and PR in each immune cell subset was also compared by examining the MFI of the GR and PR antibodies.

The cellular frequencies and MFI values for each immune cell type from the 6 donors (n=6) were plotted. Statistical analysis was performed using GraphPad Prism software Version 10.1.0 (264). The flow cytometry data was analysed using one-way ANOVA for multiple comparisons.

Chapter 3: Results and discussion: GR and PR expression in the FGT

3.1. Results

3.1.1. Cervical explant donor information

This section aims to investigate GR and PR protein expression in FGT cells, including immune cells. Ectocervical tissue explants were obtained from three premenopausal women undergoing hysterectomy for benign reasons. One donor was not on any HC method (PROG 173), the HC use status was unknown for one donor (PROG 175), while another donor was using the Mirena contraceptive (PROG 179). Endogenous LH, FSH, E_2, and progesterone levels are tabulated (**Table 3.1**), and the stages of their respective menstrual cycles are determined according to the NHLS guidelines (**Table 6.1, Appendix 6.1**) (Kratz et al., 2004).

Table 3.1: Serum concentrations of endogenous hormones, phase of menstrual cycle and type of HC use of tissue donors.

Patient number	Hormone concentrations				Phase of menstrual cycle	Type of HC use
	LH*[1]	FSH*[2]	E_2*[3]	Progesterone*[4]		
PROG 173	4.4	8.1	303	<0.2	Follicular	None
PROG 175	3.8	2.7	447	26.5	Luteal	N/A
PROG 179	1.3	5.3	128	<0.2	Luteal	Mirena

*[1] IU/L; *[2] IU/L; *[3] pmol/L; *[4] nmol/L; N/A = not available

3.1.2. Unconjugated anti-GR and anti-PR antibodies do not cross-react with PR and GR, respectively

Unconjugated primary antibodies against GR and PR were tested for cross-reactivity to determine whether the GR antibody binds to the PR and the PR antibody binds to the GR. COS1 cells were used as a model to assess the cross-reactivity of antibodies by overexpressing GR or PR, respectively. This cell line does not express endogenous PR and is easy to transfect. GR and PR expression were assessed by probing with anti-GR and anti-PR antibodies and confirmed by western blot analysis. With the mouse anti-GR antibody, a band corresponding to ~ 95 kDa, corresponding with the molecular weight of GR, was obtained (**Figure 3.1A, lane 3**). Endogenous expression of GR in untransfected and mock-transfected samples was not observed (**Figure 3.1A, lanes 1 and 2**). No signal was detected in COS1 cells transfected with PR (**Figure 3.1A, lane 4**). Similarly, the mouse anti-PR antibody did not bind to overexpressed GR, as a signal was not obtained in cells transfected with GR when the mouse anti-PR antibody was used for immunoblotting (**Figure 3.1B, lane 3**). Two bands at ~ 96 kDa and ~ 116 kDa corresponding to the molecular weights of PR-A and PR-B, respectively, were detected in protein lysates of COS1 cells transfected with PR (**Figure 3.1B, lane 4**). Endogenous expression of PR was not observed in untransfected and mock-transfected COS1 cells (**Figure 3.1B, lanes 1 and 2**). These results demonstrate that the GR and PR primary antibodies did not cross-react.

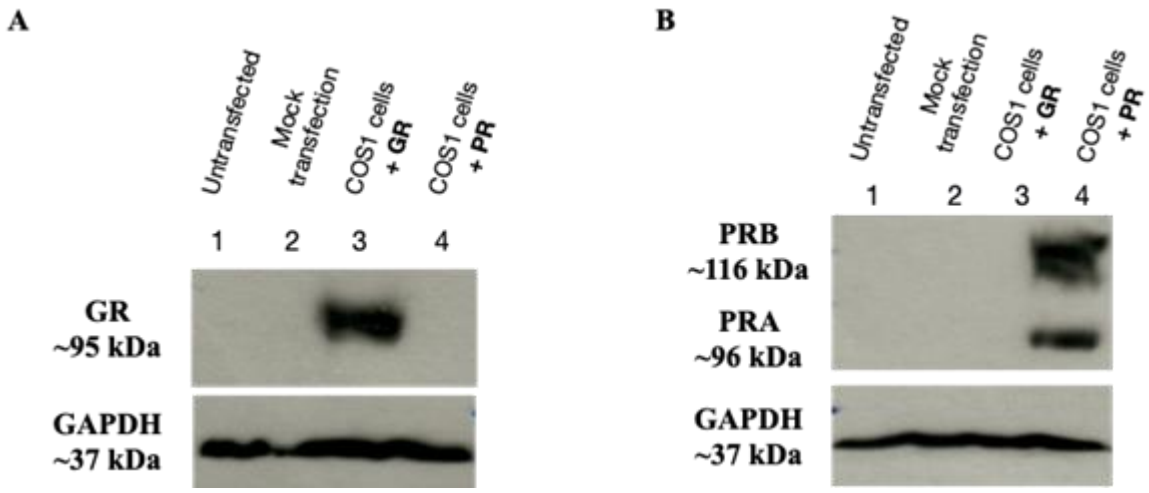

Figure 3.1: Unconjugated primary antibodies of GR and PR do not cross-react to their non-corresponding proteins as examined by western blot analysis. COS1 cells were transfected with 500 ng pcDNA3-hGR (lane 3) or pMT-PRB (lane 4). An untransfected control (lane 1) and a mock-transfected control (lane 2) were included. Twenty-four hrs later, the cells were harvested, equal amounts of protein were separated on a 0.8% SDS-PAGE gel, transferred onto nitrocellulose membranes, and the membranes were probed with either mouse anti-GR (**A**) or mouse anti-PR (**B**) to test for cross-reactivity of the antibodies.

While western blot analysis showed that the GR and PR antibodies did not cross-react under denaturing conditions, it is possible that cross-reactivity could occur under non-denaturing conditions. Therefore, cross-reactivity was investigated by immunofluorescence. Following overexpression of exogenous GR and PR in COS1 cells, the cells were stained for either GR or PR by immunofluorescence and visualised on a confocal microscope. When the cells were stained for GR, faint green fluorescence was observed in some but not all nuclei of mock-transfected COS1 cells (**Figure 3.2A, row 1**), indicating that COS1 cells express low levels of GR protein, consistent with the literature (Yudt and Cidlowski, 2001). In GR-transfected COS1 cells, the fluorescence of GR staining was at a higher intensity compared to mock-transfected COS1 cells, thus confirming the successful transfection and expression of GR. GR fluorescence

staining was also visible in the cytoplasm adjacent to the nuclei of GR-transfected COS1 cells compared to mock-transfected COS1 cells (**Figure 3.2A, row 2**). In the PR-transfected COS1 cells, faint fluorescence for GR staining signal was observed (**Figure 3.2A, row 3**). The fluorescence of GR staining was of the same intensity in mock- and PR-transfected cells, indicating that the faint signal in the PR-transfected COS1 cells was due to the low amount of endogenous GR protein in COS1 cells (**Figure 3.2A, row 1 and row 3**). This suggests that the GR primary antibody does not cross-react with overexpressed PR protein.

Fluorescence staining of PR was not apparent in mock-transfected COS1 cells, indicating that COS1 cells do not express endogenous PR. (**Figure 3.2B, row 1**). Similarly, in GR-transfected COS1 cells, PR fluorescence staining was not observed (**Figure 3.2B, row 2**). This suggests that the mouse anti-PR antibody did not cross-react with overexpressed GR proteins in GR-transfected COS1 cells in western blots. Moreover, fluorescence staining of PR was observed in COS1 cells transfected with PR, thus confirming successful transfection and PR expression. PR fluorescence staining was also seen in the cytoplasm of PR-transfected COS1 cells (**Figure 3.2B, row 3**).

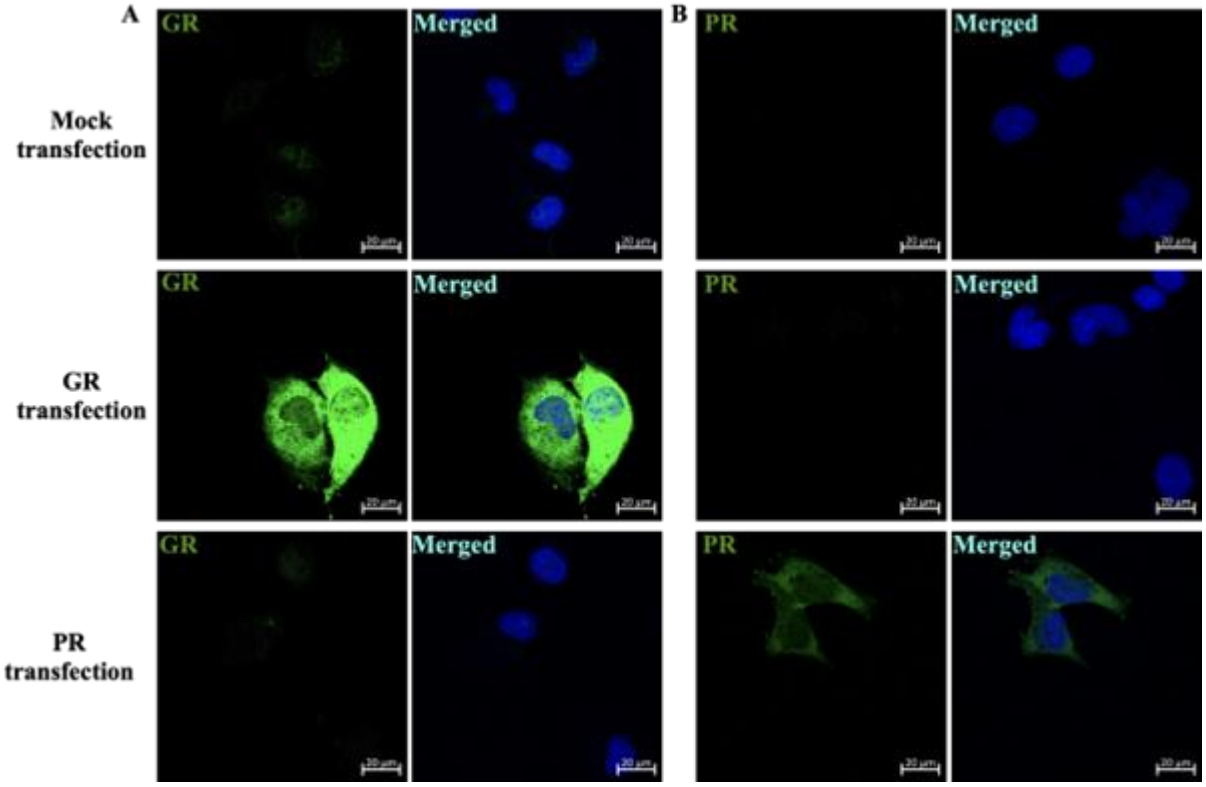

Figure 3.2: Immunofluorescent staining of transfected COS1 cells demonstrates that unconjugated primary antibodies of GR and PR do not cross-react to PR and GR, respectively. GR and PR were overexpressed in COS1 cells and the transfected cells were stained with anti-GR or anti-PR antibodies. A mock-transfection control was included to visualise endogenous expression of GR or PR proteins. The cells were visualised on a confocal microscope on the AF488 channel (panel 1) to detect GR or PR and the AF488 channel was merged with the DAPI channel (panel 2) to confirm the presence of cell nuclei. (**A**) Confocal images of COS1 cells stained with mouse anti-GR antibody following exogenous expression of GR or PR. (**B**) Confocal images of COS1 cells stained with mouse anti-PR following exogenous expression of GR or PR.

Altogether, the results from western blot analysis and immunofluorescence staining in GR and PR overexpressed COS1 cells validate that primary antibodies for GR and PR do not cross-

react, thus confirming their suitability for the detection of GR and PR in ectocervical tissue samples by immunofluorescent staining.

3.1.3. In the ectocervix, GR is highly expressed in epithelial cells while PR is primarily expressed in stromal cells

GR and PR expression were characterised by cell type in ectocervical tissue explants by immunofluorescence staining. The ectocervix was observed to comprise two distinct cellular compartments: the epithelium and the stroma (**Figure 3.3A, panel 2**). Epithelial cells were tightly packed and stacked in several layers facing towards the exterior of the FGT, while stromal cells were scattered and located on the interior side of the ectocervix (**Figure 3.3B, panel 2**). Confocal z-stacks images were captured from both the epithelium and the stroma to compare the spatial expression of the two receptors.

GR was observed in most epithelial cells, while, in the stroma, fewer cells were positive for GR (**Figure 3.3A**). Epithelial cells appeared to have a stronger fluorescence signal, indicative of higher GR expression density per cell, compared to the stromal cells (**Figure 3.3B**). In addition, GR seems to be localised to the nuclei of the cells, as the nuclei staining overlaps with GR staining (**Figure 3.3, merged images**).

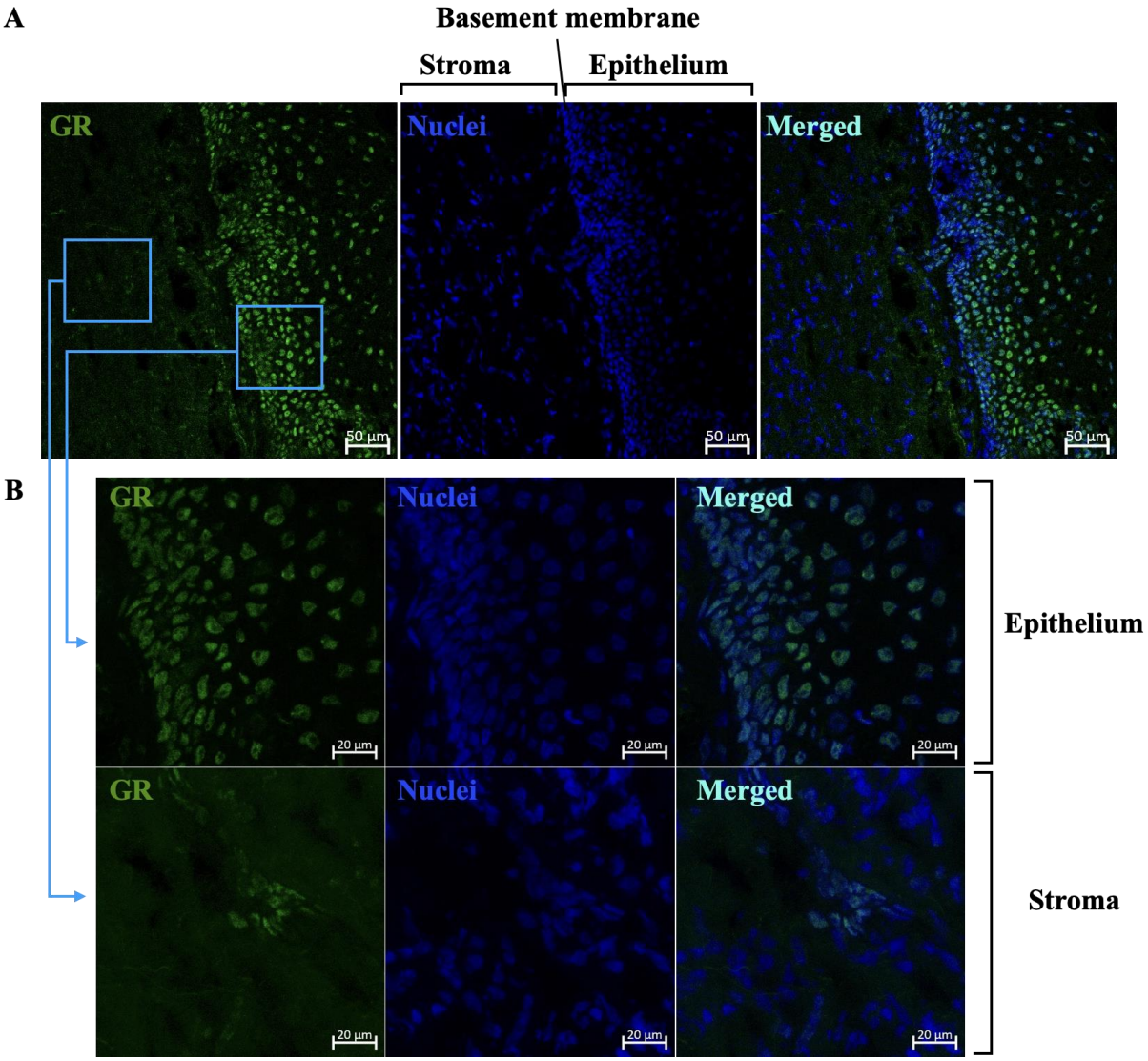

Figure 3.3: GR expression in ectocervical epithelial and stromal cells. Ectocervical tissue sections of 8 µm were stained for immunofluorescence using mouse anti-GR antibody (green fluorescence) and counterstained with Hoescht (blue). (**A**) A snapshot was captured at 20X magnification for examining GR expression across the ectocervical epithelial and stromal layers. (**B**) MIP of z-stacks images taken at 63X magnification comparing GR expression between epithelial and stromal cells. Panel 1: Green fluorescence (GR staining) visualised on the AF488 channel; Panel 2: Nuclei staining (Hoescht) visualised on the DAPI channel; Panel 3: Merged image of both channels. Confocal images of a representative donor (PROG 179) are shown. The blue squares represent the fields of view that were selected for imaging at higher magnification and the corresponding images are indicated by blue arrows.

Fluorescence staining of PR was visible in comparatively fewer cells of the epithelium (**Figure 3.4**). PR was primarily detected in the stroma where fluorescently stained nuclei were apparent in some stromal cells (**Figure 3.5**). PR expression was apparent in stromal regions deeper within the ectocervical tissue (**Figure 3.5**) and fluorescence staining of PR was visible in the nuclei of the ectocervical cells (**Figure 3.4B and 3.5B**).

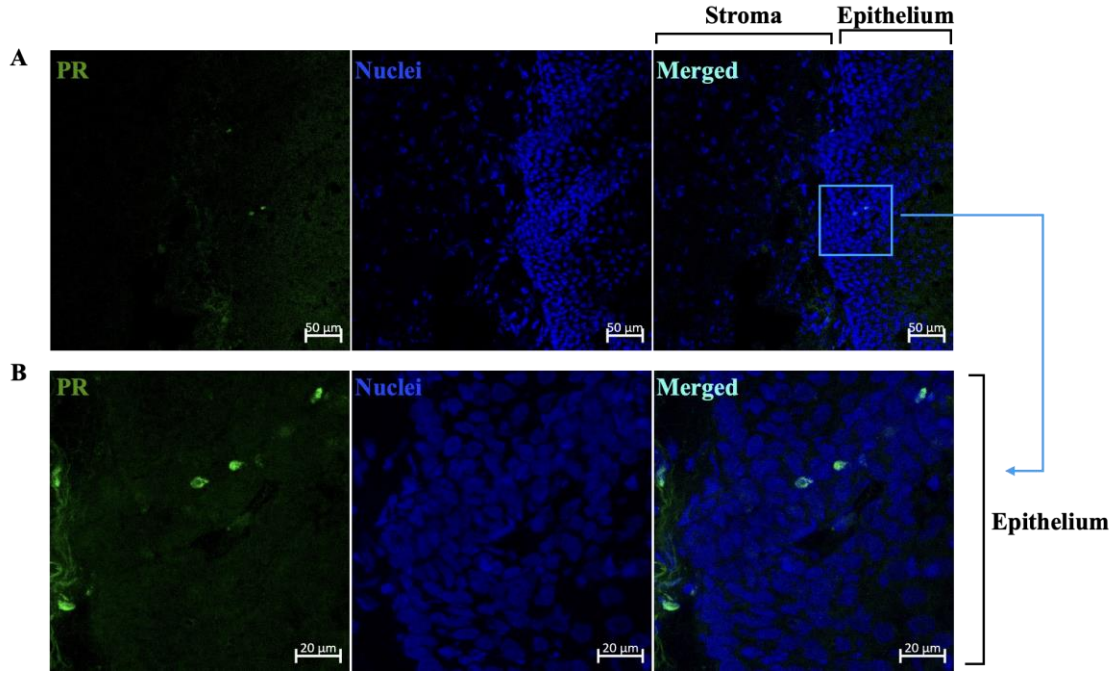

Figure 3.4: PR expression in ectocervical epithelial and stromal tissues. Ectocervical sections of 8 µm were stained for immunofluorescence with mouse anti-PR and anti-mouse AF488 antibodies and were counterstained with Hoescht. The stained sections were eventually imaged by confocal microscopy. (**A**) A snapshot image taken at 20X magnification visualising staining of PR at the epithelial-stromal junction. (**B**) MIP of z-stacks images taken at 63X magnification showing PR staining in epithelial cells. Panel 1: Green fluorescence (PR staining) visualised on the AF488 channel; Panel 2: Nuclei staining (Hoescht) visualised on the DAPI channel; Panel 3: Merged image of both channels. Confocal images of a representative donor (PROG 179) are shown. The blue square represents a field of view that

was selected in the epithelium for imaging at higher magnification and the image is indicated by a blue arrow.

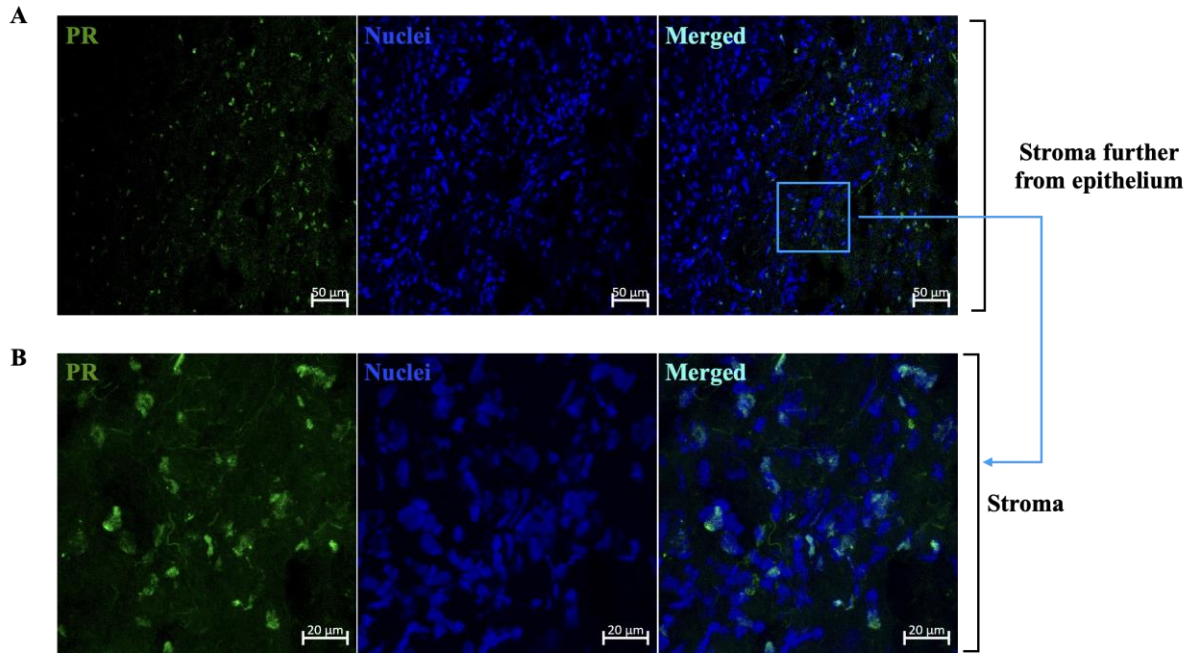

Figure 3.5: PR expression in ectocervical stromal cells. Ectocervical tissue explants were sectioned at 8 µm and stained with anti-PR and anti-mouse AF488. The sections were eventually counterstained with Hoescht and visualised by confocal microscopy. (**A**) A snapshot taken at 20X magnification in a specific region in the stroma distal to the epithelium to visualise fluorescence staining of PR. (**B**) A region from the field of view in (**A**) was focused at 63X magnification showing PR staining in stromal cells. Panel 1: Green fluorescence (PR staining) visualised on the AF488 channel; Panel 2: Hoescht staining (Nuclei staining) visualised on the DAPI channel; Panel 3: Merged image of both channels. The blue square represents a field of view that was selected in the stroma for imaging at higher magnification and the image is indicated by a blue arrow.

Furthermore, in one of the three tissue donors (Prog 173), relatively faint staining of PR was observed in cells of the basal layer of the epithelial cells compared to stromal cells (**Supplementary figure 6.3.1**).

3.1.4. Some ectocervical $CD4^+$ and $CD8^+$ cells express GR, but none expresses PR

GR and PR protein expression was investigated in ectocervical $CD4^+$ and $CD8^+$ immune cells. This was achieved by double-labelling for the extracellular immune markers CD4 and CD8, and the GR and PR. CD4 or CD8 marker staining was visualised in the Cy3 channel, GR or PR staining in the AF488 channel and nuclei (Hoescht) staining in the DAPI channel.

$CD4^+$ and $CD8^+$ cells, as indicated by the red fluorescently labelled cell surface markers, were observed at seemingly random regions throughout the ectocervical tissue, both in the epithelial and stromal layers (**Figures 3.6 - 3.9**). Snapshots were taken at 20X magnification to illustrate the spatial distribution of GR or PR in $CD4^+$ and $CD8^+$ cells in the ectocervical tissue (**Figure 3.6A, Figure 3.7A, Figure 3.8A and Figure 3.9A**). Thereafter, z-stack images were captured at 63X magnification for quantitative analysis (**Figure 3.6B, Figure 3.7B, Figure 3.8B and Figure 3.9B**).

Confocal imaging revealed that ectocervical $CD4^+$ cells express GR, as evident by the presence of green fluorescent staining for GR (**Figure 3.6A**). Moreover, it can be observed that a greater number of $CD4^+$ cells in the epithelium expressed GR compared to stromal $CD4^+$ cells (**Figure 3.6B**). GR also appeared to be expressed in some but not all $CD8^+$ cells of the ectocervix (**Figure 3.7A**). However, there was no visibly discernible difference in GR expression density per cell between the epithelial and stromal layers, as assessed by visual comparison of the intensity of green fluorescent signals in the $CD8^+$ cells (**Figure 3.7B**).

Fluorescent staining of PR was not detected in $CD4^+$ and $CD8^+$ cells at 20X (**Figure 3.8A and Figure 3.9A**) or at 63X (**Figure 3.8B and Figure 3.9B**) magnifications in either the epithelial or stromal regions of the ectocervix.

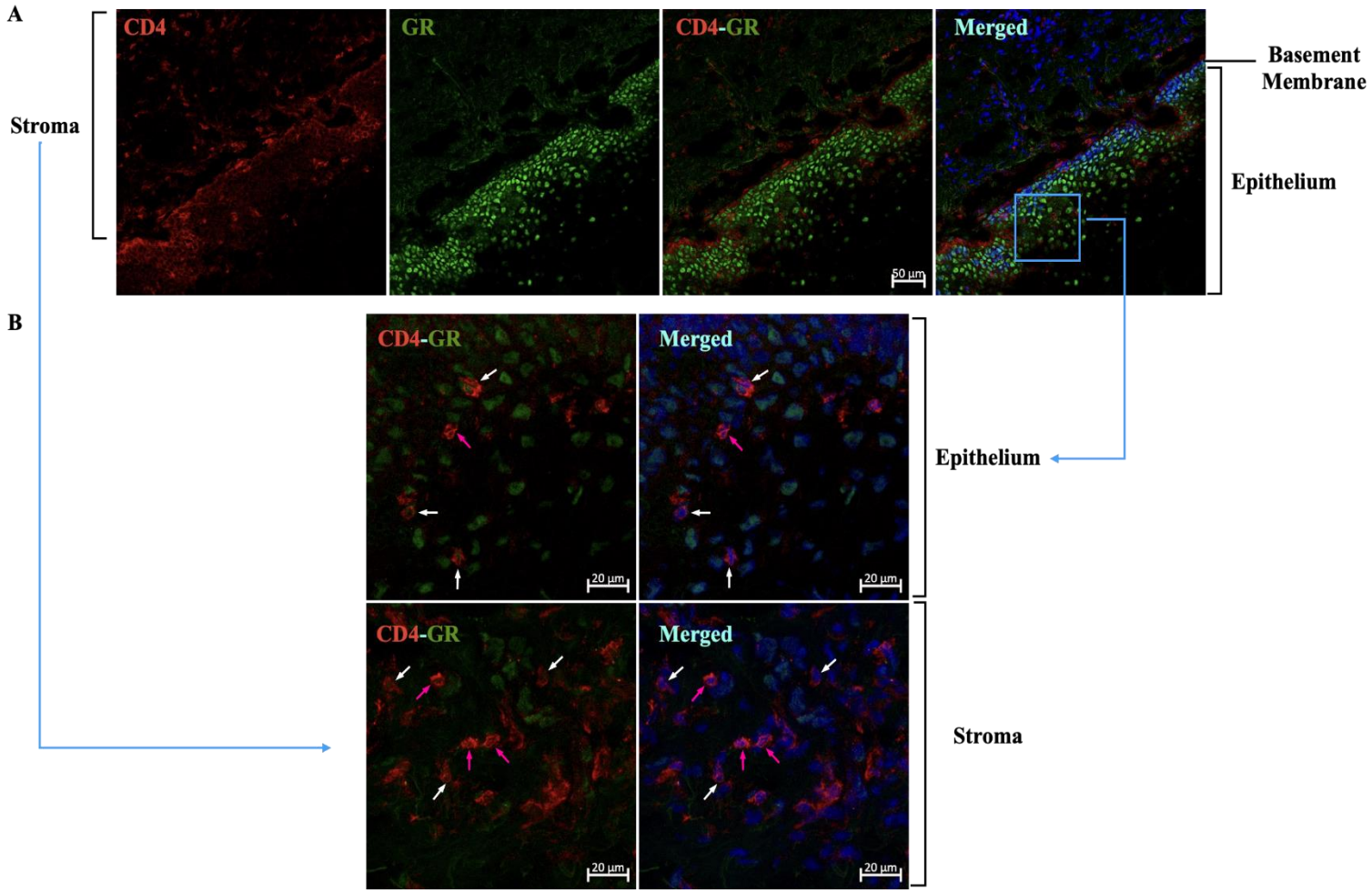

Figure 3.6: Protein expression of GR in ectocervical epithelial and stromal CD4$^+$ cells. Ectocervical tissue sections were stained sequentially by immunofluorescence for CD4 markers and GR. (A) Snapshots were captured at 20X magnification to show CD4 and GR staining across the epithelial and stromal layers. Panel 1: CD4 staining (red fluorescence); Panel 2: GR staining (green fluorescence); Panel 3: Merged image of CD4 and GR staining; Panel 4: Merged image of all channels. (B) Fields of view in epithelial and stromal regions were focused at 63X magnification to examine GR staining in CD4$^+$ cells, z-stacks images were captured and converted to MIP. Panel 1: Merged images of CD4 and GR staining. Panel 2: Merged images of all channels. White arrows demonstrate CD4$^+$ cells with visible green fluorescent staining for GR, whereas pink arrows indicate CD4$^+$ cells without apparent green fluorescent staining for GR. Confocal images of a representative donor (PROG 179) are shown.

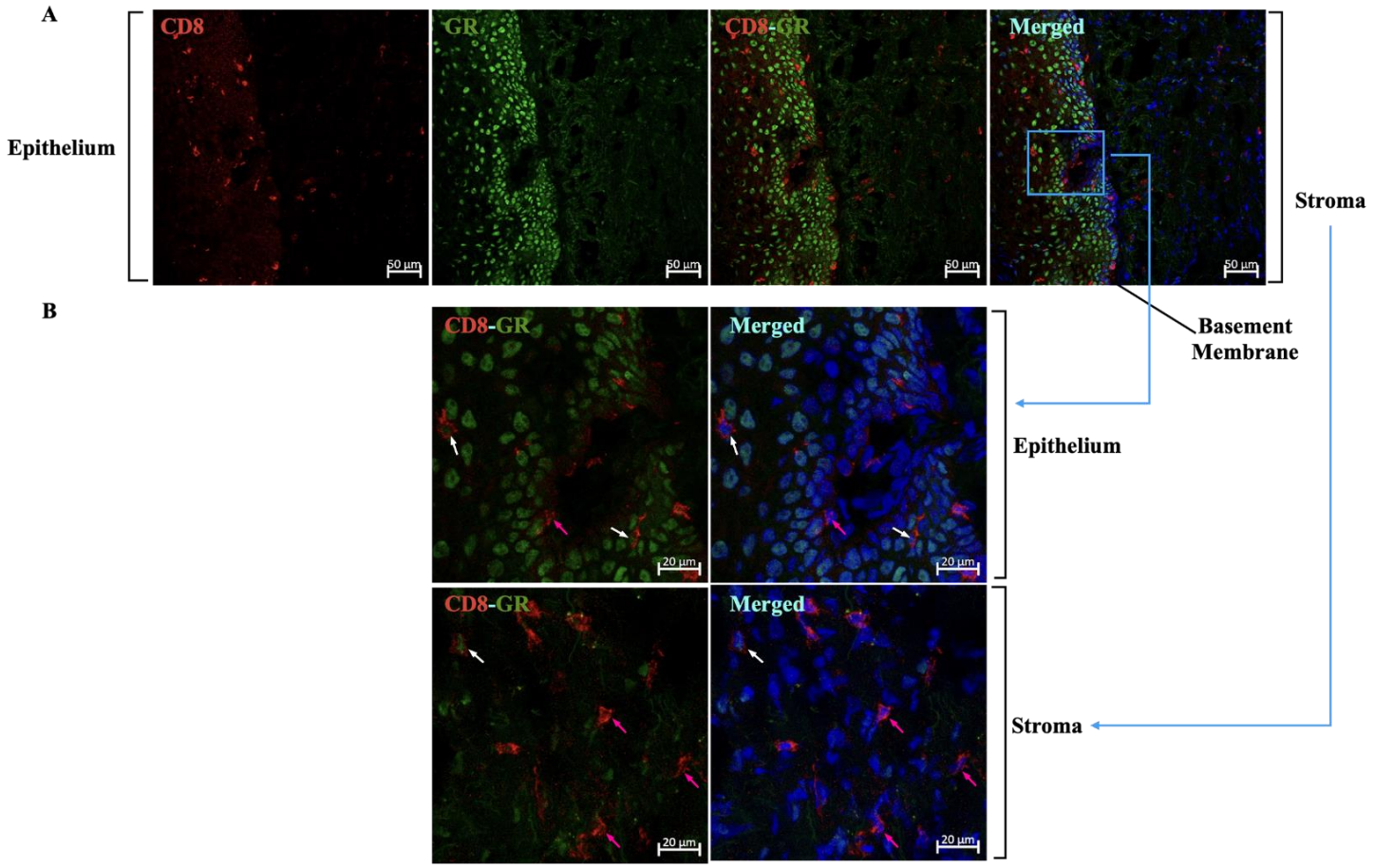

Figure 3.7: Protein expression of GR in ectocervical epithelial and stromal CD8$^+$ cells. Ectocervical tissue sections were stained sequentially by immunofluorescence for CD8 markers and GR. (A) Snapshots were captured at 20X magnification to show CD8 and GR staining across the epithelial and stromal layers. Panel 1: CD8 staining (red fluorescence); Panel 2: GR staining (green fluorescence); Panel 3: Merged image of CD4 and GR staining; Panel 4: Merged image of all channels. (B) Fields of view in epithelial and stromal regions were focused at 63X magnification to examine GR staining in CD8$^+$ cells, z-stacks images were captured and converted to MIP. Panel 1: Merged images of CD8 and GR staining. Panel 2: Merged images of all channels. White arrows demonstrate CD8$^+$ cells with visible green fluorescent staining for GR, whereas pink arrows indicate CD8$^+$ cells without apparent green fluorescent staining for GR. Confocal images of a representative donor (PROG 179) are shown.

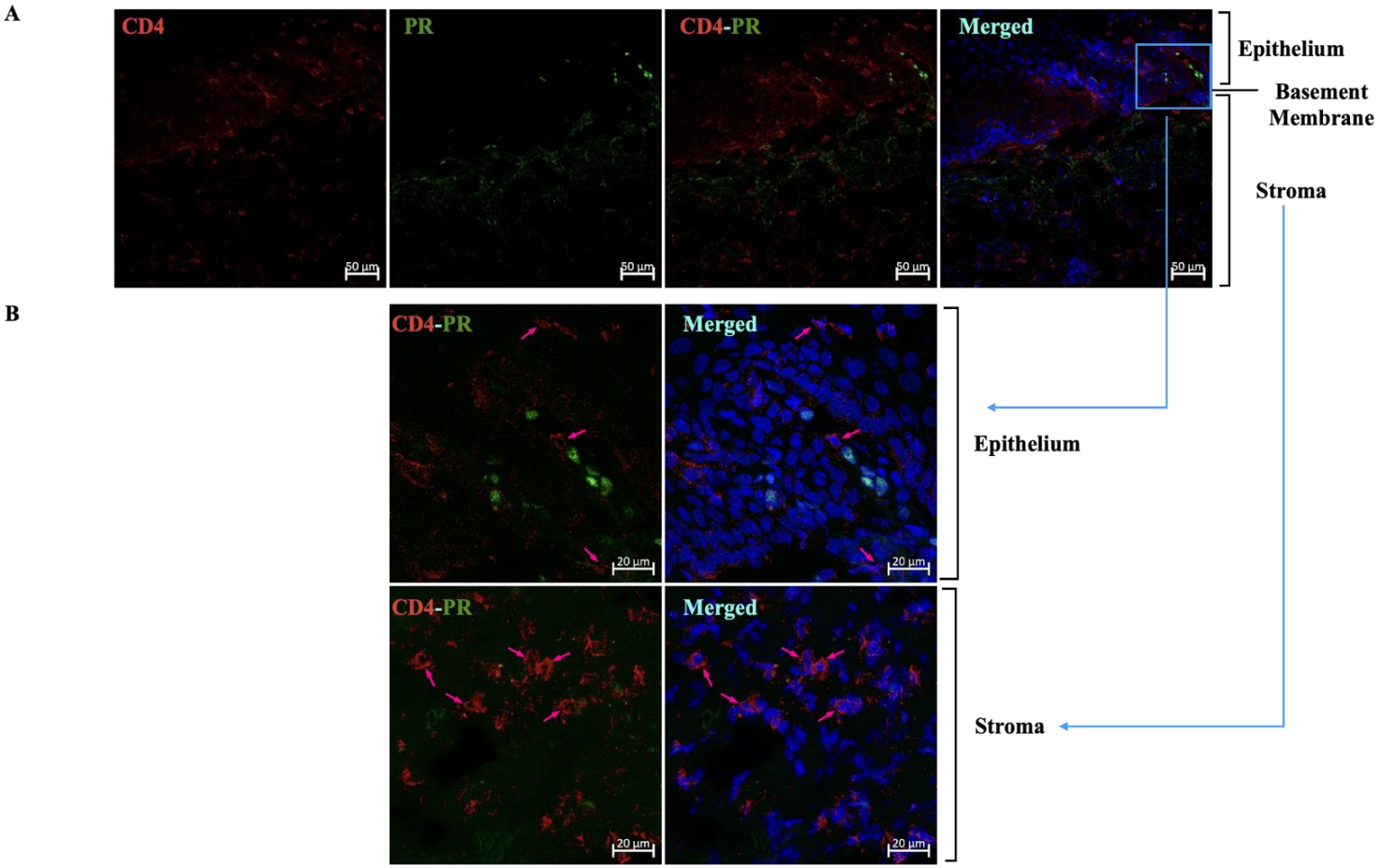

Figure 3.8: Protein expression of PR in ectocervical epithelial and stromal CD4⁺ cells. Ectocervical tissue sections were stained sequentially by immunofluorescence for CD4 markers and PR. (A) Snapshots were captured at 20X magnification to show CD4 and PR staining across the epithelial and stromal layers. Panel 1: CD4 staining (red fluorescence); Panel 2: PR staining (green fluorescence); Panel 3: Merged image of CD4 and PR staining; Panel 4: Merged image of all channels. (B) Fields of view in epithelial and stromal regions were focused at 63X magnification to examine PR staining in $CD4^+$ cells, z-stacks images were captured and converted to MIP. Panel 1: Merged images of CD4 and PR staining. Panel 2: Merged images of all channels. White arrows demonstrate $CD4^+$ cells with visible green fluorescent staining for PR, whereas pink arrows indicate $CD4^+$ cells without apparent green fluorescent staining for PR. Confocal images of a representative donor (PROG 179) are shown.

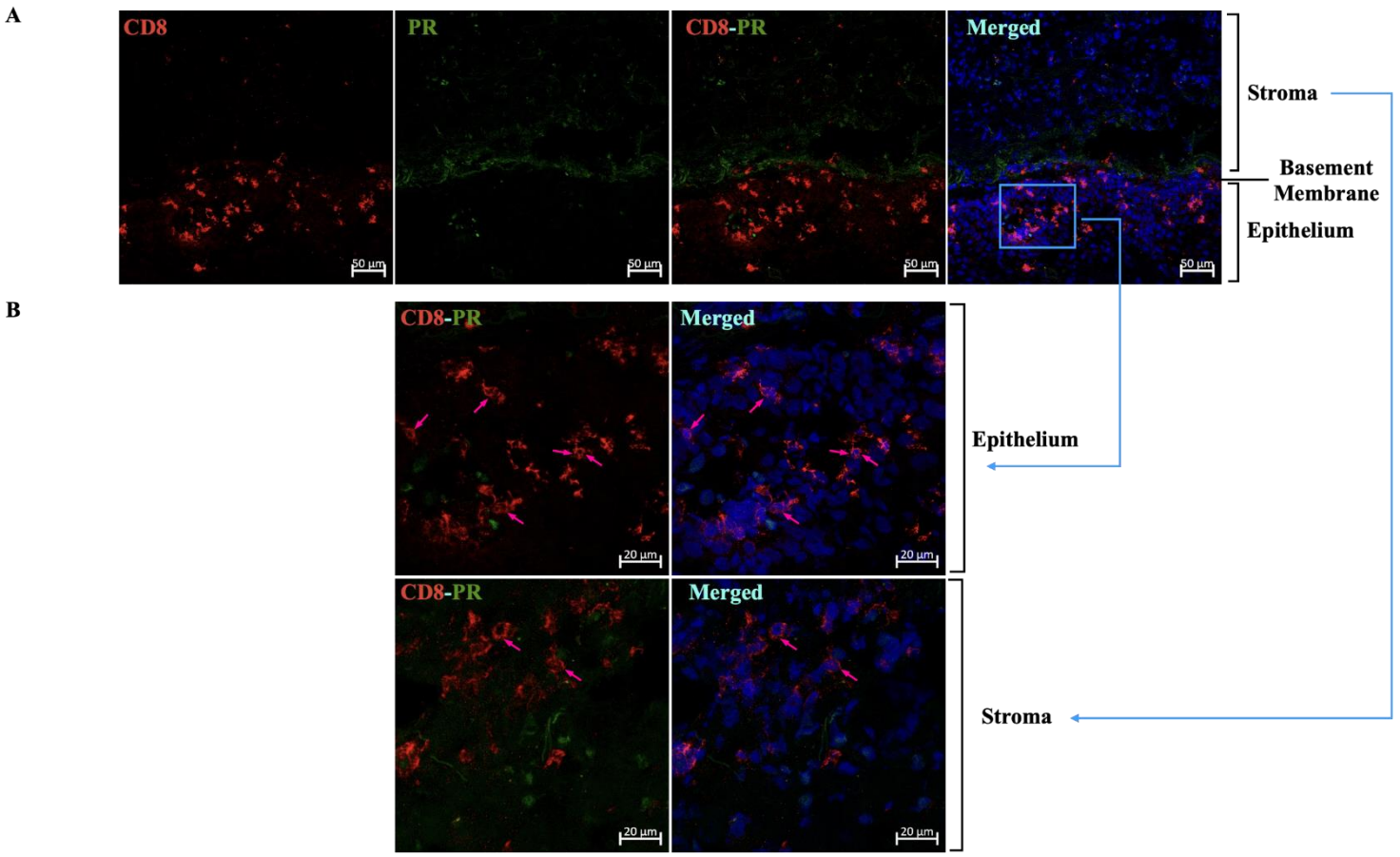

Figure 3.9: Protein expression of PR in ectocervical epithelial and stromal CD8$^+$ cells. Ectocervical tissue sections were stained sequentially by immunofluorescence for CD8 markers and PR. (A) Snapshots were captured at 20X magnification to show CD8 and PR staining across the epithelial and stromal layers. Panel 1: CD8 staining (red fluorescence); Panel 2: PR staining (green fluorescence); Panel 3: Merged image of CD4 and PR staining; Panel 4: Merged image of all channels. (B) Fields of view in epithelial and stromal regions were focused at 63X magnification to examine PR staining in CD8$^+$ cells, z-stacks images were captured and converted to MIP. Panel 1: Merged images of CD8 and PR staining. Panel 2: Merged images of all channels. White arrows demonstrate CD8$^+$ cells with visible green fluorescent staining for PR, whereas pink arrows indicate CD8$^+$ cells without apparent green fluorescent staining for PR. Confocal images of a representative donor (PROG 179) are shown.

For quantitative analysis, the MFI of the GR and PR was measured in $CD4^+$ and $CD8^+$ cells, as well as in the surrounding regions of the cells, which corresponds to background fluorescence. Confocal z-stack images of double-labelled ectocervical tissue sections were converted to MIP images, which were then used to measure the MFI of GR or PR fluorescence in the immune cells of the ectocervix. Cells that were stained for the extracellular markers CD4 or CD8, revealed red fluorescence circles around them, consistent with these markers being present on the cell surface. The cells were drawn around the red fluorescence in the Cy3 channel (**Figure 3.10C**) and the MFI in the AF488 channel (i.e., green fluorescence corresponding to GR or PR staining) (**Figure 3.10D**) of the selected region was generated by the software. For background fluorescence, rectangles were drawn in surrounding regions of the cells, and the MFI in the AF488 channel in the rectangular areas was generated. The Hoescht channel was also used to confirm the presence of nuclei, cells, or background spaces (**Figure 3.10E**). These steps were repeated for all the MIP images captured in three different regions in the epithelium and three different regions in the stroma from the three donors.

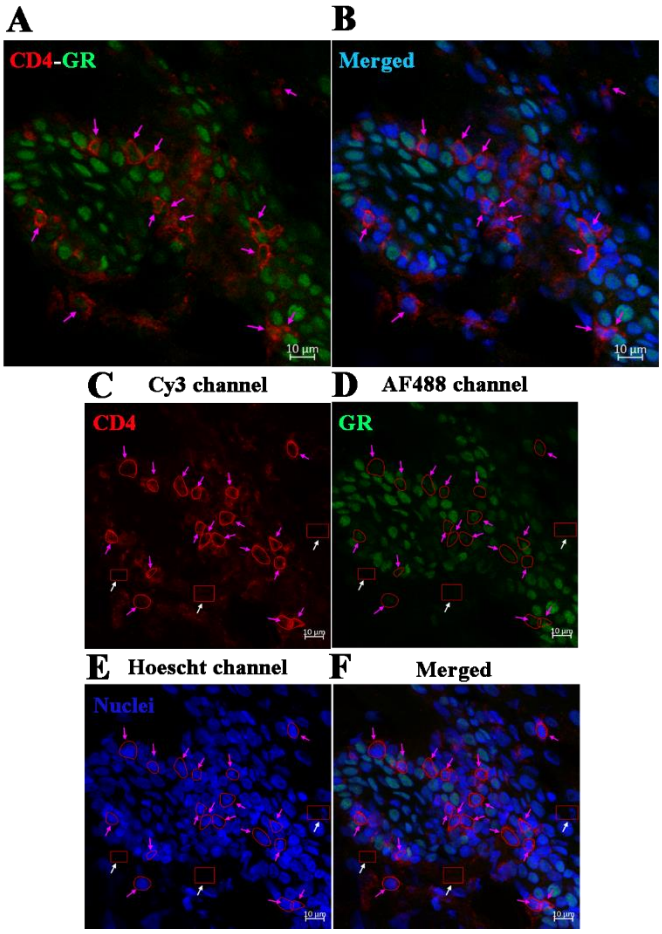

Figure 3.10: Strategy for measuring GR MFI in ectocervical CD4$^+$ cells or MFI of background regions. Z-stack images of double-labelled immunofluorescence staining of CD4 and GR were converted to MIP images. (**A**) Confocal image showing CD4 and GR staining only in the ectocervix. (**B**) Confocal image showing CD4 and GR staining with all the channels merged. (**C**) Visualisation of CD4 staining in the Cy3 channel only for drawing of CD4$^+$ cells. (**D**) Visualisation of GR staining in the AF488 channel only for GR MFI measurement. (**E**) Visualisation of nuclei staining in the DAPI (Hoescht) channel only to confirm the presence of cells/nuclei. (**F**) Merged image of all three channels in (**C**-**E**). The circular drawings represent the selection of CD4$^+$ cells and are indicated by pink arrows, whereas the rectangles represent the selected areas for background fluorescence and are indicated by white arrows.

Thereafter, the GR and PR MFI in $CD4^+$ and $CD8^+$ cells in the ectocervical epithelial and stromal tissue layers of the three tissue donors were plotted. Notably, the GR and PR MFI values for the three donors were not combined, as the stained tissue sections for PROG 173 and PROG 175 were imaged using a different confocal microscope than those for PROG 179.

GR MFI was higher than the background in only some of the ectocervical $CD4^+$ and $CD8^+$ cells (**Figure 3.11 A-C**). Additionally, GR MFI was measured in other epithelial and stromal cells that lacked CD4 and CD8 staining but displayed visible green fluorescence (green bars; **Figure 3.10 A-C**). The graphs show that some $CD4^+$ and $CD8^+$ cells exhibited lower GR MFI than these epithelial and stromal cells. This is consistent with the previous observation that the GR is expressed in some but not all $CD4^+$ and $CD8^+$ cells (**Figures 3.6 – 3.7**). Comparison of green bars between the epithelium and stromal tissues from all three donors further supports the observation that epithelial cells generally express GR at higher levels than stromal cells (**Figure 3.11 A-C**).

GR and PR expression density was also compared between $CD4^+$ and $CD8^+$ cells. Due to an insufficient number of samples for statistical analysis, trends observed only from the plots of GR and PR expression density in ectocervical $CD4^+$ and $CD8^+$ cells are reported.

GR expression density between the two immune cell subtypes across the ectocervical tissue layers varied between the donors. In all three donors, $CD4^+$ epithelial cells exhibited higher median GR expression density compared to $CD4^+$ stromal cells. For $CD8^+$ cells, GR expression density was similarly higher in the epithelium than in the stroma for two of the donors (PROG 173 and PROG 179; **Figure 3.11A and Figure 3.11C**), while the reverse trend was observed in the third donor (PROG 175; **Figure 3.11B**). Epithelial $CD4^+$ cells demonstrated higher

median GR expression compared to epithelial $CD8^+$ cells in two of the donors (PROG 173 and PROG 175). However, in the FGT tissue of the Mirena user (PROG 179), epithelial $CD8^+$ cells displayed higher median GR expression density compared to the epithelial $CD4^+$ cells. In the stroma, there seemed to be no difference in GR expression density between $CD4^+$ and $CD8^+$ cells in donor PROG 173, whereas in donors PROG 173 and PROG 175, stromal $CD8^+$ cells had a higher GR expression density than stromal $CD4^+$ cells (**Figure 3.11A-C**). Overall, these findings suggest that there is variability in GR expression between $CD4^+$ and $CD8^+$ cells across ectocervical tissue layers as well as between different donors.

Unlike the GR, PR was more apparent in stromal cells than epithelial cells, as shown by the confocal images (**Figures 3.4 – 3.5**). This was evident when comparing the PR expression density between the epithelium and the stroma in PR^+ cells in donor PROG 175 (green bars in **Figure 3.12B**). PR MFI in those cells was higher than background MFI, confirming the presence of PR. The same comparison of PR expression density was not obtained in the other donors, PROG 173 and PROG 179 (green bars in **Figures 3.12A and 3.12C**), although fewer cells in the epithelium than stromal cells possessed PR MFI above background.

PR staining in ectocervical $CD4^+$ and $CD8^+$ cells was not observed by immunofluorescence microscopy (**Figures 3.8 – 3.9**). When comparing the PR MFI in $CD4^+$ and $CD8^+$ cells (blue bars) to the background MFI (orange bars) as well as to PR^+ cells (green bars), the PR MFI values in $CD4^+$ and $CD8^+$ cells appeared to be closer to background MFI values. This suggests that a small percentage of $CD4^+$ and $CD8^+$ cells might be expressing low levels of PR or might not be expressing PR at all (**Figure 3.12A-C**). This observation was consistent for all three donors. In the case of the Mirena tissue donor (PROG 179), PR expression was hard to detect in stromal cells by confocal microscopy (**Figure 3.5B**) due to high background fluorescence.

The PR MFI in PR^+ cells in this donor was also found to be low, just above background fluorescence (**Figure 3.12C**). Furthermore, few cells expressed PR in the epithelium (**Figure 3.4B)**, at a higher concentration than in the stroma (**Figure 3.10E**).

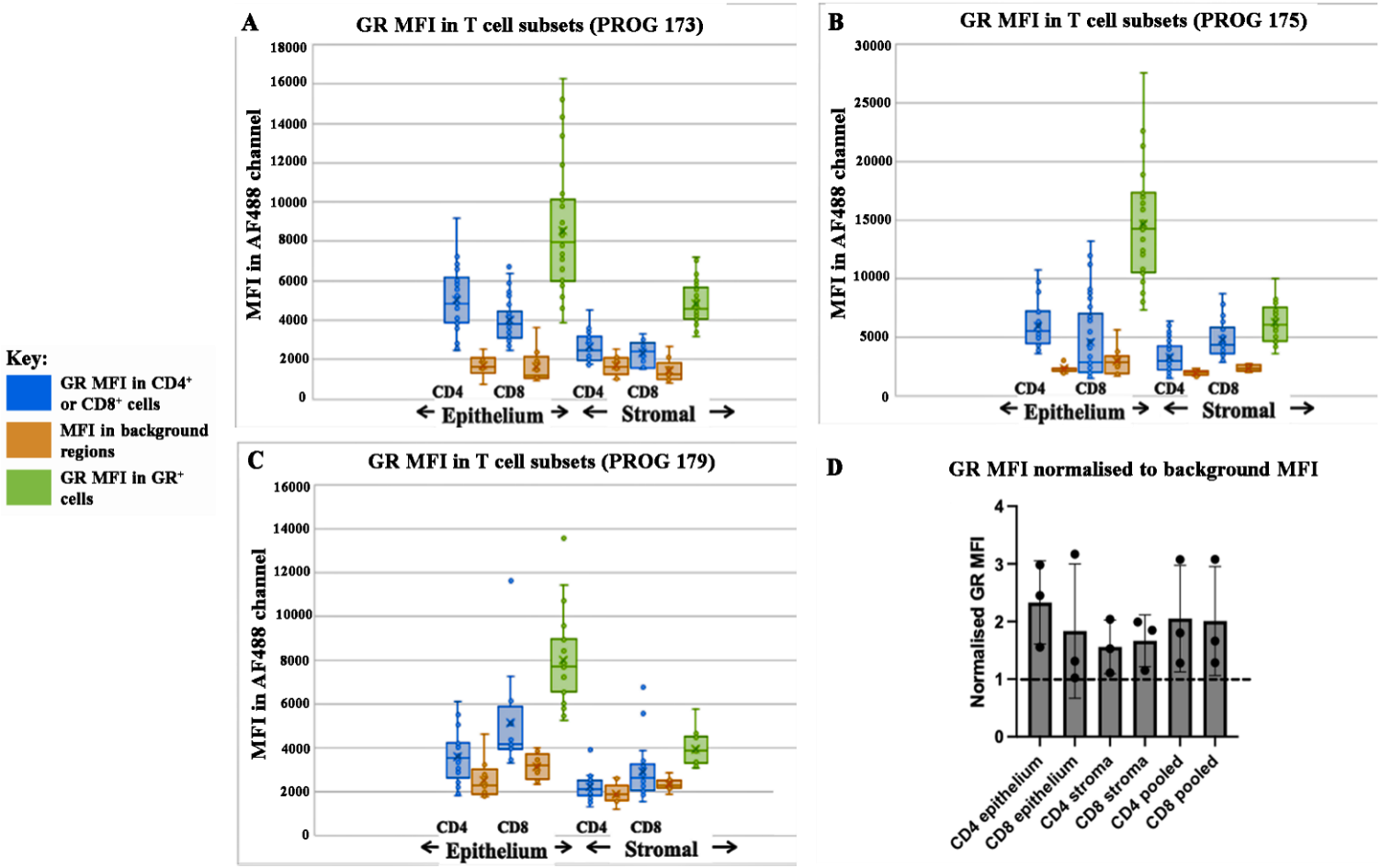

Figure 3.11: GR expression density in ectocervical CD4$^+$ and CD8$^+$ cells. The GR MFI was compared between CD4$^+$ and CD8$^+$ cells (blue bars) located in the epithelium and the stroma. The MFI of the background fluorescence in surrounding areas of the cells (orange bars) as well as in cells positively stained for GR that lacked CD4 or CD8 staining (green bars) was also plotted. The GR MFI was normalised to the background MFI. (**A**) GR MFI in CD4$^+$ and CD8$^+$ cells of the tissue donor, PROG 173, was plotted. (**B**) GR MFI in CD4$^+$ and CD8$^+$ cells of the tissue donor, PROG 175, was plotted. (**C**) GR MFI in CD4$^+$ and CD8$^+$ cells of the tissue donor, PROG 179, was plotted. (**D**) GR expression density in CD4$^+$ and CD8$^+$ cells was normalised to the background fluorescence. The data of the three donors were pooled (n=3).

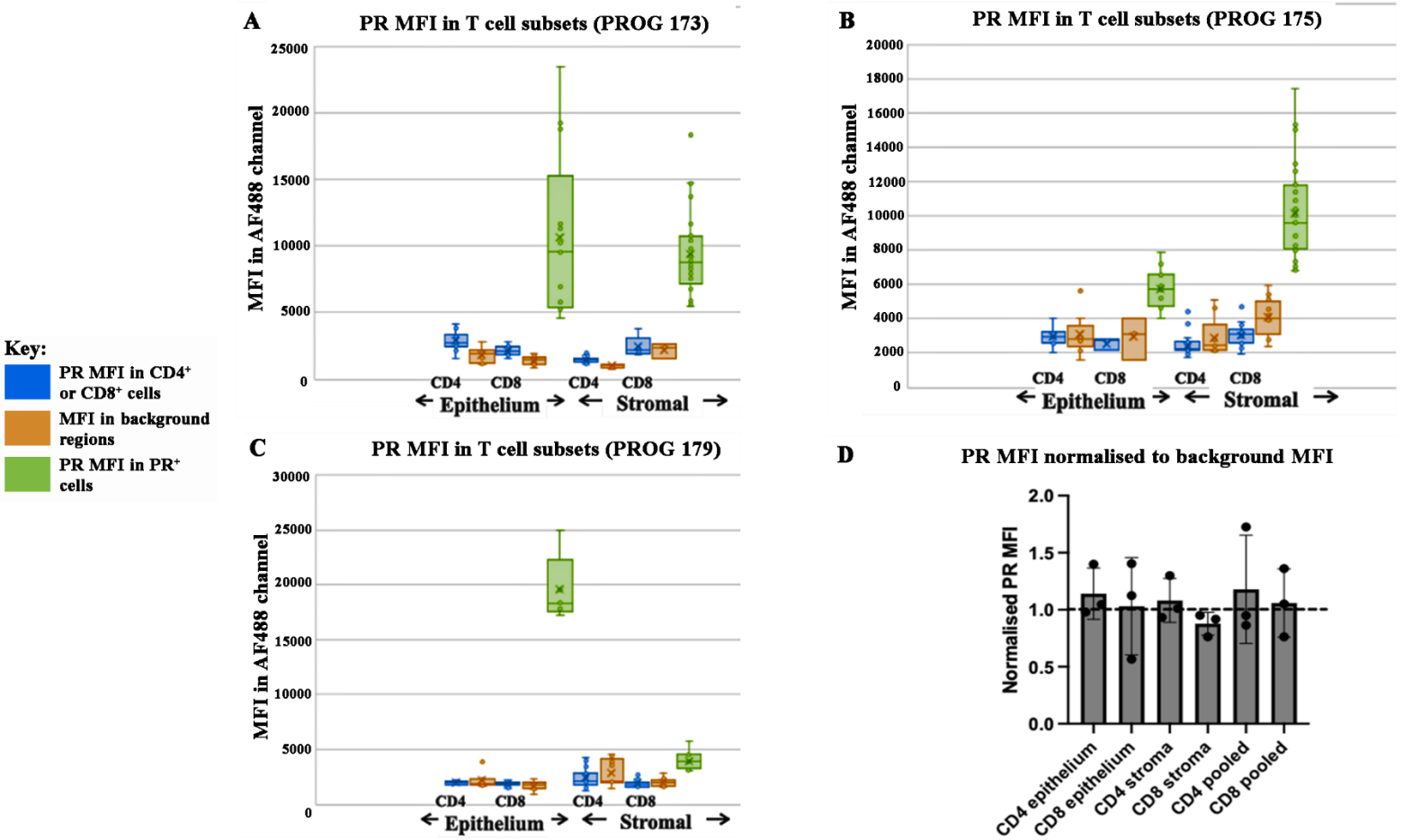

Figure 3.12: PR expression density in ectocervical CD4$^+$ and CD8$^+$ cells. The PR MFI was compared between CD4$^+$ and CD8$^+$ cells (blue bars) located in the epithelium and the stroma. The MFI of the background fluorescence in surrounding areas of the cells (orange bars) as well as in cells positively stained for PR that lacked CD4 or CD8 staining (green bars) was also plotted. The PR MFI was also normalised to the background MFI. (**A**) PR MFI in CD4$^+$ and CD8$^+$ cells of the tissue donor, PROG 173, was plotted. (**B**) PR MFI in CD4$^+$ and CD8$^+$ cells of the tissue donor, PROG 175, was plotted. (**C**) PR MFI in CD4$^+$ and CD8$^+$ cells of the tissue donor, PROG 179, was plotted. (**D**) GR expression density in CD4$^+$ and CD8$^+$ cells was normalised to the background fluorescence. The data of the three donors were pooled (n=3).

Next, the relative expression of GR to PR in $CD4^+$ compared to $CD8^+$ FGT cells was assessed in the three donors. This was done by first normalising the GR MFI or PR MFI values to the background MFI (**Figure 3.11D** and **Figure 3.12D**. Data for the three donors was pooled since MFIs were normalised to their respective background fluorescence. Moreover, GR or PR MFI values of $CD4^+$ and $CD8^+$ cells from the epithelium and the stroma were also pooled and were normalised to pooled background MFI.

The normalised GR MFI in ectocervical $CD4^+$ and $CD8^+$ cells was above 1, thus confirming GR expression. The normalised GR MFIs were higher in $CD4^+$ and $CD8^+$ epithelial cells compared to $CD4^+$ and $CD8^+$ stromal cells, more so for $CD4^+$ cells. The normalised GR MFIs were the most variable in $CD8^+$ epithelial cells among the three donors, and $CD4^+$ epithelial cells displayed the highest normalised GR expression density in the ectocervix. When pooling the data for epithelial and stromal cells, the normalised GR protein expression of $CD4^+$ and $CD8^+$ cells was similar (**Figure 3.11D**). The sample size was insufficient for formal statistical analysis, but there was no detectable trend in differences in normalised GR expression between ectocervical $CD4^+$ and $CD8^+$ cells.

In contrast, normalised PR MFI values are close to or below 1, suggesting undetectable PR expression in ectocervical $CD4^+$ and $CD8^+$ cells (**Figure 3.12D**) for all three donors. This observation was consistent across the epithelial and stromal tissues as well as when MFI values from the two regions were pooled. For one of the donors; however, the normalised PR MFI of pooled $CD4^+$ cells was above 1.5 (**Figure 3.12D**).

Following normalisation, the fold difference, i.e. the ratio of normalised GR MFI to normalised PR MFI was calculated (**Figure 3.13**). The ratios of the normalised GR to PR MFIs for each

immune cell subset, i.e. $CD4^+$ or $CD8^+$ FGT cells, in the epithelium and the stroma were computed and plotted. The ratios of normalised GR MFI to normalised PR MFI of $CD4^+$ and $CD8^+$ cells pooled from the epithelium and the stroma were also determined. In the epithelium, $CD4^+$ cells displayed a higher GR:PR ratio than did $CD8^+$ cells, whilst in the stroma the reverse was true. In the pooled groups, there appears to be no difference between $CD4^+$ and $CD8^+$ cells, and the ratios were variable between the three donors (**Figure 3.13**). Overall, there seemed to be no trend in GR:PR ratios between ectocervical $CD4^+$ and $CD8^+$ cells.

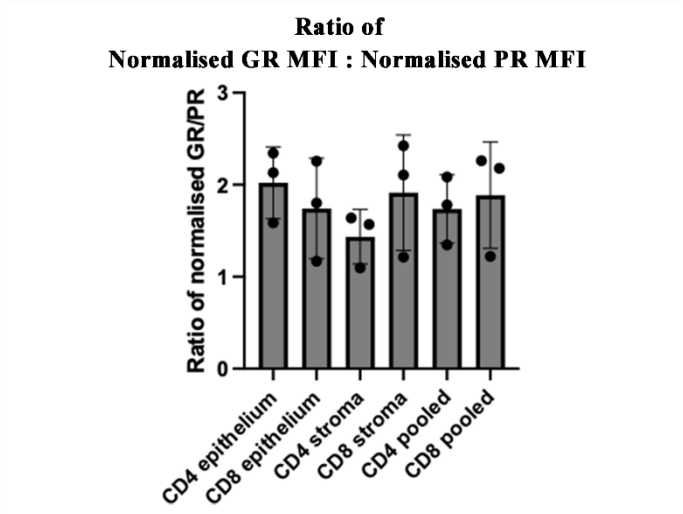

Figure 3.13: Relative expression of GR to PR in ectocervical $CD4^+$ and $CD8^+$ cells. The ratios of the normalised GR MFI to the normalised PR MFI were calculated and plotted. MFI values in both the epithelium and the stroma were also pooled, normalised to background MFI and the normalised GR to PR ratios were calculated.

3.2. Discussion:

3.2.1. Detection of GR and PR protein expression in the ectocervix

GR and PR ligands are known to exhibit reciprocal receptor cross-reactivity (Africander et al., 2011) due to significant homology between the SRs (Griekspoor et al., 2007) (Szapary et al., 2008). As a result, it is plausible that antibodies targeting those SRs may also cross-react. Despite this phenomenon, studies (summarised in **Tables 1.1** and **1.2**) reporting detection of GR or PR protein expression often overlook or fail to assess antibody-specificity. In the context of this study, the use of highly specific antibodies is crucial for the accurate detection of GR and PR proteins, prompting the assessment of potential antibody cross-reactivity. This evaluation was conducted in COS1 cells overexpressing the target proteins by employing two complementary protein detection techniques, namely western blot analysis and immunofluorescence microscopy. The results from both methods indicate that the primary antibodies of GR and PR were optimal for precise detection of the proteins by immunofluorescence assays.

This study employs a sensitive technique, i.e immunofluorescence staining coupled with confocal microscopy, to investigate the expression of GR and PR in the ectocervix *ex vivo*. In contrast with traditional protein detection methods such as immunohistochemistry and western blot analysis, confocal microscopy permits the acquisition of detailed three-dimensional images and thus represents a powerful tool for immunofluorescence staining (Jew et al., 2003). The average intensity of fluorescent staining in a specific region or cell can also be quantified (Honzel et al., 2024). The expression density of GR and PR proteins in $CD4^+$ and $CD8^+$ FGT cells was thereby determined to investigate and quantitatively compare their expression levels.

PR protein expression in tissues of the lower FGT, including in the epithelium and stroma of the ectocervix, is well-documented (Ackerman et al., 2016, WHO, 2024). In contrast, GR protein expression across different compartments and cell types within the lower FGT tissue

remains largely unexplored. This thesis presents the first investigation into GR protein expression in human ectocervical epithelial and stromal tissues. Furthermore, this study introduces the comparison of GR and PR expression levels in $CD4^+$ and $CD8^+$ immune cells within the FGT, which is also novel.

As hypothesised, this study demonstrates that GR and PR are expressed in both epithelial and stromal cells, although their distribution varies between the two cell types. A notable observation was that GR expression is predominantly localised in the epithelial tissue, whereas PR expression is primarily observed in stromal cells, suggesting that the expression of SRs is not uniform across ectocervical compartments. Previous research by (Buxant et al., 2009) supports our findings that GR is expressed in the ectocervix, but these authors did not delineate between the epithelium and stroma. Another study reported ubiquitous GR expression by immunofluorescence in stromal fibroblast cells cultured from cervical tissue (Ackerman et al., 2016). However, in this current study, GR or PR staining are present in only a subset of stromal cells, and the specific cell types expressing these receptors remain unidentified, as specific markers for fibroblasts, nerve cells or other stromal components were not used for the staining process. In this thesis, PR expression also appears to be lower in epithelial cells compared to stromal cells, consistent with Ackerman et al., 2016.

This study also demonstrates that GR proteins are expressed in some, rather than all, of $CD4^+$ and $CD8^+$ in the FGT. This finding is novel and contrasts with the initial hypothesis which anticipated the ubiquitous presence of GR proteins ACROSS all FGT $CD4^+$ and $CD8^+$ cells. Furthermore, this thesis provides the first evidence that PR protein expression is undetectable by immunofluorescence in FGT $CD4^+$ and $CD8^+$ cells.

3.2.2. GR, but not PR, is likely to be involved in the functions of the epithelial layers of the ectocervix

Results showing predominant expression of GR in epithelial cells of the ectocervix suggest that the GR may play a crucial role in regulating the functions of the ectocervical epithelial barrier *in vivo*. Ectocervical epithelial cells are exposed to the exterior and, therefore, to pathogens in the FGT (Yeaman et al., 2004), against which they mount immune responses. The stratified layer of cells acts as a physical barrier and tight junctions between the cells prevent the entry of microbes (De Tomasi et al., 2019). Some cervical epithelial cells express MHC class II molecules that bind to processed antigens and present them to $CD4^+$ T cells. Anti-microbial peptides, cytokines and chemokines are also secreted by epithelial cells to coordinate the recruitment and differentiation of innate and adaptive immune cells (Wira et al., 2005b). Hence, ectocervical cells mount innate and adaptive immune responses by acting as APCs and by secreting cytokines and chemokines (Wira and Rossoll, 1995).

The thesis data further demonstrates that PR is mostly limited to the stroma rather than the epithelium and that stromal cells express both GR and PR. Primary stromal fibroblasts were observed by others to express both GR and PR (Ackerman et al., 2016). The primary role of stromal fibroblasts is to prepare the ectocervix for implantation and successful pregnancy in response to high levels of progesterone, via the PR. The stroma provides mechanical support to the cervix during pregnancy as it comprises collagen fibres, smooth muscle and elastin (Nott et al., 2016). Stromal fibroblasts also interact with epithelial cells through paracrine signalling, by secreting cytokines and chemokines (Wira et al., 2005b, Nott et al., 2016). Together with previous findings, the thesis results suggest that both GR and PR may play a role in mediating

the effects of progestogens at relevant concentrations, regulating various functions of stromal cells in cervical tissue.

In vitro studies demonstrated that progesterone and the progestin MPA regulated immunomodulatory genes, including the genes for IL-12p40, IL-12p35, and IL-10 in Ect1/E6E7 cells. When GR expression was silenced by siRNA in these cells, the immunomodulatory effects of progesterone and MPA were reversed (Louw-du Toit et al., 2014). These data suggest that the regulation of some key immune markers by progestogens in ectocervical epithelial cells is mediated via the GR. Further research showed that biological processes, including maintenance of barrier integrity, antigen presentation and innate and adaptive immunity, are impacted by high progesterone levels and progestins, which could result in increased vulnerability to STIs (Wira and Rossoll, 1995, De Tomasi et al., 2019, Bradley et al., 2022, Edfeldt et al., 2022).

Progesterone has an affinity (K_i) of 215 nM and is a weak agonist for the human GR (Stanczyk et al., 2013). Progesterone concentrations can reach 80 nM during the luteal phase and up to 1 µM during pregnancy (Lissauer et al., 2015, Thurman et al., 2016, Polikarpova et al., 2019, Bick et al., 2022). MPA has a K_i of 10.8 nM for the GR and therefore is 20 times more likely to bind to the GR than progesterone (Africander et al., 2011). Serum concentration of MPA in women using HCs or MHT can peak up to 420 nM (Koubovec et al., 2005). The thesis results showing that epithelial cells predominantly express GR with minimal PR suggest that there is likely to be considerable cross-reaction of progestogens with the GR during the luteal phase and pregnancy, as well as in women using MPA. Altogether, these findings underscore the relevance of potential progestogen binding to the GR under conditions where physiological progestogen levels are elevated.

Moreover, cross-reaction is likely to be more pronounced in cells expressing a relatively higher GR to PR ratio, as found for ectocervical epithelial cells compared to ectocervical stromal cells. This implies that changes in response to progesterone and MPA in ectocervical epithelial cells may potentially occur mainly via the GR. In ectocervical stromal cells, responsiveness to progestogens is speculated to be mediated via the GR and PR. Hence, the relative level of GR to PR is crucial for predicting whether progesterone and MPA act via the PR and/or the GR at high concentrations. This may also result in differential biological outcomes between the epithelial and stromal cells due to their differential relative expression of GR and PR in response to progesterone and MPA. These ratios could potentially also be regulated, for example during the menstrual cycle, resulting in another level of control of differential responses.

3.2.3. GR, but not PR, contributes to the functions of FGT immune cells

This study highlights the presence of $CD4^+$ and $CD8^+$ cells within the epithelial and stromal regions of the ectocervix, although their frequencies were not quantified as in other studies (Trifonova et al., 2014). Nevertheless, the numbers and distribution of immune cell populations in the FGT are dynamic and can be modulated by hormonal fluctuations or in response to infections (White et al., 1997, Yeaman et al., 2003, Wira and Fahey, 2008, Yeaman et al., 2004) Wira et al., 2015). For instance, clinical comparisons between women using DMPA and those not on HC revealed distinct differences in immune cell distribution in the FGT. $CD4^+CCR5^+$ cells and $CD4^+Langerin^+$ cells were found to be more abundant and were superficially located in the ectocervical epithelium in DMPA users compared to non-HC- users (Chandra et al.,

2012, Edfeldt et al., 2022). It was reported that the numbers of $CD8^+$ cells and $CD8^+$ cytotoxic T lymphocyte activity remain stable throughout the menstrual cycle in the lower FGT, ensuring constant protection against pathogens (White et al., 1997, Wira et al., 2015). The expression of HIV-1 coreceptors CCR5 and CXCR4 on ectocervical epithelial and stromal leukocytes such as $CD4^+$, $CD8^+$ and $CD14^+$ cells increases vulnerability to HIV-1 infection (Hapgood et al., 2014b(Yeaman et al., 2004) Wira et al., 2015). Coupled with our results that GR proteins were expressed by some $CD4^+$ and $CD8^+$ cells, these studies support a role for the GR in mediating the effects of MPA. Further investigations on ectocervical tissue explants comparing the effects of MPA, which is a GR and PR ligand, and NET, which is not a GR ligand but a PR ligand, demonstrated that MPA, but not NET, increased CD4 HIV-1 receptor and CCR5 through GR signalling. This effect could have enhanced HIV-1 infection in ectocervical tissues for viral strains that require the CCR5 co-receptor for infection (Ray et al., 2019).Thus the findings of this study, in conjunction with the studies referenced, suggest that elevated levels of progesterone and MPA *in vivo* may influence $CD4^+$ and $CD8^+$ cell numbers and/or immune functions in the FGT. These effects, potentially mediated via the GR but not the PR, may affect immune function and increase susceptibility to STIs such as HIV-1.

Chapter 4: Results and discussion: GR and PR expression in PBMCs

4.1. Results

4.1.1. The use of unconjugated primary antibodies coupled with secondary fluorescent antibodies was not successful in the detection of GR and PR by flow cytometry

This section aimed at determining GR and PR protein expression levels in systemic immune cells such as $CD3^+$, $CD4^+$, $CD8^+$ and $CD14^+$ cells of pre-menopausal women. PBMCs were isolated from buffy coats of women aged 16-40 years old and were stained for extracellular immune markers, GR, and PR, by flow cytometry. The frequency of cells positive for GR and PR in each immune cell subset was determined.

As mentioned previously in **Section 2.11.2.3**, a mixture of unconjugated primary antibodies for GR and PR with fluorescent secondary antibodies was used for staining of GR and PR in PBMCs. When analysing the flow cytometry results, positive signals for GR and PR (Q2) were observed in $CD3^+$, $CD4^+$, $CD8^+$ and $CD14^+$ cell populations of the primary antibody staining control, i.e., the sample that excluded anti-GR and anti-PR antibodies. By way of example, the scatter plot of the $CD3^+$ cell population indicates that a frequency of 96.5% of $CD3^+$ cells were GR^+PR^+ (**Figure 4.1A**). Similarly, positive signals (Q2) were observed in $CD3^+$, $CD4^+$, $CD8^+$ and $CD14^+$ cell populations when all the primary and secondary antibodies were added, i.e., in a fully-stained PBMC sample. The scatter plot in the $CD3^+$ cell population shows a frequency of 83.6% cells that are GR^+PR^+ (**Figure 4.1B**).

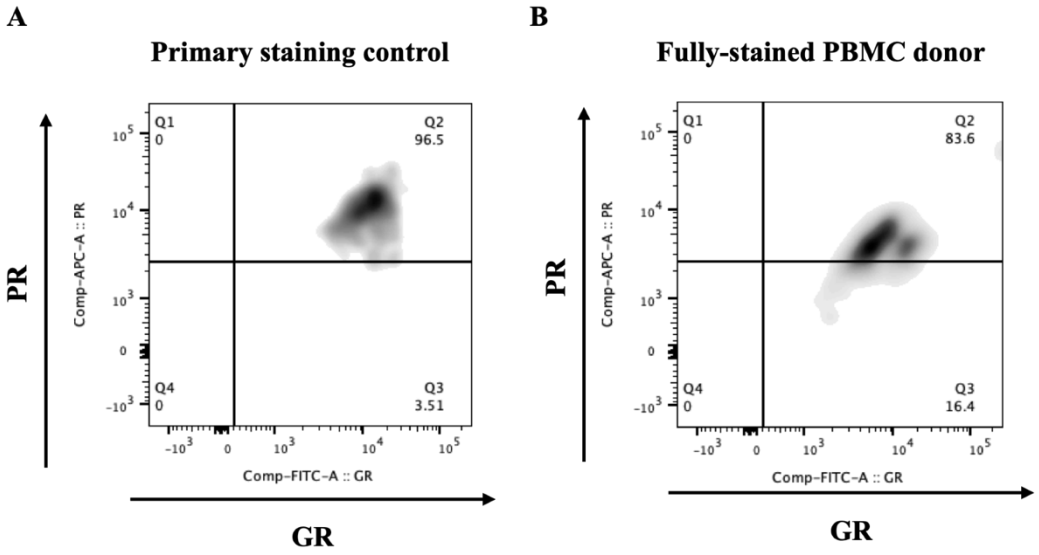

Figure 4.1: Detection of GR and PR in the $CD3^+$ cell population of primary staining control and a fully-stained PBMC sample using flow cytometry. In the primary staining control, the primary antibodies of GR and PR were not added, while in the fully-stained PBMC sample, all the antibodies were added. (**A**) Scatter plot showing staining of GR and PR in the $CD3^+$ cell subset in a primary antibody staining control. (**B**) Scatter plot showing staining of GR and PR in the $CD3^+$ cell subset in a fully-stained PBMC sample.

It was concluded that there is a possibility that the anti-mouse secondary antibodies were binding to the mouse primary antibodies of the extracellular markers CD3, CD4, CD8 and CD14, as the antibodies were raised in mice. Therefore, unconjugated primary antibodies for GR and PR were not used for GR and PR analyses by flow cytometry in PBMCs.

4.1.2. Conjugated primary antibodies for GR and PR do not exhibit reciprocal receptor cross-reaction

Based on the previous section, the conjugated primary antibodies GR FITC and PR eFluor^{TM} 660 were used for GR and PR detection, respectively, by flow cytometry. These antibodies were first tested for cross-reactivity using flow cytometry in COS1 cells with overexpressed GR or PR. A mock transfection control, where the cells were incubated with transfection reagent without plasmids for GR or PR was included to account for endogenous expression of GR and PR. Controls consisting of an unstained (no antibodies and no Zombie dye) and a Zombie-only control (no antibodies) were also included (refer to **Section 2.11.1**). The cells were stained with GR antibody and/or PR antibody.

Gating strategies were established using the unstained and Zombie-only controls to set the alive GR- and PR- gates (**Figure 4.2**). In the unstained control, COS1 cells were excluded from cellular debris using the side scatter (SSC-A) and forward scatter (FSC-A) plots. Thereafter, single cells were selected from the COS1 cells before the alive cell population gate was set. These gates were applied to a Zombie-only control where the live cell population was adjusted; cells that were dead took up the Zombie dye and were located higher on the Zombie axis. Within the live cell population, quadrant gates were created on the GR and PR axes to select $GR^{+}PR^{-}$, $GR^{-}PR^{+}$ and $GR^{+}PR^{+}$ cell populations. All gates were then applied to the stained samples – GR-stained samples, PR-stained samples and GR and PR-stained samples – to determine the cellular frequency of cells positive for GR and/or PR.

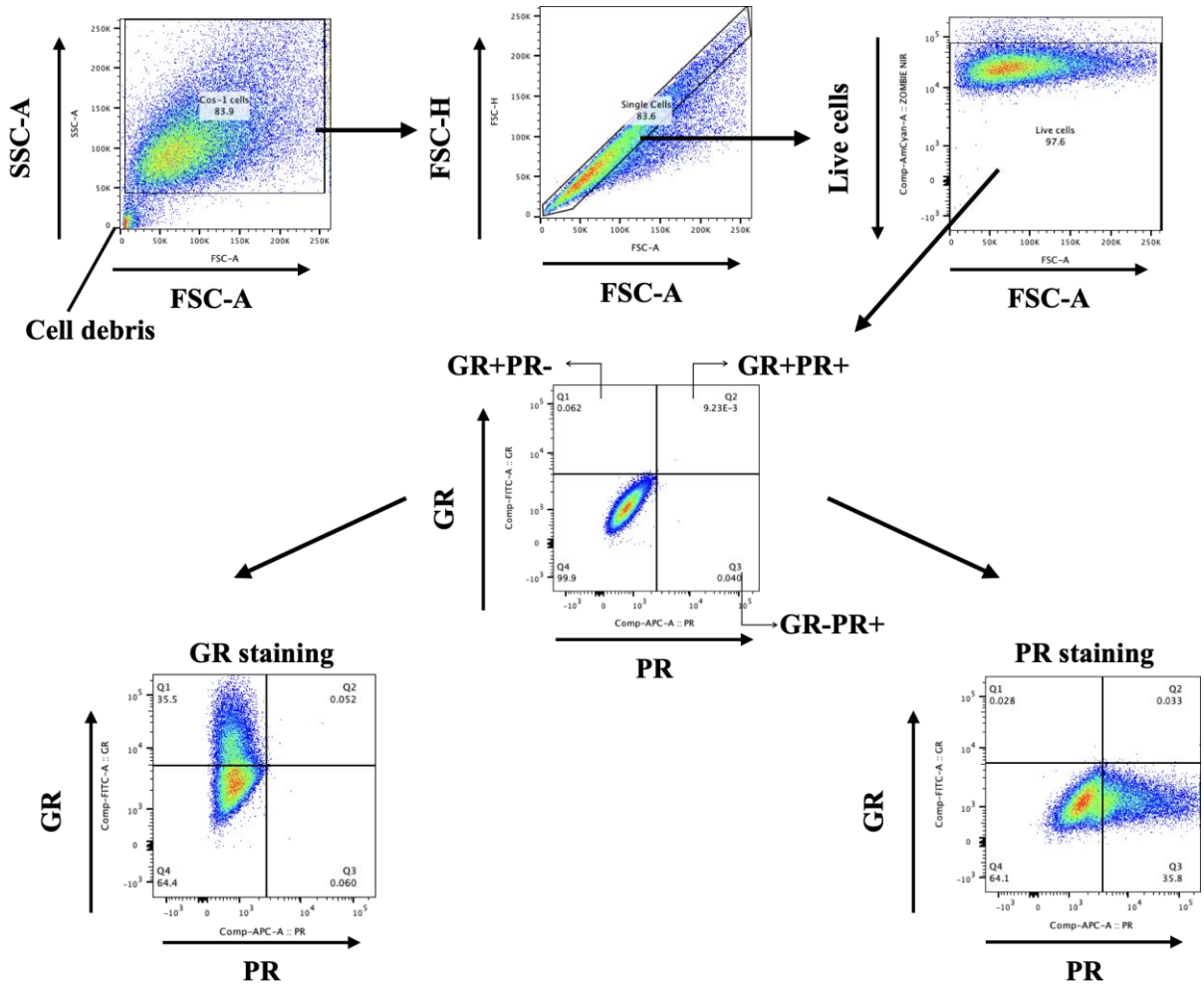

Figure 4.2: Strategies employed for gating of COS1 cells using the unstained and Zombie-only controls. In the unstained control sample, COS1 cells were not stained for Zombie, GR and PR while in the Zombie-only control, COS1 cells were stained for Zombie but not GR and GR. The unstained control was used to exclude COS1 cells from debris and to gate for single cells. Gates were then applied to the Zombie-only control. Live cells followed by GR-negative and PR-negative cells were gated. Gates were applied to samples stained with GR, PR and both GR and PR, to determine the cellular frequencies of the stained cells.

Staining for GR in COS1 cells revealed the presence of GR in the mock transfection and PR transfection groups, suggesting that COS1 cells endogenously express GR. This is consistent with the immunofluorescence results showing endogenous GR expression in COS1 cells. The

cellular frequency of GR^+ COS1 cells increased from 39.1% in the mock transfection group to 50.9% in the GR transfection group upon staining for GR (**Figure 4.3A, panel 1 and panel 2**), suggesting that transfection of the pcDNA3-hGR plasmid successfully resulted in the expression of GR. Similarly, co-staining for GR and PR demonstrated an increase in GR^+ cell frequency to 53.5% in GR-overexpressing cells as compared to 38.6% in mock transfection group (**Figure 4.3C, panel 1 and panel 2**). The observed frequency of GR^+ cells varied between 30.6% and 53.5% in both mock transfection and GR transfection groups, showing that endogenous and exogenous GR was not expressed in all COS1 cells. Staining for GR showed only a negligible increase in GR^+ cell frequency to 40.9 % in cells overexpressing exogenous PR as compared to 39.1% in cells that underwent mock transfection (**Figure 4.3A, panel 1 and panel 3**). Furthermore, co-staining for GR and PR did not result to increase GR^+ cellular frequency in cells of the PR transfection group (30.6% GR^+) as compared to cells of the mock transfection group (38.6% GR^+) (**Figure 4.3C, panel 1 and panel 3**), indicating that the GR antibody was not cross-reacting with overexpressed PR proteins.

When staining of PR was performed, an increase to 34.1% of PR^+ cells (**Figure 4.3B, panel 3**) was observed in cells overexpressed with PR compared to cells in the mock transfection group stained for PR, where 1.38% were PR^+ (**Figure 4.3B, panel 1**). Similar observation was seen during co-staining of GR and PR where the cellular frequency of PR^+ cells also increased to 34.2% when overexpressed with PR, compared to 0.23% PR^+ in cells of the mock transfection group (**Figure 4.3C, panel 1 and panel 3**). These results suggest that COS1 cells do not express PR endogenously and that the expression of PR was successful in COS1 cells following transfection with the pMT-hPRB vector. Staining for PR seemed to be absent in cells overexpressing GR and in cells of the mock transfection group as the frequency PR^+ cells was below 1% (**Figure 4.3B, panel 1 and panel 3**). Additionally, co-staining for GR and PR also

revealed very low frequency of PR^+ cells (< 1%) during GR and mock transfections (**Figure 4.3B, panel 1 and panel 2**). Taken together the results suggest the PR antibody was not cross-reacting to endogenous and exogenous GR proteins.

It can be concluded from these results that the conjugated GR FITC antibody does not cross-react with the PR, and the conjugated PR eFluor^{TM} 660 antibody does not cross-react with the GR.

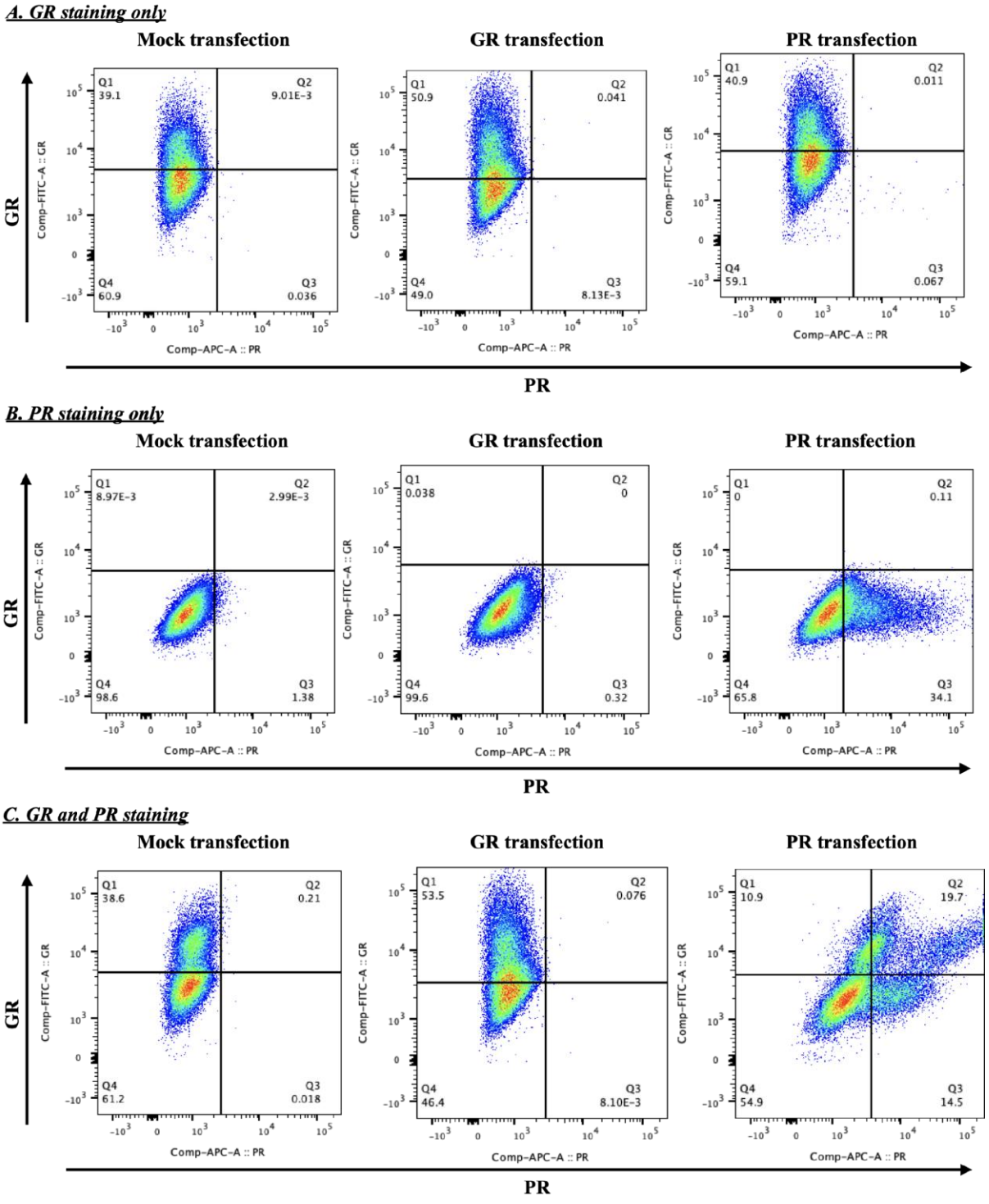

Figure 4.3: Scatter plots of transfected COS1 cells showing the results of cross-reactivity tests of GR and PR conjugated antibodies using flow cytometry. COS1 cells were transfected with either GR or PR, stained with GR and PR primary antibodies and analysed with flow cytometry. The mock-transfected cells were transfected with transfection reagent only and served as a control, to investigate endogenous expression of the proteins. (**A**) Scatter

plots of mock-, GR- and PR-transfected COS1 cells stained with GR FITC antibody. (**B**) Scatter plots of mock-, GR- and PR-transfected COS1 cells stained with PR eFluor^{TM} 660 antibody. (**C**) Scatter plots of mock-, GR- and PR-transfected COS1 cells stained with GR FITC and PR eFluor^{TM} 660 antibodies.

4.1.3. Gating of GR and PR in immune cell subtype

Having shown that the conjugated GR and PR antibodies do not cross-react, GR and PR protein levels in systemic immune cell subsets were investigated. PBMCs isolated from buffy coats of six pre-menopausal women aged 18 to 40 years old were stained for the extracellular immune cell markers CD3, CD4, CD8 and CD14, as well as the intracellular SRs, GR and PR.

A set of gates was created and is shown in **Figures 4.4-4.8** for analysis by flow cytometry of GR and PR in immune cells. Lymphocyte and monocyte populations were first selected from FSC/SSC plots based on size and granularity in the unstained control population. Single-cell and live-cell (Zombie-) populations were then gated from the respective cell types (lymphocytes or monocytes), and the live-cell gates were adjusted in the Zombie-only control sample (refer to **Section 2.11.3** for more details on the controls). CD3 and CD14 FMO control samples were then used to set gates for T cells, i.e. $CD3^+$ cells and monocytes ($CD14^+$), respectively (**Figure 4.4**). From the $CD3^+$ cell population, $CD4^+$ and $CD8^+$ cells were identified on the CD8/CD4 axes using the CD4 FMO and CD8 FMO, respectively (**Figure 4.5**). Thereafter, in each immune cell subset, GR and PR gates were selected using GR (**Figure 4.6**) and PR FMOs (**Figure 4.7**). Gating for PR and GR was also conducted on a GR-negative and PR-negative control sample (**Figure 4.**). The results in the GR-negative and PR-negative

control samples (**Figure 4.8**) were consistent with the observations in the GR FMO (**Figure 4.6**) and the PR FMO (**Figure 4.7**).

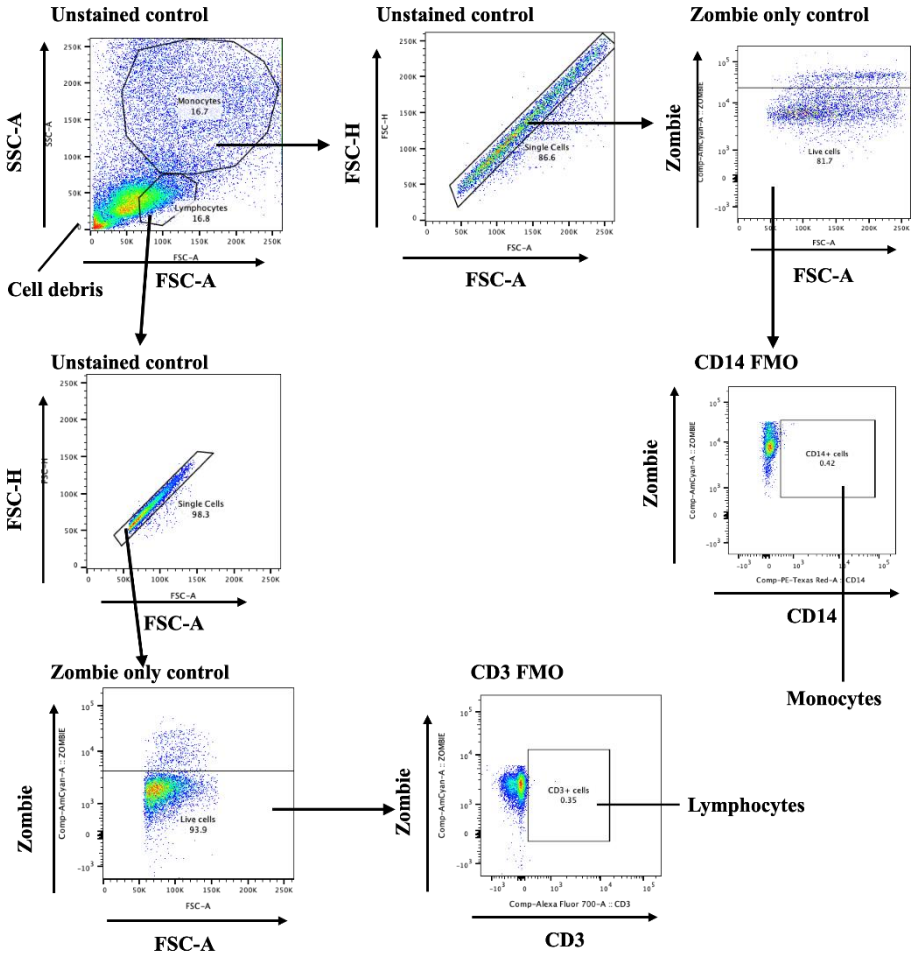

Figure 4.4: Scatter plots of PBMCs showing strategies employed for gating of lymphocytes and monocytes. Using an unstained control, gates for lymphocyte and monocyte cell populations were set according to cell size and granularity. Single cells were gated from each of the populations and the gates were applied to Zombie-only control samples. Using the Zombie-only control sample, live cells were selected on the Zombie axis. From the live cells, gates for $CD3^+$ cells and $CD14^+$ cells were set up using the CD3 FMO and CD14 FMO samples, respectively.

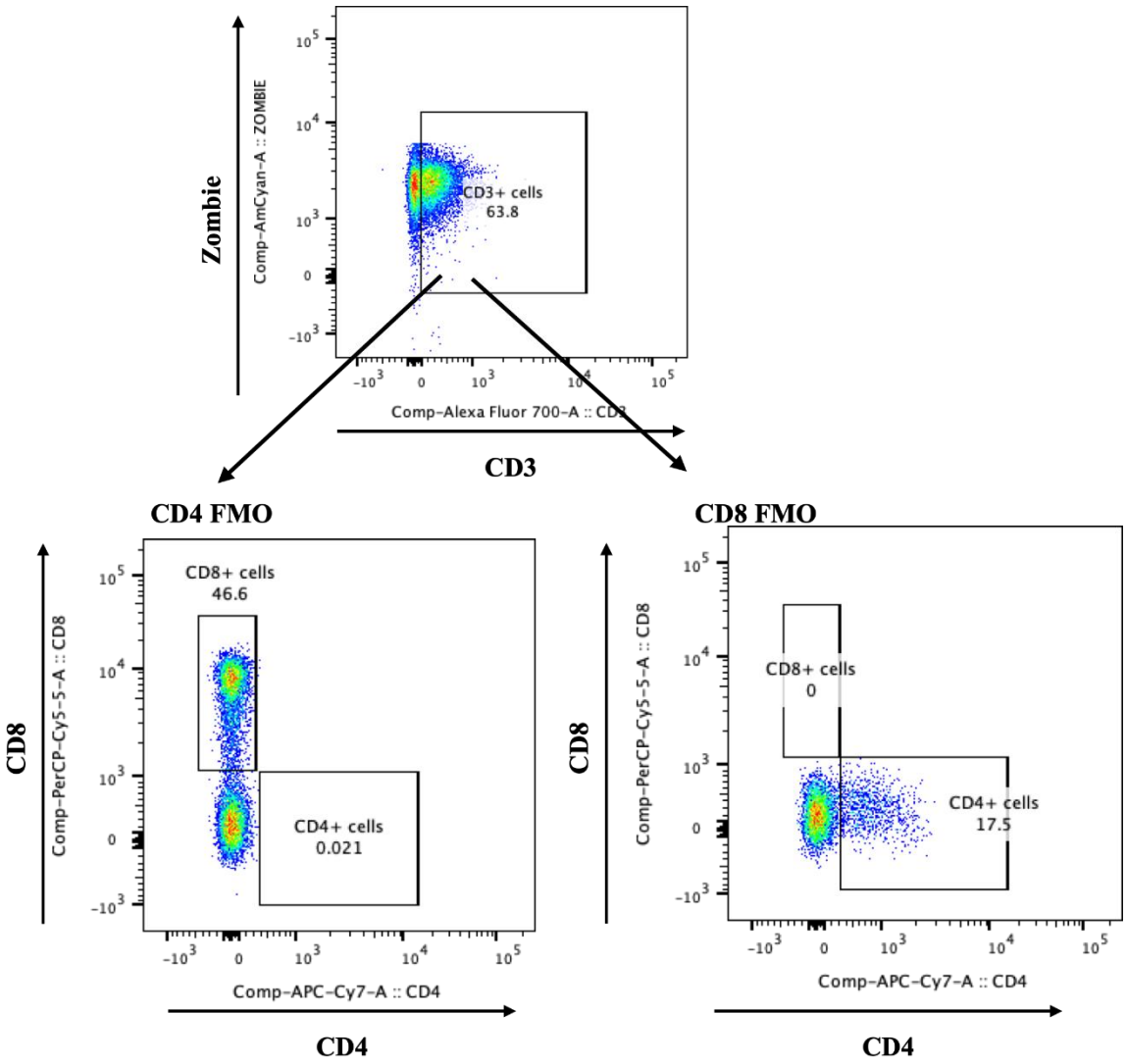

Figure 4.5: Gating of $CD4^+$ and $CD8^+$ cells using the CD4 FMO and CD8 FMO samples, respectively. The gates established in the CD3 FMO sample were applied to the CD4 and CD8 FMO samples. $CD3^+$ cells were selected and a gate for $CD4^+$ cells was created in the CD4 FMO sample, while for $CD8^+$ cells, a gate was created in the CD8 FMO sample.

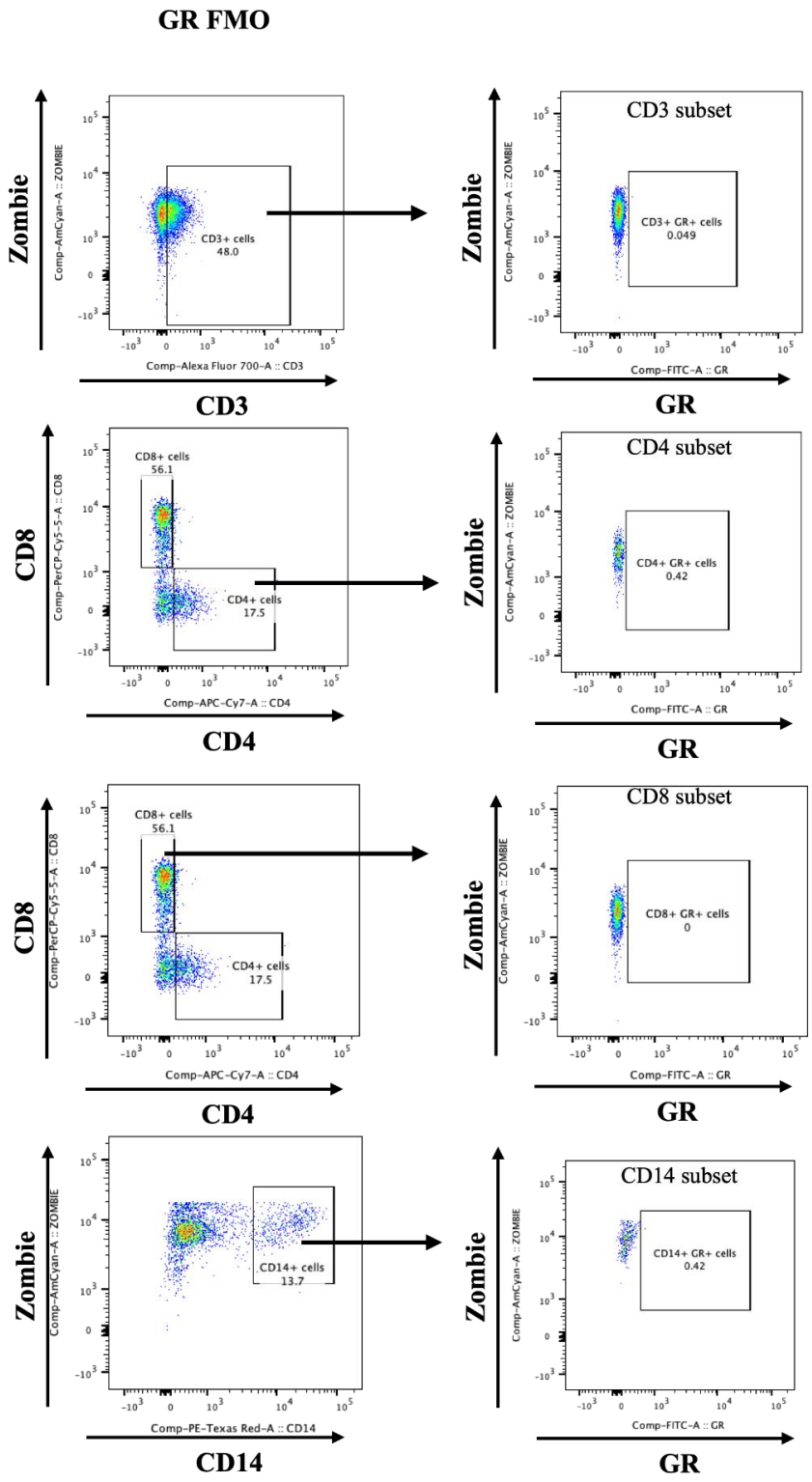

Figure 4.6: Scatter plots showing gating of GR in immune cell subsets. In the GR FMO, PBMCs were stained for CD3, CD4, CD8, CD14, GR and Zombie-only. Using the GR FMO, each immune cell population was selected and gates for GR^+ cells were created for each immune cell subset.

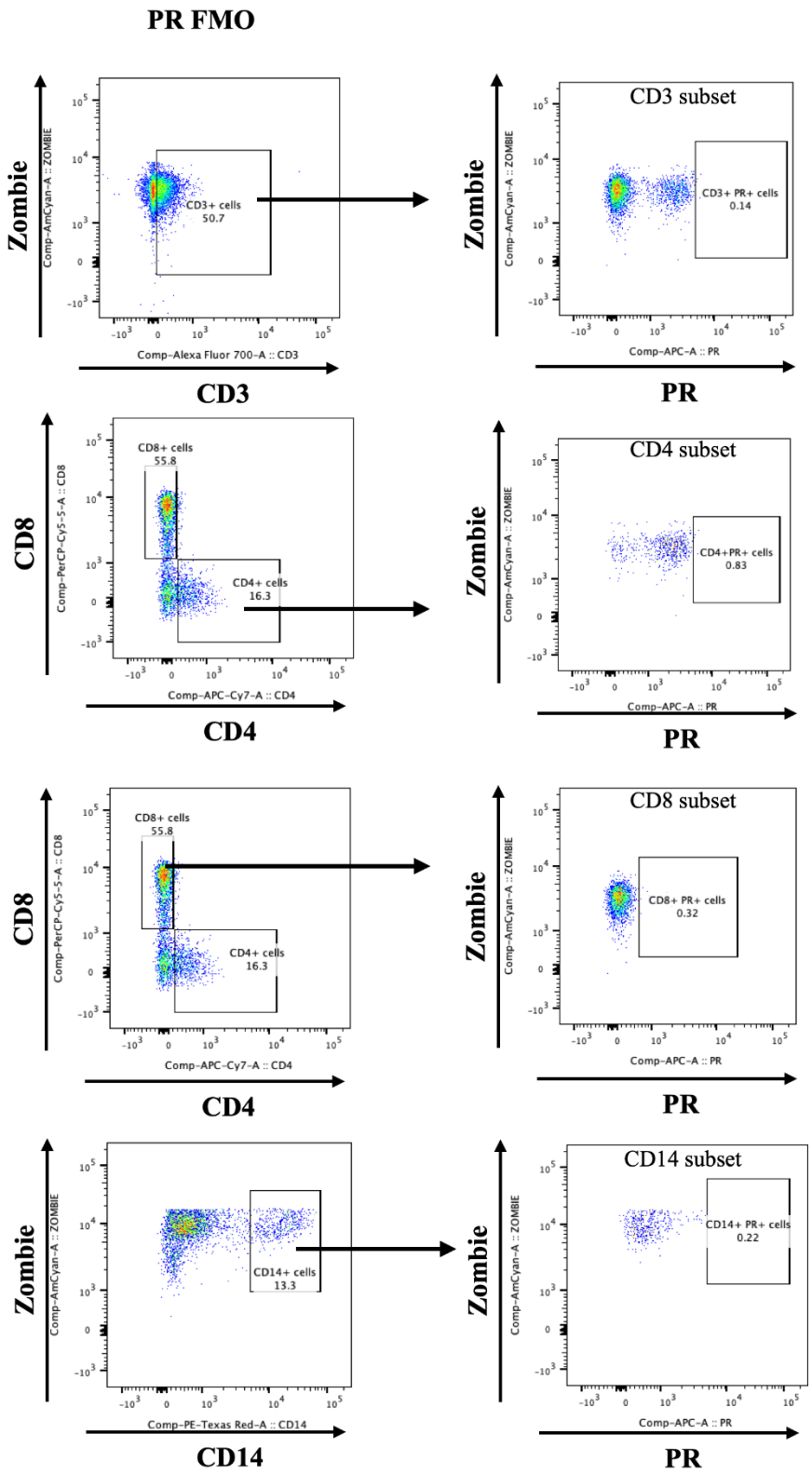

Figure 4.7: Scatter plots showing gating of PR in immune cell subsets. Using the PR FMO, each immune cell population was selected, and the PR gates were created for each cell. In the GR FMO, PBMCs were stained for CD3, CD4, CD8, CD14, PR and Zombie only.

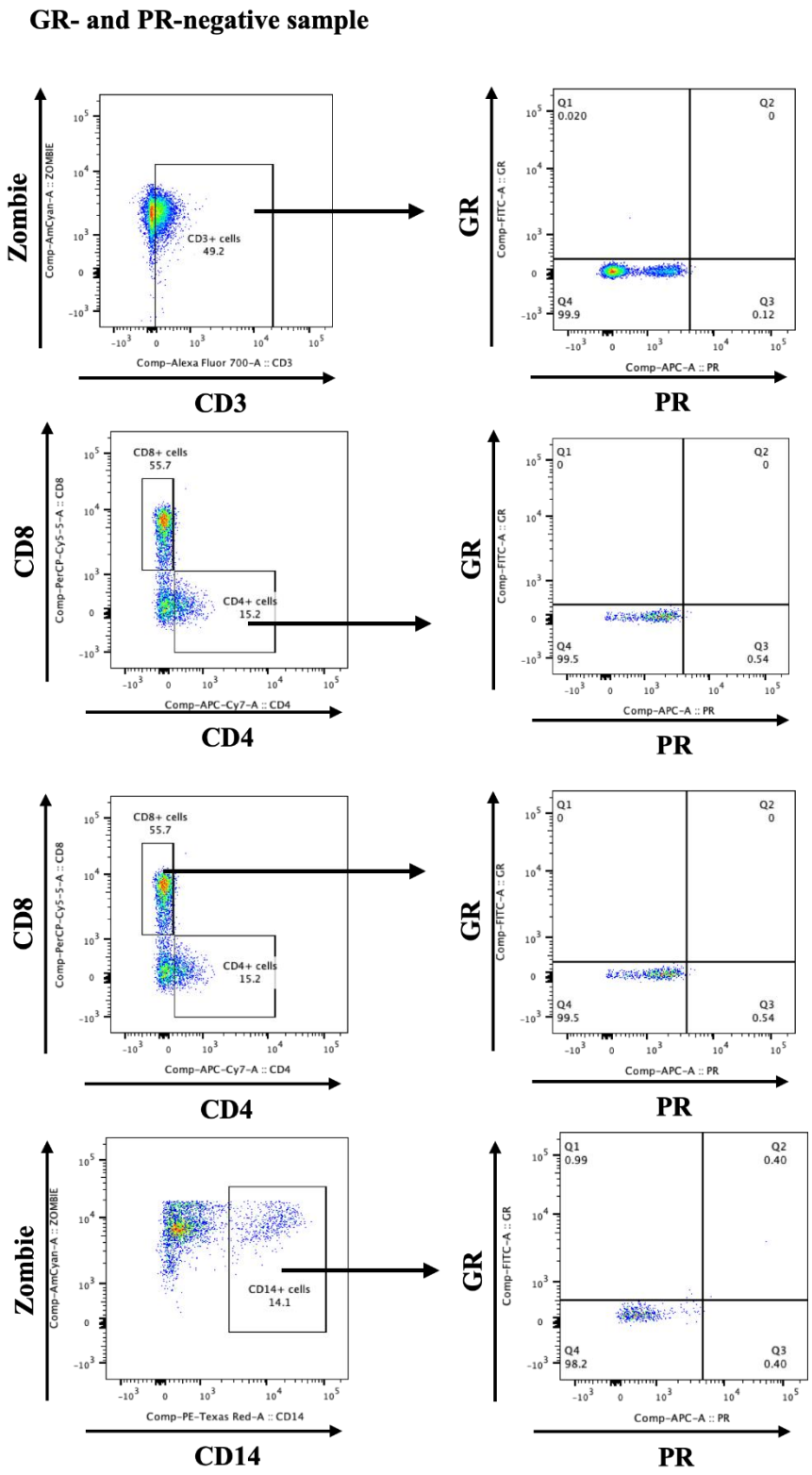

Figure 4.8: Scatter plots showing gating of GR and PR in immune cell subsets, $CD3^+$, $CD4^+$, $CD8^+$ and $CD14^+$ using the GR- and PR-negative control sample. In the GR- and PR-negative sample, PBMCs were stained for CD3, CD4, CD8, CD14 and Zombie only.

4.1.4. GR is expressed in systemic $CD3^+$, $CD4^+$, $CD8^+$ and $CD14^+$ cells with similar expression densities

All the gates created as described in **Section 4.1.3** were applied to all the fully-stained samples of the six donors. Following gating, immune cells that were GR^+ were identified in the stained samples of all six donors. High frequencies of cells positive for GR ranging from 99.3% to 100% were observed in $CD3^+$, $CD4^+$ and $CD8^+$ cells (**Figure 4.9A**). The frequency of cells positive for GR was compared between all the immune cells from the six donors. In the CD14 subset, the frequency of GR^+ cells ranged from 70.7% to 79.1% (**Figure 4.9A**). The frequencies of $CD3^+$, $CD4^+$ and $CD8^+$ cells positive for GR were significantly lower than the frequency of $CD14^+$ cells positive for GR (**Figure 4.9A**). The cellular frequency of GR^+ cells was not statistically different between $CD3^+$, $CD4^+$ and $CD8^+$ cells in the six donor samples (**Figure 4.9A**). This suggests that GR is highly expressed in almost all systemic lymphocytes, namely $CD3^+$, $CD4^+$ and $CD8^+$ T cells, while a smaller proportion of monocytes express GR. The GR expression density was also compared according to GR MFI. The expression density of GR exhibited variability across different immune cell types and between the donor samples. Although it appears that $CD14^+$ cells possess a lower GR expression density, it was shown that there was no significant difference in GR expression density among $CD3^+$, $CD4^+$, $CD8^+$ and $CD14^+$ cells (**Figure 4.9B**).

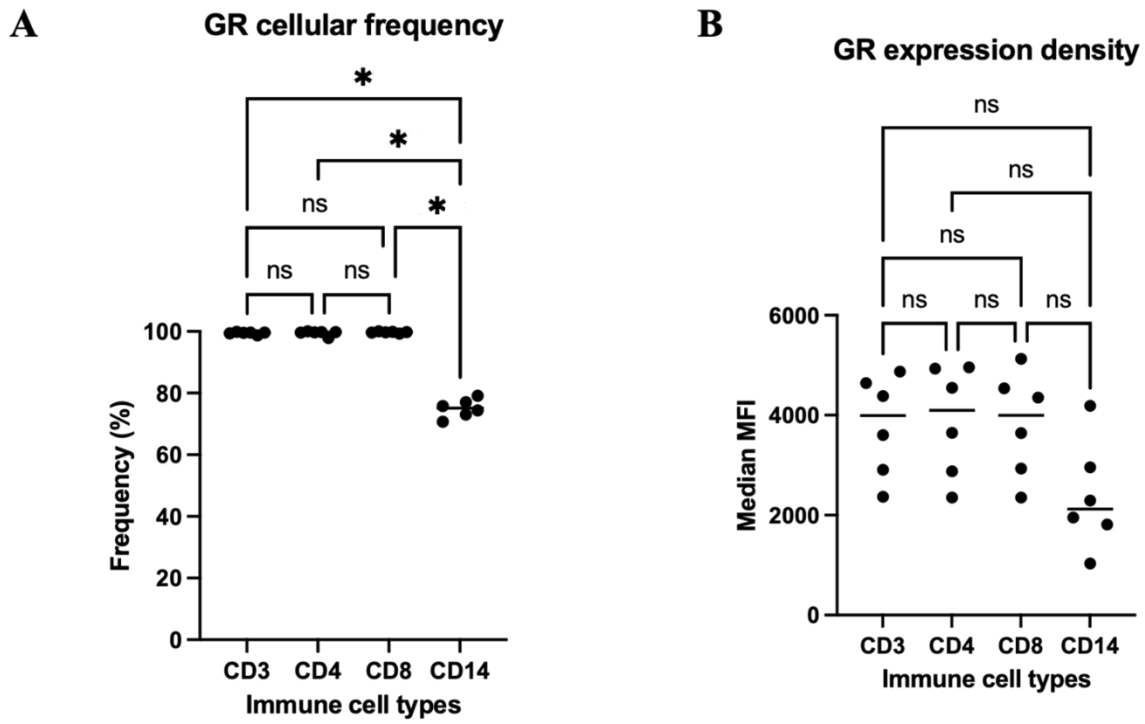

Figure 4.9: GR is ubiquitously expressed in CD3$^+$, CD4$^+$, and CD8$^+$ T cells, and CD14$^+$ cells, with CD14$^+$ cells having a significantly lower frequency and non-significantly lower density of the GR. (**A**) Frequencies of GR$^+$ cells for each immune cell type (n=6). (**B**) GR expression densities for each immune cell type (n=6). For statistical analysis, one-way ANOVA (non-parametric or mixed) was performed on pooled data of the six donors (n=6). ns = not significant; * = significant difference; p-value <0.05.

4.1.5. PR protein expression is likely to be absent in systemic CD3$^+$, CD4$^+$, CD8$^+$ and CD14$^+$ cells

PR protein expression in PBMCs was investigated by flow cytometry. Immune cell populations, including CD3, CD4, CD8 and CD14 populations, were gated as shown previously (**Figures 4.7 – 4.8)**. Using the PR FMO control sample, which did not include the PR eFluor^{TM} 660 antibody, PR gates were created. Surprisingly, two distinct populations were

observed on the PR axis in the $CD3^+$, $CD4^+$ and $CD14^+$ immune cell subsets although the PR antibody was not added (**Figure 4.7**). This observation was also apparent on the PR axis in the GR- and PR-negative samples (**Figure 4.8**). There might be spillover of another antibody in the channel that was recording signal for the PR eFluor™ 660. Such spillover might be due to the mouse anti-CD4 APC Fire 750, as this signal was higher in the $CD4^+$ subset than in other cell populations (**Figure 4.7**). Considering the above, the gates were set up just above the two signals.

In the fully-stained samples, there was no signal above the non-specific signals in the $CD3^+$, $CD4^+$, $CD8^+$ and $CD14^+$ cells. The results were similar to what was observed in the PR FMO (**Figure 4.6**). This suggests that PR was not present in $CD3^+$, $CD4^+$, $CD8^+$ and $CD14^+$ cells. The cellular frequencies were plotted while the PR MFI could not be determined as very few cells, possibly none, expressed PR (**Figure 4.10**).

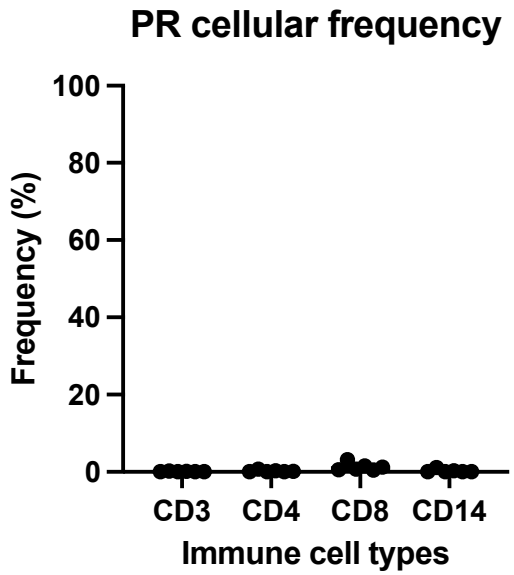

Figure 4.10: Cellular frequency of $CD3^+$, $CD4^+$, $CD8^+$ and $CD14^+$ cells displaying positive signal for PR above the non-specific signals observed in the PR FMO sample is negligible. Data from the six fully-stained donor samples were pooled and plotted (n=6).

4.2. Discussion

4.2.1. Detection of GR and PR protein expression in PBMCs

Data in the literature on GR expression in systemic immune cells, including $CD3^+$, $CD4^+$, $CD8^+$ and $CD14^+$ cells, is scant, whilst data on PR expression is inconclusive. The flow cytometry results of this study provide new information on the comparison of GR and PR protein expression among systemic $CD3^+$, $CD4^+$, $CD8^+$ and $CD14^+$ cells based on cellular frequency and expression density. In addition, the primary antibodies for GR and PR conjugated to their fluorophores were assessed for cross-reactivity using flow cytometry.

For this study, the expression of GR and PR was analysed using flow cytometry, a highly sensitive technique for protein detection. However, several challenges were encountered during the process. Previously, unconjugated mouse primary antibodies coupled with fluorescently labelled mouse secondary antibodies were used, resulting in species cross-reactivity of secondary antibodies to other antibodies raised in mice. Therefore, conjugated primary antibodies for GR and PR were used for subsequent experiments, and they were evaluated for cross-reactivity. Although GR and PR are structurally similar, the cross-reactivity of anti-PR and anti-GR antibodies does not appear to have been previously investigated. Cross-reactivity was investigated in this thesis in COS1 cells overexpressing GR or PR, but this was not the ideal cell line because COS1 cells endogenously express GR. Flow cytometry detected low endogenous GR protein levels in COS1 cells, unlike western blot analysis, showing that flow cytometry was more sensitive. Since the endogenous GR protein in COS1 cells could interfere

with the assessment of cross-reactivity between the GR-conjugated primary antibody and overexpressed PR protein, a mock-transfected control was included in the flow cytometry experiments. This control allowed for a comparison with the results for cells overexpressing PR when GR staining was performed to evaluate the cross-reactivity of the anti-GR antibody with PR protein.

When analysing the flow cytometry results, non-specific signals were observed in the channel detecting fluorescence from the conjugated PR antibody. These signals appeared in the PR FMO sample, which lacked the PR antibody, as well as in the GR- and PR- negative sample, which excluded the anti-GR and anti-PR antibodies. These signals suggest possible spillover from fluorophores of other antibodies into the channel designated for the anti-PR antibody, since two distinct cell populations were observed on the scatter plots of the PR FMO as well as the GR- and PR-negative samples. This is a common issue in multiparametric flow cytometry, where overlapping emission spectra from multiple fluorophores can lead to signal spillover and false-positive results (Bhowmick and Bushnell, 2024). Therefore, the choice of antibodies and the use of appropriate controls, such as FMO and compensation controls, were crucial to minimise non-specific signals that can result in false positives. Despite these efforts, the non-specific signals could not be eliminated in this study and future studies using different antibody panels will have to be optimised. Therefore, in this study, gating strategies were applied to try and distinguish PR-positive populations above the background non-specific signals.

It is demonstrated by flow cytometry in this present study that GR is expressed at a high cellular frequency in systemic T lymphocytes, namely $CD3^+$, $CD4^+$ and $CD8^+$ cells. A lower frequency of systemic monocytes ($CD14^+$ cells) express GR, compared to T lymphocytes. Previous

research in sorted $CD3^+$, $CD4^+$, $CD8^+$ and $CD14^+$ cells demonstrated that GR mRNA expression is ubiquitous, however, the researchers did not provide a comparative analysis of GR expression across these cell types (Brundin et al., 2021). In this present study, the GR expression density did not differ between systemic $CD3^+$, $CD4^+$, $CD8^+$ and $CD14^+$ cells. Another study, which compared systemic $CD3^+$ and $CD14^+$ cells, demonstrated that the expression density of GR was not significantly different between these immune subsets, but the cellular frequency was not assessed (Du et al., 2009).

Despite the challenges encountered in analysing PR expression, the data indicate that PR is not expressed in systemic $CD3^+$, $CD4^+$, $CD8^+$ and $CD14^+$ cells. When the samples were stained with the PR antibody, no signal was obtained above the background non-specific signal, and the fully-stained samples produced results nearly identical to the PR FMO samples. According to data in the literature, purified $CD3^+$, $CD4^+$ cells and peripheral leukocytes displayed little to no immunoreactivity for PR, while sorted $CD56^+$ cells were observed to express PR by confocal microscopy and flow cytometry (Arruvito et al., 2008, Dosiou et al., 2008). Other studies which examined PR by western blot analysis in unsorted PBMCs also showed undetectable PR expression (Tomasicchio et al., 2013). Similarly, transcription of PR mRNA in sorted $CD3^+$, $CD4^+$, $CD8^+$ and $CD14^+$ cells was investigated and was not detected (Brundin et al., 2021). Hence, our findings align with the published literature, providing compelling evidence that PR proteins are not expressed in systemic $CD3^+$, $CD4^+$, $CD8^+$ and $CD14^+$ cells.

4.2.2. PR-mediated effects may be minimal in systemic $CD3^+$, $CD4^+$, $CD8^+$ and $CD14^+$ cells

The effects of progestogens are thought to be mediated primarily via the PR. However, the lack of conclusive detection of PR in systemic $CD3^+$, $CD4^+$, $CD8^+$ and $CD14^+$ cells suggests that the PR may not be playing a significant role in endocrine signalling in these cells. Despite this, accumulating evidence supports the role of progesterone and progestins in regulating immunomodulatory genes in immune cells. For example, research conducted with PBMCs obtained from healthy maternal and male donors showed that exogenous progesterone dose-dependently regulates the production of cytokines such as IFN-γ, TNF-α, IL-5, IL-1, IL-4, IL-5 and IL-10, in $CD4^+$ and $CD8^+$ T cells (Lissauer et al., 2015). In PBMCs isolated from women at various stages of the menstrual cycle, several immunomodulatory genes were shown to be significantly upregulated in the ovulatory and mid-luteal phase, during which time progesterone levels peak in the menstrual cycle, compared to the follicular phase. These genes are involved in pro-inflammatory and Th1/Th2 responses and include the genes for IL-1β, TNF-α, IFN-γ and NFκB1 (Brundin et al., 2021). Progesterone was reported to regulate the expression of IL-1β, TNFα, and IL-6 cytokines at both mRNA and protein levels in $CD4^+$ T cells and $CD8^+$ T cells from healthy pregnant women, as well as in THP-1 monocytes (Polikarpova et al., 2019). Increased progesterone levels are associated with impaired cytotoxic activity of peripheral $CD8^+$ cells during pregnancy, potentially contributing to maternal-foetal immune tolerance (Yao et al., 2017). Interestingly, the above-mentioned reports detected the presence of membrane PR (mPR), particularly in systemic immune cells, including $CD3^+$, $CD4^+$, $CD8^+$ and $CD14^+$ cells (Lissauer et al., 2015, Polikarpova et al., 2019), suggesting that the immunomodulatory effects of progestogens might be mediated via the mPR rather than the classical nuclear PR in systemic immune cells. Notably, mPR is structurally unrelated to nuclear PR and acts via non-genomic signalling pathways (Wehling, 1997). Studies performed in a human breast cancer cell line demonstrated that progesterone has a high binding affinity of K_d of 4-8 nM to recombinant human mPR, while the progestins DHT and NET displayed no

competitive binding to mPR. The relative binding affinity of MPA to mPR is yet to be determined (Thomas et al., 2007, Thomas, 2008, Stanczyk et al., 2013). Taken together these findings highlight the need for further investigation into the actions, binding affinities and responses of progestogens mediated via the mPR in systemic immune cells.

While some non-genomic effects due to progesterone may be mediated by the mPR in the absence of nuclear PR, SR receptor theory suggest that the majority of progesterone-induced effects, as well as those of other progestins are often regulated by other SRs, such as AR, ER, GR and MR (Hapgood et al., 2014b). For instance, progesterone, MPA, NET and LNG have been shown to bind to the AR, where they can act as agonists or antagonists (Kemppainen et al., 1999, Africander et al., 2011, Africander et al., 2014, Louw-du Toit et al., 2017). Other studies showed that MPA and NET do not activate the MR at contraceptive doses, while progesterone displayed both agonistic and antagonistic activity via the MR (Fuhrmann et al., 1996, Quinkler and Diederich, 2002, Africander et al., 2013). MPA and NET did not activate the ER at normal serum concentrations of HC users, but progesterone seemed to exhibit anti-estrogenic properties (Louw-du Toit et al., 2017). Therefore, further research is needed to delineate the contributions of non-genomic versus genomic pathways and to explore how progestogens interact with multiple SRs in different tissue types, including immune cells.

4.2.3. High expression of GR relative to PR in PBMCs suggest that ligands that bind to both receptors likely exert more GR effects in systemic $CD3^+$, $CD4^+$, $CD8^+$ and $CD14^+$ cells

Given that GR is known for its role in immune function, it is not surprising that it was expressed in systemic immune cells, including $CD3^+$, $CD4^+$, $CD8^+$ and $CD14^+$ cells. The GR expression densities among $CD3^+$, $CD4^+$, $CD8^+$ and $CD14^+$ cells were not significantly different, while the cellular frequency of GR^+ cells in T lymphocytes ($CD3^+$, $CD4^+$ and $CD8^+$ cells) was significantly higher than in monocytes ($CD14^+$ cells). T lymphocytes are key components of the adaptive immune system that regulate immune function by secreting cytokines and chemokines (Swain et al., 2012). Monocytes are professional antigen-presenting cells and phagocytes that form part of the innate immune system (Kapellos et al., 2019). The difference in the cellular frequency of GR-expressing T lymphocytes and GR-expressing monocytes may be attributed to their specific functions. The higher frequency of T lymphocytes compared to monocytes expressing GR may occur because T lymphocytes induce specific cell-mediated responses to foreign pathogens requiring regulation by glucocorticoids, while monocytes phagocytose pathogens to control infections.

The thesis findings describing the relatively high expression of GR in systemic $CD3^+$, $CD4^+$, $CD8^+$ and $CD14^+$ cells suggest that progesterone and progestins may exert glucocorticoid-like effects in these systemic immune cells. Progesterone and NET have a relatively low binding affinity for the GR, while MPA possesses a relatively high binding affinity for the GR. (Africander et al., 2011, Hapgood et al., 2014b). Studies in human leukocytes *in vitro* have shown that MPA exhibits more potent competitive binding to the GR than that of the endogenous glucocorticoid, cortisol (Kontula et al., 1983). Dose-response analyses conducted *in vitro* indicated that progesterone exhibits weak agonistic activity via the GR, MPA exhibits partial to full agonistic properties, while NET does not activate gene regulation via the GR. MPA also induced regulation of anti- and pro-inflammatory genes via the GR at concentrations ranging from 1-100 nM *in vitro* (Govender et al., 2014, Hapgood et al., 2014a, Maritz et al.,

2018). Serum concentrations of MPA can reach up to 65 nM, while NET concentrations range from 10 to 50 nM post-HCs administration (Africander et al., 2011, Hapgood et al., 2014b, Govender et al., 2014). Endogenous progesterone concentrations in serum peak at 80 nM during the luteal phase and may reach up to 1 µM during pregnancy (Lissauer et al., 2015). Altogether, these data highlight the potential for systemic immune cells to respond to progestogens via the GR. The relatively high serum concentrations of endogenous progesterone during the luteal phase of the menstrual cycle and pregnancy as well as MPA following HC administration may result in significant GR-mediated effects on immune cells' gene regulation.

It is well known that the GR modulates the expression of anti- and pro-inflammatory cytokines and chemokines (Lawrence, 2009, Cruz-Topete and Cidlowski, 2014, Moss and Jaffe, 2015, Fedotcheva et al., 2022). At physiological serum concentrations, progesterone and progestins can act via the GR in systemic immune cells (Hapgood et al., 2018, Fedotcheva et al., 2022). Similar to GCs, progesterone possesses anti-inflammatory and immunomodulatory properties (Fedotcheva et al., 2022). Treatment of PBMCs with progesterone *in vitro* suppressed secretion of RANTES, MIP1α, and MIP1β in $CD8^+$ cells (Vassiliadou et al., 1999). High exogenous progesterone levels promoted Th2-type anti-inflammatory responses in a human $CD4^+$ T cell line by increasing the production of IL-4 and IL-10 (Piccinni et al., 1995, Mauvais-Jarvis et al., 2020). MPA was also demonstrated *in vitro* to repress the IL-2 gene, an effect similar to that of the synthetic glucocorticoid, dexamethasone in normal human lymphocytes (Bamberger et al., 1999). Other *in vitro* studies reported that MPA, but not NET and LNG, inhibited the activation of human primary T cells and plasmacytoid dendritic cells (Huijbregts et al., 2014). Hence, these findings suggest that progesterone and certain progestins, particularly MPA, may mimic glucocorticoid-like effects in immune cells through GR-mediated pathways.

Further research also supported a mechanism by which the GR was involved in mediating the actions of MPA and/or progesterone. In primary $CD4^+$ T cells, MPA increased apoptosis similarly to the glucocorticoids, dexamethasone and cortisol, while progesterone and NET did not (Tomasicchio et al., 2013). By using the GR antagonist, RU486, the authors showed that the increase in apoptosis was mediated by a mechanism involving the GR (Tomasicchio et al., 2013). Moreover, MPA exhibited glucocorticoid activity similar to dexamethasone, by suppressing the human IL-2 promoter and protein levels of IL-2 and IL-6 in PBMCs *in vitro.* Some of these effects were reversed when GR was knocked down by siRNA. (Bick, 2018, Maritz et al., 2018). These reports provide evidence that certain progestogen can exert potent glucocorticoid-like effects in immune cells via the GR.

Altogether, the findings of this study and other reported studies support a role for the GR in regulating immune responses in systemic $CD3^+$, $CD4^+$, $CD8^+$ and $CD14^+$ cells, particularly in response to elevated levels of progesterone and MPA at normal concentrations in HC users.

Chapter 5: Conclusions, Limitations and Future Perspectives

5.1. Conclusions

The sequence and structural homology between GR and PR have led researchers to explore the cross-receptor binding of their ligands. Cross-receptor binding is also applicable to cross-reactivity of their antibodies, which can result in erroneous outcomes when using sensitive protein detection methods, particularly immunofluorescence staining and flow cytometry. Hence, this study analysed the potential cross-reactivity of GR and PR primary antibodies to improve the reliability of protein detection methods. Using overexpression strategies in COS1 cells, none of the primary antibodies to GR and PR used for detection cross-reacted to their non-corresponding proteins.

GR was discovered to be expressed in both FGT and systemic tissues as well as all types of immune cells investigated, consistent with its pleiotropic functions in humans. GR expression was not detected in every FGT $CD4^+$ and $CD8^+$ cell, while flow cytometry results indicate that GR expression is ubiquitous in T lymphocytes, i.e., $CD3^+$, $CD4^+$ and $CD8^+$ cells, as well as in $CD14^+$ monocytes. The difference in GR expression observed between FGT and systemic immune cells may be due to inconsistencies in sensitivity between the two detection methods. However, these differences they may also reflect real differences in the GR expression levels in FGT immune cells versus systemic cell types, which are likely to be exposed to different signals that may regulate the levels of the receptor. On the other hand, PR expression was limited to cells of the stroma and a small number of cells of the epithelium in the FGT. However, PR expression levels in systemic $CD3^+$, $CD4^+$, $CD8^+$ and $CD14^+$ cells are either

relatively undetectable compared to the GR, or absent. Nevertheless, undetectable PR expression in FGT $CD4^+$ and $CD8^+$ cells by immunofluorescence staining is consistent with the flow cytometry results, providing compelling evidence that PR expression was relatively low or absent in both FGT and systemic immune cells.

Additionally, the discovery of relatively high levels of the GR compared to the PR in FGT epithelial cells, FGT $CD4^+$ and FGT $CD8^+$ cells, as well as systemic $CD3^+$, $CD4^+$, $CD8^+$ and $CD14^+$ cells, indicates that progestogens may exhibit substantial binding to the GR in these tissues and cells relevant for control of immunity and women's reproductive health. However, the receptor-specific actions of progestogens depend on their relative affinities for GR vs PR, concentration of endogenous steroids and functional activities across different SRs, which are hard to predict. While off-target binding of progesterone to the GR may contribute to immune changes to support foetal-maternal tolerance when progesterone levels are high, off-target GR binding by progestins can lead to effects on immunoregulatory genes coding for coreceptors, cytokines, chemokines, and anti- and pro-inflammatory markers. These changes could influence barrier integrity in the FGT epithelium, as well as recruitment, differentiation and distribution of FGT resident or systemic immune cells, with implications for immunity in women on progestin-based MHT or HCs.

5.2. Limitations

This study focused on the investigation of GR and PR levels, but other SRs, such as the AR and MR, also exhibit homology in their sequence and structures. Off-target binding of PR ligands to these SRs is also an important line of research, and the primary antibodies of GR and PR may bind to these SRs, though this was not examined. Moreover, GR and PR exist in

multiple isoforms with variable ligand-binding and transcriptional activity profiles. The antibodies used in this study targeted the primary isoforms, GRα, PR-A and PR-B, but did not comprehensively account for all possible isoforms. Notably, a recent report has shown variable expression levels of PR isoforms A, B and C in systemic $CD4^+$, $CD8^+$ and $CD56^+$ cells, suggesting an isoform-specific distribution between immune cell types but did not assess cross-reactivity of primary antibodies (Holmberg et al., 2024). In the FGT, PR isoforms A and B have also been shown to be expressed (Ackerman et al., 2016, Ray et al., 2019).

Furthermore, while PR expression was confirmed in some ectocervical cells, the cell types expressing PR remains unknown, as specific markers for fibroblasts, smooth muscles, and lymphatic, nerve and vascular cells were not investigated by immunofluorescence. Simultaneous analysis of GR and PR expression in FGT tissue explants was also attempted but was hindered as the unconjugated antibodies were of the same species, and there seemed to be some compatibility issues with the conjugated antibodies. Ultimately, the co-localisation of GR and PR within individual cells could not be determined via this strategy.

Additionally, the number of donors of ectocervical tissue explants (n=3) and blood bank donors (n=6) was small, limiting the scope of statistical analysis. The tissue explants were also not visualised on the same microscope due to technical issues. Moreover, the PBMC donors could not be classified according to their phase of the menstrual cycle due to a lack of data on their hormone levels. The expression levels of SRs, particularly GR and PR, are regulated by multiple signalling molecules including endogenous and exogenous hormones, such as progesterone, progestins and E_2 (Ackerman et al., 2016, Bick et al., 2022). This was not accounted for in this study as the sample sizes were small, and information on the hormone levels of both the tissue the PBMC donors was not available.

5.3. Future perspectives

Some refinements on the technical aspects for the detection of GR and PR, particularly by flow cytometry, are required, to fully eliminate non-specific signals. This can be addressed by optimising antibody selection for all the markers or correcting for fluorescence spillover, *i.e.*, removing signal from all the fluorochromes except for the antibody of interest. Regarding immunofluorescence staining of tissue explants, simultaneous detection of GR and PR could reveal whether individual FGT cells and immune cells express GR or PR or both. Furthermore, it was beyond the scope of this study to analyse GR and PR expression in all cell types. This includes fibroblasts cells, smooth muscle cells in FGT tissue as well as other immune cells in FGT tissues and PBMCs such as monocytes ($CD14^+$ cells) in the FGT, which are known to be susceptible to viruses, and NK cells ($CD56^+$ cells), which are a key component of immune regulation during pregnancy. Since NK cells are the only immune cells known to express PR, this line of investigation may provide a more comprehensive understanding of PR expression patterns across immune cell types. Thus, these above-mentioned suggestions may produce a more comprehensive understanding results on PR expression in immune cells and provide more detailed information on the expression of GR and PR.

Further research should also explore the expression of other SRs, namely, the AR, ER and MR, as PR ligands are known to cross-react with these receptors (Africander et al., 2011). The cross-reactivity of the antibodies to other SRs should also be assessed, as well as those of GR and PR. Furthermore, the expression of specific SR isoforms, the binding affinities, relative affinities and potencies of the PR ligands for the multiple SRs and their isoforms could be

investigated, which would provide information on the possible SRs mediating responses in specific types of cells.

Additionally, larger FGT sample collections from women across different menstrual cycle phases or those using HCs are needed, to better understand how hormonal fluctuations influence SR expression. A similar approach for PBMC samples would allow the exploration of differences in SR expression, if any, in $CD3^+$, $CD4^+$, $CD8^+$ and $CD14^+$ cells. In addition, it may be valuable to perform *in vitro* stimulation of FGT tissues and PBMCs with physiological concentrations of reproductive hormones/progestins – such as during follicular vs luteal phase of the menstrual cycle, pre- vs post-menopausal, pregnancy or in women before and after contraceptive initiation – to assess the impact of hormonal variations on SR expression in these cells.

Lastly, further research is warranted to explore the association between SR levels and cross-receptor binding with altered immune regulation or increased susceptibility to STIs. For example, changes in expression levels of co-receptors and inflammatory markers or distribution of susceptible target cells in response to changes in the GR to PR ratio could be explored. This may shed light on mechanisms by which differential immune regulation is associated with SR ligands.

Chapter 6: Appendix

6.1. NHLS guidelines for menstrual phase cycle

Supplementary Table 6.1: Reference concentrations of endogenous reproductive hormones, LH, FSH, E_2 and progesterone across distinct phases of the menstrual cycle, as established by the NHLS (Kratz et al., 2004).

LH reference ranges	
Follicular phase	2.4 – 12.6 IU/L
Ovulatory phase	14.0 – 95.6 IU/L
Luteal phase	1.0 – 11.4 IU/L
Postmenopausal	7.7 – 58.5 IU/L
FSH reference ranges	
Follicular phase	3.5 – 12.5 IU/L
Ovulatory phase	4.7 – 21.5 IU/L
Luteal phase	1.7 – 7.7 IU/L
Postmenopausal	25.8 – 134.8 IU/L
E_2 reference ranges	
Follicular phase	46 – 608 pmol/L
Ovulatory phase	315 – 1828 pmol/L
Luteal phase	161 – 775 pmol/L
Postmenopausal	<18 – 201 pmol/L
Progesterone reference ranges	
Follicular phase	0.6 – 4.7 nmol/L
Ovulatory phase	2.4 – 9.4 nmol/L
Luteal phase	5.3 – 86.0 nmol/L
Postmenopausal	0.3 – 2.5 nmol/L

6.2. Immunofluorescence controls

Single-stain controls of extracellular markers were visualised by immunofluorescence and were set up as negative controls for GR and PR staining. This was to ensure, as far as possible, that signals obtained for GR and PR are specific. Tissue sections were stained as previously

described with the same combinations and dilutions of primary and secondary antibodies, except that primary antibodies for GR and PR were replaced with 1% BSA in PBS-T. As expected, green fluorescence for GR and PR in the AF488 channel was not detected in the ectocervical cells when tissue explants were stained for either CD4 or CD8 only. This indicates that non-specific immunofluorescence signals for GR or PR in CD4 and CD8 cells were not obtained.

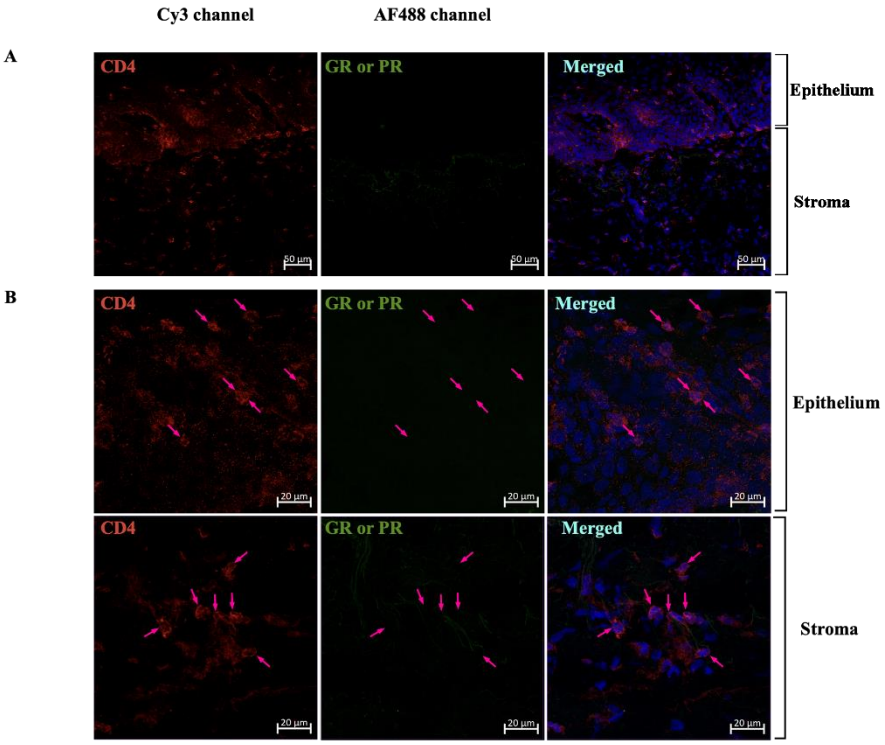

Supplementary Figure 6.2.1: Single stain control of CD4 markers. Ectocervical tissue sections were stained with rabbit anti-CD4 and anti-rabbit Cy3 antibodies, followed by anti-mouse AF488 secondary antibodies. (A) A snapshot was captured at 20X magnification, showing $CD4^+$ cells in the epithelial and stromal layers of the ectocervix. (**B**) MIP of z-stack images at 63X magnification capturing $CD4^+$ cells in the epithelial and stromal tissue layers. Panel 1: Red fluorescence (CD4 staining) visualised on the Cy3 channel; Panel 2: Green fluorescence (GR staining) visualised on the AF488 channel; Panel 3: Merged image of both

channels with DAPI channel (nuclei staining). Confocal images of a representative donor (PROG 179) are shown. The pink arrows indicate cells positive staining for CD4 markers.

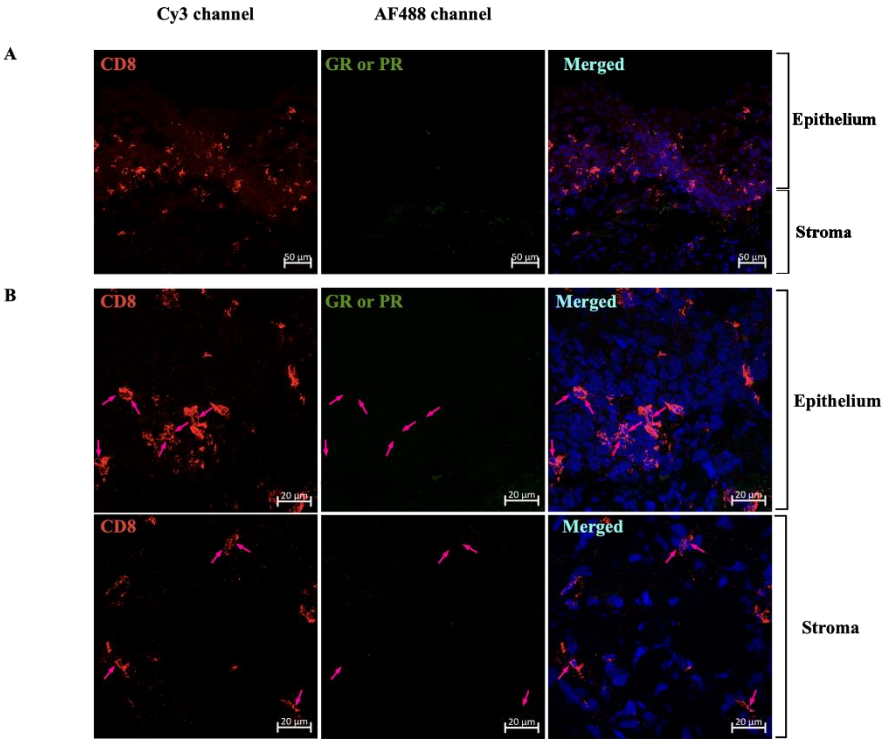

Supplementary Figure 6.2.2: Single stain control of CD8. Ectocervical tissue sections were stained with rabbit anti-CD8 and anti-rabbit Cy3 antibodies, followed by anti-mouse AF488 secondary antibodies. (A) A snapshot was captured at 20X magnification, showing $CD8^+$ cells in the epithelial and stromal layers of the ectocervix. (**B**) MIP of z-stack images at 63X magnification capturing $CD8^+$ cells in the epithelial and stromal tissue layers. Panel 1: red fluorescence (CD8 staining) visualised on the Cy3 channel; Panel 2: green fluorescence (GR staining) visualised on the AF488 channel; Panel 3: merged image of both channels with DAPI channel (nuclei staining). Confocal images of a representative donor (PROG 179) are shown. The pink arrows indicate cells positive staining for CD4 markers.

6.3. PR expression in ectocervical epithelial cells

PR protein expression was also detected in the basal epithelial layer of the ectocervix in one of the donors, PROG 173, where relatively faint fluorescence of PR staining was visible in cells of the basal membrane. Fluorescently labelled nuclei were also apparent in ectocervical stromal cells of the same donor. Merged images indicate that PR is expressed in the nuclei of the cells.

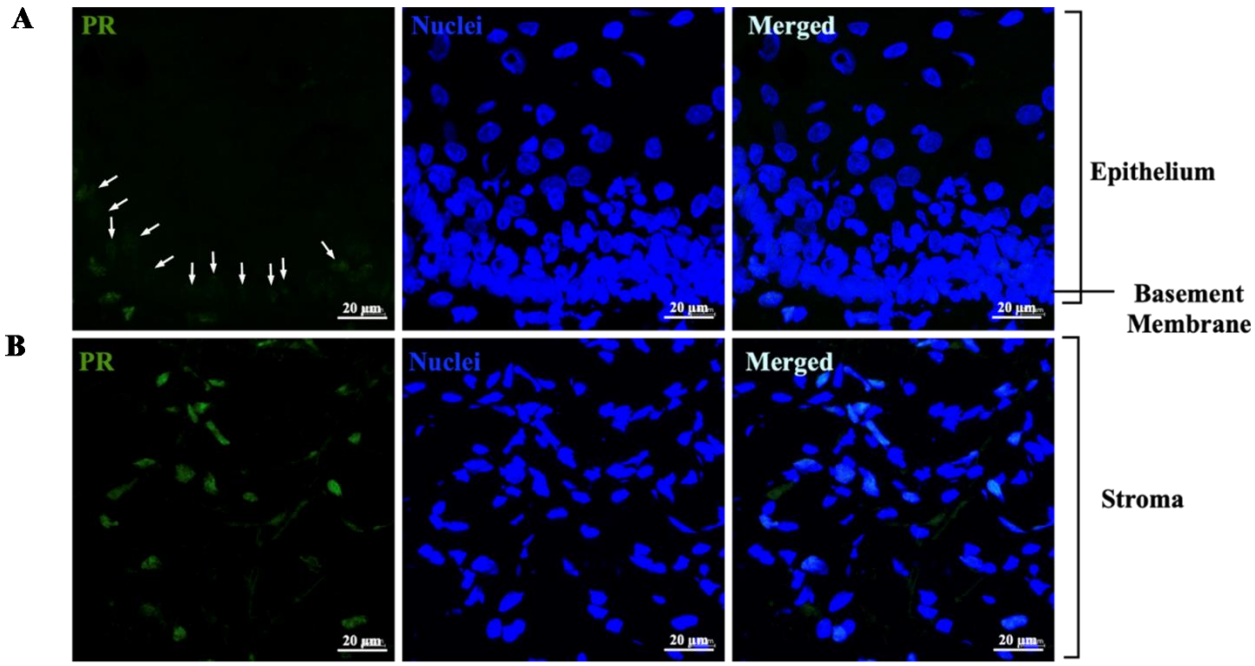

Supplementary Figure 6.3.1: Relatively faint staining of PR in ectocervical epithelial cells. Ectocervical tissue explants were sectioned at 8 µm, and the sections were stained with anti-PR and anti-mouse AF488. The sections were then counterstained with Hoescht and visualised by confocal microscopy. (A) MIP of z-stack images captured at 63X magnification in the epithelial region. (B) MIP of z-stack images captured at 63X magnification in the stromal region. Panel 1: green fluorescence (PR staining) visualised on the AF488 channel; Panel 2: nuclei staining (Hoescht) visualised on the DAPI channel; Panel 3: merged image of both

channels. Confocal images of the donor, PROG 173, are shown. The white arrows indicate epithelial cells with faint green fluorescence staining for PR.

6.4. Ethics approval

UNIVERSITY OF CAPE TOWN
Faculty of Health Sciences
Human Research Ethics Committee

Room 45 E-52-E-Floor- Old Main Building
Groote Schuur Hospital
Observatory 7925
Telephone [021] 406 6492
Email: hrec-submissions@uct.ac.za
Website: https://health.uct.ac.za/home/human-research-ethics

26 September 2022

HREC REF: 590/2022

Prof J Hapgood
Division of Molecular & Cell Biology
University Avenue, UCT
Email: janet.hapgood@uct.ac.za
Student: Apppre003@myuct.ac.za

Dear Prof Hapgood

PROJECT TITLE: RELATIVE LEVELS OF GLUCOCORTICOID AND PROGESTERONE RECEPTOR: IMPLICATIONS FOR CONTRACEPTION AND HIV-SUB-STUDY LINKED TO 210/2011 (MSC CANDIDATE-MISS PRETTYSHA APPADOO)

Thank you for submitting your study to the Faculty of Health Sciences Human Research Ethics Committee (HREC) for review.

It is a pleasure to inform you that the HREC has **formally approved** the above-mentioned study.

Approval is granted for one year until the 30 September 2023.

Please submit a progress form, using the standardised Annual Report Form (FHS016) if the study continues beyond the approval period. Please submit a Standard Closure form if the study is completed within the approval period.
(Forms can be found on our website: www.health.uct.ac.za/fhs/research/humanethics/forms)

The HREC acknowledge that the student: Miss Prettysha Appadoo will also be involved in this study.

Please quote the HREC REF 590/2022 in all your correspondence.

Please note that the ongoing ethical conduct of the study remains the responsibility of the principal investigator.

Please note that for all studies approved by the HREC, the principal investigator **must** obtain appropriate institutional approval, where necessary, before the research may occur.

Yours sincerely

PROFESSOR M BLOCKMAN
CHAIRPERSON, FACULTY OF HEALTH SCIENCES HUMAN RESEARCH ETHICS COMMITTEE
Federal Wide Assurance Number: FWA00001637. Institutional Review Board (IRB) number: IRB00001938 NHREC-registration number: REC-210208-007

HREC/ref 590.2022

This serves to confirm that the University of Cape Town Human Research Ethics Committee complies to the Ethics Standards for Clinical Research with a new drug in patients, based on the Medical Research Council (MRC-SA), Food and Drug Administration (FDA-USA), International Council for Harmonisation of Technical Requirements for Pharmaceuticals for Human Use: Good Clinical Practice (ICH GCP), South African Good Clinical Practice Guidelines (DoH 2020), based on the Association of the British Pharmaceutical Industry Guidelines (ABPI), and Declaration of Helsinki (2013) guidelines. The Human Research Ethics Committee granting this approval is in compliance with the ICH Harmonised Tripartite Guidelines E6: Note for Guidance on Good Clinical Practice (CPMP/ICH/135/95) and FDA Code Federal Regulation Part 50, 56 and 312.

HREC/ref 590.2022

UNIVERSITY OF CAPE TOWN
IYUNIVESITHI YASEKAPA • UNIVERSITEIT VAN KAAPSTAD

FACULTY OF HEALTH SCIENCES
Human Research Ethics Committee

FHS017: Annual Progress Report / Renewal

Record Reviews/Audits/Collection of Biological Specimens/Repositories/Databases/Registries

HREC office use only (FWA00001637; IRB00001938)			
This serves as notification of annual approval, including any documentation described below.			
☑ Approved	Annual progress report	Approved until/next renewal date	30.9.2024
☐ Not approved	See attached comments		
Signature Chairperson of the HREC/ Designee		Date Signed	11/9/2023

Note: Please note that incomplete submissions will not be reviewed.
Please email this form and supporting documents (if applicable) in a combined pdf-file to hrec-enquiries@uct.ac.za.

HUMAN RESEARCH ETHICS COMMITTEE
11 SEP 2023
HEALTH SCIENCES FACULTY
UNIVERSITY OF CAPE TOWN

Please clarify your plan for research-related activities during COVID-19 lockdown

Principal Investigator to complete the following:

1. Protocol information

Date (when submitting this form)	08/09/2023		
HREC REF Number	590/2022	Current Ethics Approval was granted until	30/09/2023
Protocol title	Relative levels of glucocorticoid and progesterone receptors: Implications for contraception and HIV		
Principal Investigator	Prof. Janet Hapgood		
Department / Office Internal Mail Address	Department of Molecular and Cell Biology Molecular and Cell Biology Building, 22 University Avenue, University of Cape Town, Rondebosch 7700		
1.1 Does this protocol receive US Federal funding?		☐ Yes	✔ No

2. Protocol status (tick ✓)

✔	Research-related activities are ongoing
☐	Data collection is complete, data analysis only
Please indicate (in the block below) the titles and HREC reference numbers of any projects currently making use of the Database/registry/repository.	

3. Protocol summary

Total number of records or specimens collected, reviewed or stored since the original approval		26
Total number of records or specimens collected, reviewed or stored since last progress report		26
Have any research-related outputs (e.g. publications, abstracts, conference presentations) resulted from this research? If yes, please list and attach with this report.	☐ Yes	✔ No

4. Signature

Signature of PI		Date	08/09/2023

UNIVERSITY OF CAPE TOWN
IYUNIVESITHI YASEKAPA • UNIVERSITEIT VAN KAAPSTAD

FACULTY OF HEALTH SCIENCES
Human Research Ethics Committee

FHS017: Annual Progress Report / Renewal

Record Reviews/Audits/Collection of Biological Specimens/Repositories/Databases/Registries

HREC office use only (FWA00001637; IRB00001938)			
This serves as notification of annual approval, including any documentation described below.			
☑ Approved	Annual progress report	Approved until/next renewal date	30.9.2025
☐ Not approved	See attached comments		
Signature Chairperson of the HREC/ Designee		Date Signed	18/9/2024

Note: Please note that incomplete submissions will not be reviewed.
Our website address: **https://health.uct.ac.za/home/human-research-ethics**

HUMAN RESEARCH ETHICS COMMITTEE
17 SEP 2024
HEALTH SCIENCES FACULTY
UNIVERSITY OF CAPE TOWN

Please email this form and supporting documents (if applicable) in a combined pdf-file to hrec-enquiries@uct.ac.za.

Principal Investigator to complete the following:

1. Protocol information

Date (when submitting this form)	16/09/2024		
HREC REF Number	590/2022	Current Ethics Approval was granted until	30/09/2024
Protocol title	Relative levels of glucocorticoid and progesterone receptors: Implications for contraception and HIV		
Principal Investigator	Prof. Janet Hapgood		
Department and email address	Department of Molecular and Cell Biology Molecular and Cell Biology Building, 22 University Avenue, University of Cape Town, Rondebosch 7700		
1.1 Does this protocol receive US Federal funding?		☐ Yes	✓ No

2. Protocol status (tick ✓)

☐	Research-related activities are ongoing
✓	Data collection is complete, data analysis only
☐	Publication or thesis submitted and final completion?
Please indicate (in the block below) the titles and HREC reference numbers of any projects currently making use of the Database/registry/repository.	

3. Protocol summary

Total number of records or specimens collected, reviewed or stored since the original approval		39
Total number of records or specimens collected, reviewed or stored since last progress report		13
Have any research-related outputs (e.g. publications, abstracts, conference presentations) resulted from this research? If yes, please list and attach with this report.	☐ Yes	✓ No
Please complete the Closure form (FHS019) if the study is completed within the approval period		

4. Signature

Signature of PI		Date	16/09/2024

References

ACKERMAN, W. E., SUMMERFIELD, T. L., MESIANO, S., SCHATZ, F., LOCKWOOD, C. J. & KNISS, D. A. 2016. Agonist-Dependent Downregulation of Progesterone Receptors in Human Cervical Stromal Fibroblasts. *Reproductive sciences (Thousand Oaks, Calif.),* 23, 112-123.

AFRICANDER, D., LOUW, R. & HAPGOOD, J. P. 2013. Investigating the anti-mineralocorticoid properties of synthetic progestins used in hormone therapy. *Biochemical and Biophysical Research Communications,* 433, 305-310.

AFRICANDER, D., VERHOOG, N. & HAPGOOD, J. P. 2011. Molecular mechanisms of steroid receptor-mediated actions by synthetic progestins used in HRT and contraception. *Steroids,* 76, 636-652.

AFRICANDER, D. J., STORBECK, K.-H. & HAPGOOD, J. P. 2014. A comparative study of the androgenic properties of progesterone and the progestins, medroxyprogesterone acetate (MPA) and norethisterone acetate (NET-A). *The Journal of Steroid Biochemistry and Molecular Biology,* 143, 404-415.

ALTIERI, B., MUSCOGIURI, G., PASCHOU, S., VRYONIDOU - BOMPOTA, A., DELLA CASA, S., PONTECORVI, A., FASSNACHT, M., RONCHI, C. & NEWELL-PRICE, J. 2018. Adrenocortical incidentalomas and bone: from molecular insights to clinical perspectives. *Endocrine,* 62.

ANDERSSON, G., LUNDGREN, S., HEBY, M., NODIN, B., ELEBRO, J. & JIRSTRÖM, K. 2019. Clinical significance of stromal ER and PR expression in periampullary adenocarcinoma. *Biomarker Research,* 7.

AQUILA, S. & DE AMICIS, F. 2014. Steroid receptors and their ligands: effects on male gamete functions. *Exp Cell Res,* 328, 303-13.

ARRIZA, J. L., WEINBERGER, C., CERELLI, G., GLASER, T. M., HANDELIN, B. L., HOUSMAN, D. E. & EVANS, R. M. 1987. Cloning of human mineralocorticoid receptor complementary DNA: structural and functional kinship with the glucocorticoid receptor. *Science,* 237, 268-75.

ARRUVITO, L., GIULIANELLI, S., FLORES, A. C., PALADINO, N., BARBOZA, M., LANARI, C. & FAINBOIM, L. 2008. NK cells expressing a progesterone receptor are susceptible to progesterone-induced apoptosis. *J Immunol,* 180, 5746-53.

ASIN, S. N., HEIMBERG, A. M., ESZTERHAS, S. K., ROLLENHAGEN, C. & HOWELL, A. L. 2008. Estradiol and progesterone regulate HIV type 1 replication in peripheral blood cells. *AIDS Res Hum Retroviruses,* 24, 701-16.

BAMBERGER, A. M., MILDE-LANGOSCH, K., LÖNING, T. & BAMBERGER, C. M. 2001. The glucocorticoid receptor is specifically expressed in the stromal compartment of the human endometrium. *J Clin Endocrinol Metab,* 86, 5071-4.

BAMBERGER, C. M., ELSE, T., BAMBERGER, A. M., BEIL, F. U. & SCHULTE, H. M. 1999. Dissociative glucocorticoid activity of medroxyprogesterone acetate in normal human lymphocytes. *J Clin Endocrinol Metab,* 84, 4055-61.

BARNES, P. J. 1998. Anti-inflammatory Actions of Glucocorticoids: Molecular Mechanisms. *Clinical Science,* 94, 557-572.

BEATO, M. & KLUG, J. 2000. Steroid hormone receptors: an update. *Hum Reprod Update,* 6, 225-36.

BHOWMICK, D. & BUSHNELL, T. P. 2024. How to Measure "Spillover Spread". *Methods Mol Biol,* 2779, 69-83.

BICK, A. J. 2018. ***Cross talk between the glucocorticoid receptor and the progesterone receptor in modulation of progestin responses and HIV-1 infection.*** **Doctor of Philosophy, University of Cape Town.**

BICK, A. J., AVENANT, C., TOMASICCHIO, M., VAN DER SPUY, Z. & HAPGOOD, J. P. 2022. Increased HIV-1 infection in PBMCs treated in vitro with menstrual cycle phase hormones or medroxyprogesterone acetate likely occurs via different mechanisms. ***American Journal of Reproductive Immunology,*** **88, e13643.**

BICK, A. J., LOUW-DU TOIT, R., SKOSANA, S. B., AFRICANDER, D. & HAPGOOD, J. P. 2021. Pharmacokinetics, metabolism and serum concentrations of progestins used in contraception. ***Pharmacology & therapeutics (Oxford),*** **222, 107789-107789.**

BOUMPAS, D. T., CHROUSOS, G. P., WILDER, R. L., CUPPS, T. R. & BALOW, J. E. 1993. Glucocorticoid therapy for immune-mediated diseases: basic and clinical correlates. ***Ann Intern Med,*** **119, 1198-208.**

BRADLEY, F., FRANZÉN BOGER, M., KALDHUSDAL, V., ÅHLBERG, A., EDFELDT, G., LAJOIE, J., BERGSTRÖM, S., OMOLLO, K., DAMDIMOPOULOS, A., CZARNEWSKI, P., MÅNBERG, A., OYUGI, J., KIMANI, J., NILSSON, P., FOWKE, K., TJERNLUND, A. & BROLIDEN, K. 2022. Multi-omics analysis of the cervical epithelial integrity of women using depot medroxyprogesterone acetate. ***PLOS Pathogens,*** **18, e1010494.**

BRUNDIN, P. M. A., LANDGREN, B.-M., FJÄLLSTRÖM, P., SHAMEKH, M. M., GUSTAFSSON, J.-Å., JOHANSSON, A. F. & NALVARTE, I. 2021. Expression of Sex Hormone Receptor and Immune Response Genes in Peripheral Blood Mononuclear Cells During the Menstrual Cycle. ***Frontiers in endocrinology (Lausanne),*** **12, 721813-721813.**

BUXANT, F., BUCELLA, D., ANAF, V., SIMON, P. & NOEL, J.-C. 2009. Glucocorticoid receptor expression in cervical intraepithelial neoplasia and invasive squamous cell carcinoma of the cervix. ***European journal of gynaecological oncology,*** **30, 259-62.**

BYRNE, E. H., ANAHTAR, M. N., COHEN, K. E., MOODLEY, A., PADAVATTAN, N., ISMAIL, N., BOWMAN, B. A., OLSON, G. S., MABHULA, A., LESLIE, A., NDUNG'U, T., WALKER, B. D., GHEBREMICHAEL, M. S., DONG, K. L. & KWON, D. S. 2016. Association between injectable progestin-only contraceptives and HIV acquisition and HIV target cell frequency in the female genital tract in South African women: a prospective cohort study. ***Lancet Infect Dis,*** **16, 441-8.**

CAIRNS, C., CAIRNS, W. & OKRET, S. 1993. Inhibition of gene expression by steroid hormone receptors via a negative glucocorticoid response element: evidence for the involvement of DNA-binding and agonistic effects of the antiglucocorticoid/antiprogestin RU486. ***DNA Cell Biol,*** **12, 695-702.**

CANO, A., SERRA, V., RIVERA, J., MONMENEU, R. & MARZO, C. 1990. Expression of estrogen receptors, progesterone receptors, and an estrogen receptor-associated protein in the human cervix during the menstrual cycle and menopause. ***Fertil Steril,*** **54, 1058-64.**

CARATTI, G., MATTHEWS, L., POOLMAN, T., KERSHAW, S., BAXTER, M. & RAY, D. 2015. Glucocorticoid receptor function in health and disease. ***Clin Endocrinol (Oxf),*** **83, 441-8.**

CHANDRA, N., THURMAN, A. R., ANDERSON, S., CUNNINGHAM, T. D., YOUSEFIEH, N., MAUCK, C. & DONCEL, G. F. 2012. Depot Medroxyprogesterone Acetate Increases Immune Cell Numbers and Activation Markers in Human Vaginal Mucosal Tissues. ***AIDS Research and Human Retroviruses,*** **29, 592-601.**

CONNEELY, O. M., MULAC-JERICEVIC, B., DEMAYO, F., LYDON, J. P. & O'MALLEY, B. W. 2002. Reproductive functions of progesterone receptors. ***Recent Prog Horm Res,*** **57, 339-55.**

CRUZ-TOPETE, D. & CIDLOWSKI, J. A. 2014. One Hormone, Two Actions: Anti- and Pro-Inflammatory Effects of Glucocorticoids. ***Neuroimmunomodulation,*** **22, 20-32.**

DE TOMASI, J. B., OPATA, M. M. & MOWA, C. N. 2019. Immunity in the Cervix: Interphase between Immune and Cervical Epithelial Cells. ***Journal of immunology research,*** **2019, 7693183-13.**

DEHM, S. M. & TINDALL, D. J. 2007. Androgen receptor structural and functional elements: role and regulation in prostate cancer. ***Mol Endocrinol,*** **21, 2855-63.**

DINH, D. T., BREEN, J., AKISON, L. K., DEMAYO, F. J., BROWN, H. M., ROBKER, R. L. & RUSSELL, D. L. 2019. Tissue-specific progesterone receptor-chromatin binding and the regulation of progesterone-dependent gene expression. ***Scientific Reports,*** **9, 11966.**

DONAGHY, H., STEBBING, J. & PATTERSON, S. 2004. Antigen presentation and the role of dendritic cells in HIV. ***Curr Opin Infect Dis,*** **17, 1-6.**

DOSIOU, C., HAMILTON, A. E., PANG, Y., OVERGAARD, M. T., TULAC, S., DONG, J., THOMAS, P. & GIUDICE, L. C. 2008. Expression of membrane progesterone receptors on human T lymphocytes and Jurkat cells and activation of G-proteins by progesterone. ***J Endocrinol,*** **196, 67-77.**

DU, J., LI, M., ZHANG, D., ZHU, X., ZHANG, W., GU, W., FENG, Y., ZHAI, X. & LING, C. 2009. Flow cytometry analysis of glucocorticoid receptor expression and binding in steroid-sensitive and steroid-resistant patients with systemic lupus erythematosus. ***Arthritis Research & Therapy,*** **11, R108.**

EDFELDT, G., LAJOIE, J., RÖHL, M., OYUGI, J., ÅHLBERG, A., KHALILZADEH-BINICY, B., BRADLEY, F., MACK, M., KIMANI, J., OMOLLO, K., WÄHLBY, C., FOWKE, K. R., BROLIDEN, K. & TJERNLUND, A. 2022. Regular Use of Depot Medroxyprogesterone Acetate Causes Thinning of the Superficial Lining and Apical Distribution of Human Immunodeficiency Virus Target Cells in the Human Ectocervix. ***The Journal of infectious diseases,*** **225, 1151-1161.**

FEDOTCHEVA, T. A., FEDOTCHEVA, N. I. & SHIMANOVSKY, N. L. 2022. Progesterone as an Anti-Inflammatory Drug and Immunomodulator: New Aspects in Hormonal Regulation of the Inflammation. ***Biomolecules,*** **12, 1299.**

FUHRMANN, U., KRATTENMACHER, R., SLATER, E. P. & FRITZEMEIER, K.-H. 1996. The novel progestin drospirenone and its natural counterpart progesterone: Biochemical profile and antiandrogenic potential. ***Contraception (Stoneham),*** **54, 243-251.**

GAEGGELER, H.-P., GONZALEZ-RODRIGUEZ, E., JAEGER, N. F., LOFFING-CUENI, D., NORREGAARD, R., LOFFING, J., HORISBERGER, J.-D. & ROSSIER, B. C. 2005. Mineralocorticoid versus Glucocorticoid Receptor Occupancy Mediating Aldosterone-Stimulated Sodium Transport in a Novel Renal Cell Line. ***Journal of the American Society of Nephrology,*** **16.**

GALON, J., FRANCHIMONT, D., HIROI, N., FREY, G., BOETTNER, A., EHRHART-BORNSTEIN, M., O'SHEA, J. J., CHROUSOS, G. P. & BORNSTEIN, S. R. 2002. Gene profiling reveals unknown enhancing and suppressive actions of glucocorticoids on immune cells. ***Faseb j,*** **16, 61-71.**

GEHRING, U. 1998. Steroid Hormone Receptors and Heat Shock Proteins. ***In:*** **LITWACK, G. (ed.)** ***Vitamins & Hormones.*** **Academic Press.**

GIVAN, A. L., WHITE, H. D., STERN, J. E., COLBY, E., GOSSELIN, E. J., GUYRE, P. M. & WIRA, C. R. 1997. Flow cytometric analysis of leukocytes in the human female reproductive tract: comparison of fallopian tube, uterus, cervix, and vagina. ***Am J Reprod Immunol,*** **38, 350-9.**

GORINI, S., KIM, S. K., INFANTE, M., MAMMI, C., LA VIGNERA, S., FABBRI, A., JAFFE, I. Z. & CAPRIO, M. 2019. Role of Aldosterone and Mineralocorticoid Receptor in Cardiovascular Aging. ***Frontiers in Endocrinology,*** **10.**

GOVENDER, Y., AVENANT, C., VERHOOG, N. J. D., RAY, R. M., GRANTHAM, N. J., AFRICANDER, D. & HAPGOOD, J. P. 2014. The injectable-only contraceptive medroxyprogesterone acetate, unlike norethisterone acetate and progesterone, regulates inflammatory genes in endocervical cells via the glucocorticoid receptor. Public Library of Science.

GRAD, I. & PICARD, D. 2007. The glucocorticoid responses are shaped by molecular chaperones. ***Mol Cell Endocrinol,*** **275, 2-12.**

GRAHAM, J. D. & CLARKE, C. L. 1997. Physiological Action of Progesterone in Target Tissues*. ***Endocrine Reviews,*** **18, 502-519.**

GREMEL, G., BERGMAN, J., DJUREINOVIC, D., EDQVIST, P.-H., MAINDAD, V., BHARAMBE, B. M., KHAN, W. A. Z. A., NAVANI, S., ELEBRO, J., JIRSTRÖM, K., HELLBERG, D., UHLÉN, M., MICKE, P. & PONTÉN, F. 2014. A systematic analysis of commonly used antibodies in cancer diagnostics. ***Histopathology,*** **64, 293-305.**

GRIEKSPOOR, A., ZWART, W., NEEFJES, J. & MICHALIDES, R. 2007. Visualizing the action of steroid hormone receptors in living cells. ***Nucl Recept Signal,*** **5, e003.**

HAPGOOD, J. P., AFRICANDER, D., LOUW, R., RAY, R. M. & ROHWER, J. M. 2014a. Potency of progestogens used in hormonal therapy: toward understanding differential actions. ***The Journal of steroid biochemistry and molecular biology,*** **142, 39-47.**

HAPGOOD, J. P., KAUSHIC, C. & HEL, Z. 2018. Hormonal contraception and HIV-1 acquisition: biological mechanisms. ***Endocrine reviews,*** **39, 36-78.**

HAPGOOD, J. P., RAY, R. M., GOVENDER, Y., AVENANT, C. & TOMASICCHIO, M. 2014b. Differential Glucocorticoid Receptor-Mediated Effects on Immunomodulatory Gene Expression by Progestin Contraceptives: Implications for HIV-1 Pathogenesis. ***American journal of reproductive immunology (1989),*** **71, 505-512.**

HARDY, D. B., JANOWSKI, B. A., COREY, D. R. & MENDELSON, C. R. 2006. Progesterone receptor plays a major antiinflammatory role in human myometrial cells by antagonism of nuclear factor-kappaB activation of cyclooxygenase 2 expression. ***Mol Endocrinol,*** **20, 2724-33.**

HEDLEY, D. W., CHRISTIE, M., WEATHERBY, R. P. & CATERSON, I. D. 1985. Lack of correlations between plasma concentration of medroxyprogesterone acetate, hypothalamic-pituitary function, and tumour response in patients with advanced breast cancer. ***Cancer Chemother Pharmacol,*** **14, 112-5.**

HELLBERG, S., RAFFETSEDER, J., RUNDQUIST, O., MAGNUSSON, R., PAPAPAVLOU, G., JENMALM, M. C., ERNERUDH, J. & GUSTAFSSON, M. 2021. Progesterone Dampens Immune Responses in In Vitro Activated CD4+ T Cells and Affects Genes Associated With Autoimmune Diseases That Improve During Pregnancy. ***Frontiers in Immunology,*** **12.**

HOLMBERG, C. S., LEVINGER, C., ABONGWA, M., CERIANI, C., ARCHIN, N. M., SIEGEL, M., GHOSH, M. & BOSQUE, A. 2024. HIV-1 latency reversal and

immune enhancing activity of IL-15 is not influenced by sex hormones. ***JCI Insight,*** **9.**

HONZEL, E., JOSHI, A., HERNANDEZ-MORATO, I., PENNINGTON-FITZGERALD, W. & PITMAN, M. J. 2024. A comparison of confocal and epifluorescence microscopy for quantification of RNAScope and immunohistochemistry fluorescent images. ***Journal of Neuroscience Methods,*** **403, 110050.**

HORVATH, C. A., BOULET, G. A., RENOUX, V. M., DELVENNE, P. O. & BOGERS, J. P. 2010. Mechanisms of cell entry by human papillomaviruses: an overview. ***Virol J,*** **7, 11.**

HUGHES, G. C. 2011. Progesterone and autoimmune disease. ***Autoimmunity reviews,*** **11, A502-A514.**

HUIJBREGTS, R. P. H., MICHEL, K. G. & HEL, Z. 2014. Effect of progestins on immunity: medroxyprogesterone but not norethisterone or levonorgestrel suppresses the function of T cells and pDCs. ***Contraception (Stoneham),*** **90, 123-129.**

JEW, J. Y., BERGER, E. J., BERGER, R. A. & LIN, Y. T. 2003. Fluorescence immunohistochemistry and confocal scanning laser microscopy: a protocol for studies of joint innervation. ***Acta Orthop Scand,*** **74, 689-96.**

KAPELLOS, T. S., BONAGURO, L., GEMÜND, I., REUSCH, N., SAGLAM, A., HINKLEY, E. R. & SCHULTZE, J. L. 2019. Human Monocyte Subsets and Phenotypes in Major Chronic Inflammatory Diseases. ***Front Immunol,*** **10, 2035.**

KEMPPAINEN, J. A., LANGLEY, E., WONG, C.-I., BOBSEINE, K., KELCE, W. R. & WILSON, E. M. 1999. Distinguishing Androgen Receptor Agonists and Antagonists: Distinct Mechanisms of Activation by Medroxyprogesterone Acetate and Dihydrotestosterone. ***Molecular Endocrinology,*** **13, 440-454.**

KLEIVELAND, C. R. 2015. Peripheral Blood Mononuclear Cells. ***In:*** **VERHOECKX, K., COTTER, P., LÓPEZ-EXPÓSITO, I., KLEIVELAND, C., LEA, T., MACKIE, A., REQUENA, T., SWIATECKA, D. & WICHERS, H. (eds.)** ***The Impact of Food Bioactives on Health: in vitro and ex vivo models.*** **Cham: Springer International Publishing.**

KOH, C.-H., LEE, S., KWAK, M., KIM, B.-S. & CHUNG, Y. 2023. CD8 T-cell subsets: heterogeneity, functions, and therapeutic potential. ***Experimental & Molecular Medicine,*** **55, 2287-2299.**

KOMANE, M., AVENANT, C., LOUW-DU TOIT, R., AFRICANDER, D. J. & HAPGOOD, J. P. 2022. Differential off-target glucocorticoid activity of progestins used in endocrine therapy. ***Steroids,*** **182, 108998.**

KONTULA, K., PAAVONEN, T., LUUKKAINEN, T. & ANDERSSON, L. C. 1983. Binding of progestins to the glucocorticoid receptor. Correlation to their glucocorticoid-like effects on in vitro functions of human mononuclear leukocytes. ***Biochem Pharmacol,*** **32, 1511-8.**

KOUBOVEC, D., BERGHE, W. V., VERMEULEN, L., HAEGEMAN, G. & HAPGOOD, J. P. 2004. Medroxyprogesterone acetate downregulates cytokine gene expression in mouse fibroblast cells. ***Molecular and Cellular Endocrinology,*** **221, 75-85.**

KOUBOVEC, D., RONACHER, K., STUBSRUD, E., LOUW, A. & HAPGOOD, J. P. 2005. Synthetic progestins used in HRT have different glucocorticoid agonist properties. ***Mol Cell Endocrinol,*** **242, 23-32.**

KRATZ, A., FERRARO, M., SLUSS, P. M. & LEWANDROWSKI, K. B. 2004. Normal Reference Laboratory Values. ***New England Journal of Medicine,*** **351, 1548-1563.**

LAUTEN, M., CARIO, G., ASGEDOM, G., WELTE, K. & SCHRAPPE, M. 2003. Protein expression of the glucocorticoid receptor in childhood acute lymphoblastic leukemia. ***Haematologica,*** **88, 1253-8.**

LAWRENCE, T. 2009. The nuclear factor NF-kappaB pathway in inflammation. ***Cold Spring Harb Perspect Biol,*** **1, a001651.**

LEI, K., CHEN, L., GEORGIOU, E. X., SOORANNA, S. R., KHANJANI, S., BROSENS, J. J., BENNETT, P. R. & JOHNSON, M. R. 2012. Progesterone acts via the nuclear glucocorticoid receptor to suppress IL-1β-induced COX-2 expression in human term myometrial cells. ***PLoS One,*** **7, e50167.**

LIN, X., TAKAGI, W., HYODO, S., IJIRI, S., KATSU, Y. & BAKER, M. E. 2022. Regulation by Progestins, Corticosteroids, and RU486 of Transcriptional Activation of Elephant Shark and Human Progesterone Receptors: An Evolutionary Perspective. ***ACS Pharmacol Transl Sci,*** **5, 52-61.**

LISSAUER, D., ELDERSHAW, S. A., INMAN, C. F., COOMARASAMY, A., MOSS, P. A. H. & KILBY, M. D. 2015. Progesterone promotes maternal–fetal tolerance by reducing human maternal T-cell polyfunctionality and inducing a specific cytokine profile. ***European journal of immunology,*** **45, 2858-2872.**

LOUW-DU TOIT, R., HAPGOOD, J. P. & AFRICANDER, D. 2014. Medroxyprogesterone Acetate Differentially Regulates Interleukin (IL)-12 and IL-10 in a Human Ectocervical Epithelial Cell Line in a Glucocorticoid Receptor (GR)-dependent Manner. ***J Biol Chem,*** **289, 31136-49.**

LOUW-DU TOIT, R., PERKINS, M. S., HAPGOOD, J. P. & AFRICANDER, D. 2017. Comparing the androgenic and estrogenic properties of progestins used in contraception and hormone therapy. ***Biochem Biophys Res Commun,*** **491, 140-146.**

LU, N. Z., WARDELL, S. E., BURNSTEIN, K. L., DEFRANCO, D., FULLER, P. J., GIGUERE, V., HOCHBERG, R. B., MCKAY, L., RENOIR, J. M., WEIGEL, N. L., WILSON, E. M., MCDONNELL, D. P. & CIDLOWSKI, J. A. 2006. International Union of Pharmacology. LXV. The pharmacology and classification of the nuclear receptor superfamily: glucocorticoid, mineralocorticoid, progesterone, and androgen receptors. ***Pharmacol Rev,*** **58, 782-97.**

MACDONALD, K. P. A., MUNSTER, D. J., CLARK, G. J., DZIONEK, A., SCHMITZ, J. & HART, D. N. J. 2002. Characterization of human blood dendritic cell subsets. ***Blood,*** **100, 4512-4520.**

MAHAJAN, V., GUJRAL, P., JAIN, L. & PONNAMPALAM, A. P. 2022. Differential Expression of Steroid Hormone Receptors and Ten Eleven Translocation Proteins in Endometrial Cancer Cells. ***Frontiers in oncology,*** **12, 763464-763464.**

MANGELSDORF, D. J., THUMMEL, C., BEATO, M., HERRLICH, P., SCHÜTZ, G., UMESONO, K., BLUMBERG, B., KASTNER, P., MARK, M., CHAMBON, P. & EVANS, R. M. 1995. The nuclear receptor superfamily: the second decade. ***Cell,*** **83, 835-9.**

MARITZ, M. F., RAY, R. M., BICK, A. J., TOMASICCHIO, M., WOODLAND, J. G., GOVENDER, Y., AVENANT, C. & HAPGOOD, J. P. 2018. Medroxyprogesterone acetate, unlike norethisterone, increases HIV-1 replication in human peripheral blood mononuclear cells and an indicator cell line, via mechanisms involving the glucocorticoid receptor, increased CD4/CD8 ratios and CCR5 levels. ***PloS one,*** **13, e0196043-e0196043.**

MAUVAIS-JARVIS, F., KLEIN, S. L. & LEVIN, E. R. 2020. Estradiol, Progesterone, Immunomodulation, and COVID-19 Outcomes. ***Endocrinology,*** **161.**

MCEWAN, I. J. & BRINKMANN, A. O. 2000. Androgen Physiology: Receptor and Metabolic Disorders. ***In:*** **FEINGOLD, K. R., ANAWALT, B., BLACKMAN, M.**

R., BOYCE, A., CHROUSOS, G., CORPAS, E., DE HERDER, W. W., DHATARIYA, K., DUNGAN, K., HOFLAND, J., KALRA, S., KALTSAS, G., KAPOOR, N., KOCH, C., KOPP, P., KORBONITS, M., KOVACS, C. S., KUOHUNG, W., LAFERRÈRE, B., LEVY, M., MCGEE, E. A., MCLACHLAN, R., NEW, M., PURNELL, J., SAHAY, R., SHAH, A. S., SINGER, F., SPERLING, M. A., STRATAKIS, C. A., TRENCE, D. L. & WILSON, D. P. (eds.) ***Endotext.*** **South Dartmouth (MA): MDText.com, Inc.**

Copyright © 2000-2024, MDText.com, Inc.

MCMASTER, A. & RAY, D. W. 2008. Drug Insight: selective agonists and antagonists of the glucocorticoid receptor. ***Nature Clinical Practice Endocrinology & Metabolism,*** **4, 91-101.**

MONSONEGO, J., MAGDELENAT, H., CATALAN, F., COSCAS, Y., ZERAT, L. & SASTRE, X. 1991. Estrogen and progesterone receptors in cervical human papillomavirus related lesions. ***International Journal of Cancer,*** **48, 533-539.**

MOODLEY, M., MOODLEY, J., CHETTY, R. & HERRINGTON, C. S. 2003. The role of steroid contraceptive hormones in the pathogenesis of invasive cervical cancer: a review. ***Int J Gynecol Cancer,*** **13, 103-10.**

MORRISON, C. S., CHEN, P.-L., KWOK, C., BAETEN, J. M., BROWN, J., CROOK, A. M., VAN DAMME, L., DELANY-MORETLWE, S., FRANCIS, S. C., FRIEDLAND, B. A., HAYES, R. J., HEFFRON, R., KAPIGA, S., KARIM, Q. A., KARPOFF, S., KAUL, R., MCCLELLAND, R. S., MCCORMACK, S., MCGRATH, N., MYER, L., REES, H., VAN DER STRATEN, A., WATSON-JONES, D., VAN DE WIJGERT, J. H. H. M., STALTER, R. & LOW, N. 2015. Hormonal Contraception and the Risk of HIV Acquisition: An Individual Participant Data Meta-analysis. ***PLOS Medicine,*** **12, e1001778.**

MORRISON, C. S. & NANDA, K. 2012. Hormonal contraception and HIV: an unanswered question. ***The Lancet Infectious Diseases,*** **12, 2-3.**

MOSS, M. E. & JAFFE, I. Z. 2015. Mineralocorticoid Receptors in the Pathophysiology of Vascular Inflammation and Atherosclerosis. ***Frontiers in Endocrinology,*** **6.**

MSELLE, T. F., MEADOWS, S. K., ERIKSSON, M., SMITH, J. M., SHEN, L., WIRA, C. R. & SENTMAN, C. L. 2007. Unique characteristics of NK cells throughout the human female reproductive tract. ***Clin Immunol,*** **124, 69-76.**

MULAC-JERICEVIC, B., LYDON, J. P., DEMAYO, F. J. & CONNEELY, O. M. 2003. Defective mammary gland morphogenesis in mice lacking the progesterone receptor B isoform. ***Proc Natl Acad Sci U S A,*** **100, 9744-9.**

MULAC-JERICEVIC, B., MULLINAX, R. A., DEMAYO, F. J., LYDON, J. P. & CONNEELY, O. M. 2000. Subgroup of reproductive functions of progesterone mediated by progesterone receptor-B isoform. ***Science,*** **289, 1751-4.**

NAVOT, D., ANDERSON, T. L., DROESCH, K., SCOTT, R. T., KREINER, D. & ROSENWAKS, Z. 1989. Hormonal manipulation of endometrial maturation. ***J Clin Endocrinol Metab,*** **68, 801-7.**

NICOLAIDES, N. C., CHARMANDARI, E. & CHROUSOS, G. P. 2018. Glucocorticoid Receptor☆. ***In:*** **HUHTANIEMI, I. & MARTINI, L. (eds.)** ***Encyclopedia of Endocrine Diseases (Second Edition).*** **Oxford: Academic Press.**

NOTT, J. P., BONNEY, E. A., PICKERING, J. D. & SIMPSON, N. A. B. 2016. The structure and function of the cervix during pregnancy. ***Translational Research in Anatomy,*** **2, 1-7.**

OAKLEY, R. H. & CIDLOWSKI, J. A. 2011. Cellular processing of the glucocorticoid receptor gene and protein: new mechanisms for generating tissue-specific actions of glucocorticoids. ***J Biol Chem,*** **286, 3177-84.**

OAKLEY, R. H. & CIDLOWSKI, J. A. 2013. The biology of the glucocorticoid receptor: new signaling mechanisms in health and disease. ***J Allergy Clin Immunol,*** **132, 1033-44.**

OBR, A. E. & EDWARDS, D. P. 2012. The biology of progesterone receptor in the normal mammary gland and in breast cancer. ***Molecular and Cellular Endocrinology,*** **357, 4-17.**

OGARA, M. F., RODRÍGUEZ-SEGUÍ, S. A., MARINI, M., NACHT, A. S., STORTZ, M., LEVI, V., PRESMAN, D. M., VICENT, G. P. & PECCI, A. 2019. The glucocorticoid receptor interferes with progesterone receptor-dependent genomic regulation in breast cancer cells. ***Nucleic Acids Research,*** **47, 10645-10661.**

OMOLLO, K., LAJOIE, J., OYUGI, J., WESSELS, J., MWAENGO, D., KIMANI, J., KAUSHIC, C. & FOWKE, K. 2021. Differential Elevation of Inflammation and CD4 T Cell Activation in Kenyan Female Sex Workers and Non-Sex Workers Using Depot-Medroxyprogesterone Acetate. ***Frontiers in Immunology,*** **11, 598307.**

PACE, T. W. & MILLER, A. H. 2009. Cytokines and glucocorticoid receptor signaling. Relevance to major depression. ***Ann N Y Acad Sci,*** **1179, 86-105.**

PATEL, B., ELGUERO, S., THAKORE, S., DAHOUD, W., BEDAIWY, M. & MESIANO, S. 2015. Role of nuclear progesterone receptor isoforms in uterine pathophysiology. ***Hum Reprod Update,*** **21, 155-73.**

PERROT-APPLANAT, M., DENG, M., FERNANDEZ, H., LELAIDIER, C., MEDURI, G. & BOUCHARD, P. 1994. Immunohistochemical localization of estradiol and progesterone receptors in human uterus throughout pregnancy: expression in endometrial blood vessels. ***The Journal of Clinical Endocrinology & Metabolism,*** **78, 216-224.**

PICCINNI, M. P., GIUDIZI, M. G., BIAGIOTTI, R., BELONI, L., GIANNARINI, L., SAMPOGNARO, S., PARRONCHI, P., MANETTI, R., ANNUNZIATO, F., LIVI, C. & ET AL. 1995. Progesterone favors the development of human T helper cells producing Th2-type cytokines and promotes both IL-4 production and membrane CD30 expression in established Th1 cell clones. ***J Immunol,*** **155, 128-33.**

POLIKARPOVA, A. V., LEVINA, I. S., SIGAI, N. V., ZAVARZIN, I. V., MOROZOV, I. A., RUBTSOV, P. M., GUSEVA, A. A., SMIRNOVA, O. V. & SHCHELKUNOVA, T. A. 2019. Immunomodulatory effects of progesterone and selective ligands of membrane progesterone receptors. ***Steroids,*** **145, 5-18.**

POLIS, C. B., CURTIS, K. M., HANNAFORD, P. C., PHILLIPS, S. J., CHIPATO, T., KIARIE, J. N., WESTREICH, D. J. & STEYN, P. S. 2016. An updated systematic review of epidemiological evidence on hormonal contraceptive methods and HIV acquisition in women. ***Aids,*** **30, 2665-2683.**

POPPE, W. A., DRIJKONINGEN, M., IDE, P. S., LAUWERYNS, J. M. & VAN ASSCHE, F. A. 1998. Lymphocytes and dendritic cells in the normal uterine cervix. An immunohistochemical study. ***Eur J Obstet Gynecol Reprod Biol,*** **81, 277-82.**

PRATT, W. B. & TOFT, D. O. 1997. Steroid receptor interactions with heat shock protein and immunophilin chaperones. ***Endocr Rev,*** **18, 306-60.**

QUINKLER, M. & DIEDERICH, S. 2002. DIFFERENCE OF IN VIVO AND IN VITRO ANTIMINERALOCORTICOID POTENCY OF PROGESTERONE. ***Endocrine research,*** **28, 465-470.**

RAY, D. W., SUEN, C. S., BRASS, A., SODEN, J. & WHITE, A. 1999. Structure/Function of the Human Glucocorticoid Receptor: Tyrosine 735 Is Important for Transactivation. ***Molecular Endocrinology,*** **13, 1855-1863.**

RAY, R. M. 2015. ***Differential effects of progestogens on HIV-1 replication and host gene expression in primary PBMCs and cervical tissue explants.*** **Doctor of Philosophy, University of Cape Town.**

RAY, R. M., MARITZ, M. F., AVENANT, C., TOMASICCHIO, M., DLAMINI, S., VAN DER SPUY, Z. & HAPGOOD, J. P. 2019. The contraceptive medroxyprogesterone acetate, unlike norethisterone, directly increases R5 HIV-1 infection in human cervical explant tissue at physiologically relevant concentrations. ***Scientific reports,*** **9, 4334.**

RUPPRECHT, R., REUL, J. M., VAN STEENSEL, B., SPENGLER, D., SÖDER, M., BERNING, B., HOLSBOER, F. & DAMM, K. 1993. Pharmacological and functional characterization of human mineralocorticoid and glucocorticoid receptor ligands. ***Eur J Pharmacol,*** **247, 145-54.**

SABA, E., ORIGONI, M., TACCAGNI, G., FERRARI, D., DOGLIONI, C., NAVA, A., LISCO, A., GRIVEL, J. C., MARGOLIS, L. & POLI, G. 2013. Productive HIV-1 infection of human cervical tissue ex vivo is associated with the secretory phase of the menstrual cycle. ***Mucosal Immunol,*** **6, 1081-90.**

SALEHNIA, M. & ZAVAREH, S. 2013. The effects of progesterone on oocyte maturation and embryo development. ***Int J Fertil Steril,*** **7, 74-81.**

SAMBROOK, J., FRITSCH, E. F. & MANIATIS, T. 1989. ***Molecular cloning : a laboratory manual,*** **Cold Spring Harbor, N.Y, Cold Spring Harbor Laboratory Press.**

SAPOLSKY, R. M., ROMERO, L. M. & MUNCK, A. U. 2000. How do glucocorticoids influence stress responses? Integrating permissive, suppressive, stimulatory, and preparative actions. ***Endocr Rev,*** **21, 55-89.**

SHUKLA, V., BARNHOUSE, V., ACKERMAN, W. E., SUMMERFIELD, T. L., POWELL, H. M., LEIGHT, J. L., KNISS, D. A. & GHADIALI, S. N. 2018. Cellular Mechanics of Primary Human Cervical Fibroblasts: Influence of Progesterone and a Pro-inflammatory Cytokine. ***Annals of Biomedical Engineering,*** **46, 197-207.**

SMITH, R. 2007. Parturition. ***N Engl J Med,*** **356, 271-83.**

SOCHA, M. W., FLIS, W., PIETRUS, M., WARTĘGA, M. & STANKIEWICZ, M. 2022. Signaling Pathways Regulating Human Cervical Ripening in Preterm and Term Delivery. ***Cells*** **[Online], 11.**

STANCZYK, F. Z., HAPGOOD, J. P., WINER, S. & MISHELL, D. R. 2013. Progestogens Used in Postmenopausal Hormone Therapy: Differences in Their Pharmacological Properties, Intracellular Actions, and Clinical Effects. ***Endocrine reviews,*** **34, 171-208.**

SU, S. V., GURNEY, K. B. & LEE, B. 2003. Sugar and spice: viral envelope-DC-SIGN interactions in HIV pathogenesis. ***Curr HIV Res,*** **1, 87-99.**

SWAIN, S. L., MCKINSTRY, K. K. & STRUTT, T. M. 2012. Expanding roles for CD4+ T cells in immunity to viruses. ***Nature Reviews Immunology,*** **12, 136-148.**

SZAPARY, D., SONG, L. N., HE, Y. & SIMONS, S. S., JR. 2008. Differential modulation of glucocorticoid and progesterone receptor transactivation. ***Mol Cell Endocrinol,*** **283, 114-26.**

TAN, M. H. E., LI, J., XU, H. E., MELCHER, K. & YONG, E.-L. 2015. Androgen receptor: structure, role in prostate cancer and drug discovery. ***Acta Pharmacologica Sinica,*** **36, 3-23.**

THOMAS, P. 2008. Characteristics of membrane progestin receptor alpha (mPRα) and progesterone membrane receptor component one (PGMRC1) and their roles in mediating rapid progestin actions. ***Frontiers in neuroendocrinology,*** **29, 292-312.**

THOMAS, P., PANG, Y., DONG, J., GROENEN, P., KELDER, J., DE VLIEG, J., ZHU, Y. & TUBBS, C. 2007. Steroid and G Protein Binding Characteristics of the Seatrout and Human Progestin Membrane Receptor α Subtypes and Their Evolutionary Origins. ***Endocrinology (Philadelphia),*** **148, 705-718.**

THURMAN, A. R., CHANDRA, N., YOUSEFIEH, N., ZALENSKAYA, I., KIMBLE, T., ASIN, S., ROLLENHAGEN, C., ANDERSON, S. M., HEROLD, B., MESQUITA, P. M., RICHARDSON-HARMAN, N., CUNNINGHAM, T., SCHWARTZ, J. L. & DONCEL, G. F. 2016. Comparison of Follicular and Luteal Phase Mucosal Markers of HIV Susceptibility in Healthy Women. ***AIDS Res Hum Retroviruses,*** **32, 547-60.**

TIMMERMANS, S., VANDEWALLE, J. & LIBERT, C. 2022. Dimerization of the Glucocorticoid Receptor and Its Importance in (Patho)physiology: A Primer. ***Cells,*** **11, 683.**

TOMASICCHIO, M., AVENANT, C., DU TOIT, A., RAY, R. M. & HAPGOOD, J. P. 2013. The progestin-only contraceptive medroxyprogesterone acetate, but not norethisterone acetate, enhances HIV-1 Vpr-mediated apoptosis in human CD4+ T cells through the glucocorticoid receptor. ***PLoS One,*** **8, e62895.**

TRIFONOVA, R. T., BOLLMAN, B., BARTENEVA, N. S. & LIEBERMAN, J. 2018. Myeloid Cells in Intact Human Cervical Explants Capture HIV and Can Transmit It to CD4 T Cells. ***Frontiers in Immunology,*** **9.**

TRIFONOVA, R. T., LIEBERMAN, J. & VAN BAARLE, D. 2014. Distribution of immune cells in the human cervix and implications for HIV transmission. ***Am J Reprod Immunol,*** **71, 252-64.**

VANDEVYVER, S., DEJAGER, L., TUCKERMANN, J. & LIBERT, C. 2013. New Insights into the Anti-inflammatory Mechanisms of Glucocorticoids: An Emerging Role for Glucocorticoid-Receptor-Mediated Transactivation. ***Endocrinology,*** **154, 993-1007.**

VASSILIADOU, N., TUCKER, L. & ANDERSON, D. J. 1999. Progesterone-induced inhibition of chemokine receptor expression on peripheral blood mononuclear cells correlates with reduced HIV-1 infectability in vitro. ***J Immunol,*** **162, 7510-8.**

WANG, H., CRITCHLEY, H. O., KELLY, R. W., SHEN, D. & BAIRD, D. T. 1998. Progesterone receptor subtype B is differentially regulated in human endometrial stroma. ***Molecular Human Reproduction,*** **4, 407-412.**

WEHLING, M. 1997. Specific, nongenomic actions of steroid hormones. ***Annual review of physiology,*** **59, 365-393.**

WHITE, H. D., CRASSI, K. M., GIVAN, A. L., STERN, J. E., GONZALEZ, J. L., MEMOLI, V. A., GREEN, W. R. & WIRA, C. R. 1997. CD3+ CD8+ CTL activity within the human female reproductive tract: influence of stage of the menstrual cycle and menopause. ***J Immunol,*** **158, 3017-27.**

WHO. 2024. ***Histopathology of the uterine cervix - digital atlas*** **[Online]. Pubmed.gov. Available: https://screening.iarc.fr/atlashisto_detail.php?flag=1&lang=1&Id=00004108&cat=b2 [Accessed].**

WIRA, C. R. & FAHEY, J. V. 2008. A new strategy to understand how HIV infects women: identification of a window of vulnerability during the menstrual cycle. ***AIDS,*** **22, 1909-17.**

WIRA, C. R., FAHEY, J. V., RODRIGUEZ-GARCIA, M., SHEN, Z. & PATEL, M. V. 2014. Regulation of mucosal immunity in the female reproductive tract: the role of sex hormones in immune protection against sexually transmitted pathogens. ***Am J Reprod Immunol,*** **72, 236-58.**

WIRA, C. R., FAHEY, J. V., SENTMAN, C. L., PIOLI, P. A. & SHEN, L. 2005a. Innate and adaptive immunity in female genital tract: cellular responses and interactions. ***Immunol Rev,*** **206, 306-35.**

WIRA, C. R., GRANT-TSCHUDY, K. S. & CRANE-GODREAU, M. A. 2005b. Epithelial Cells in the Female Reproductive Tract: a Central Role as Sentinels of Immune Protection. ***American journal of reproductive immunology (1989),*** **53, 65-76.**

WIRA, C. R., RODRIGUEZ-GARCIA, M. & PATEL, M. V. 2015. The role of sex hormones in immune protection of the female reproductive tract. ***Nature reviews. Immunology,*** **15, 217-230.**

WIRA, C. R. & ROSSOLL, R. M. 1995. Antigen-presenting cells in the female reproductive tract: influence of sex hormones on antigen presentation in the vagina. ***Immunology,*** **84, 505-8.**

YAO, Y., LI, H., DING, J., XIA, Y. & WANG, L. 2017. Progesterone impairs antigen-non-specific immune protection by CD8 T memory cells via interferon-γ gene hypermethylation. ***PLoS Pathog,*** **13, e1006736.**

YEAMAN, G. R., ASIN, S., WELDON, S., DEMIAN, D. J., COLLINS, J. E., GONZALEZ, J. L., WIRA, C. R., FANGER, M. W. & HOWELL, A. L. 2004. Chemokine receptor expression in the human ectocervix: implications for infection by the human immunodeficiency virus-type I. ***Immunology,*** **113, 524-533.**

YEAMAN, G. R., HOWELL, A. L., WELDON, S., DEMIAN, D. J., COLLINS, J. E., O'CONNELL, D. M., ASIN, S. N., WIRA, C. R. & FANGER, M. W. 2003. Human immunodeficiency virus receptor and coreceptor expression on human uterine epithelial cells: regulation of expression during the menstrual cycle and implications for human immunodeficiency virus infection. ***Immunology,*** **109, 137-46.**

ZHOU, J. Z., WAY, S. S. & CHEN, K. 2018. Immunology of the Uterine and Vaginal Mucosae. ***Trends Immunol,*** **39, 302-314.**